Instituto Politécnico de Saúde do Norte – Escola Superior de Saúde do Vale do Ave

Mestrado em Podiatria Infantil

Ano letivo 2022/2023

Biomechanical foot assessment in pediatric patients post intervention with arthroscopic AMIC tecnique for osteochondral lesion

Trabalho apresentado ao Curso de Mestrado em Podiatria Infantil do Departamento de Ciências da Saúde do Instituto Politécnico de Saúde – Norte – Escola Superior de Saúde do Vale do Ave, para obtenção do grau de Mestre, sob orientação de LAURA PÉREZ PALMA (Ph.D.) e coorientação de UMBERTO ALFIERI MONTRASIO

Orientador: DRA. LAURA PÉREZ PALMA

Coorientador: DR. UMBERTO ALFIERI MONTRASIO

Orientando: MARIA PALMUCCI

Vila Nova de Famalicão / 2023

Ficha de catalogação

PALMUCCI, M (2023) *Biomechanical foot assessment in pediatric patients post intervention with arthroscopic AMIC tecnique for osteochondral lesion*. Relatório de estágio profissionalizante apresentado ao Curso de Mestrado em Podiatria Infantil do Departamento de Ciências da Saúde da Escola Superior de Saúde do Vale do Ave do Instituto Politécnico de Saúde do Norte.

Vila Nova de Famalicão:

1. PEDIATRIC 2. OSTEOCHONDRAL LESION 3. AMIC 4. BIOMECHANIC

DECLARAÇÃO DE INTEGRIDADE

MARIA PALMUCCI, A30688, estudante do Mestrado em Podiatria Infantil do Departamento das Ciências da Saúde da Escola Superior de Saúde do Vale do Ave do Instituto Politécnico de Saúde do Norte, declaro ter atuado com absoluta integridade na elaboração deste RELATÓRIO DE ESTÁGIO/TRABALHO DE MESTRADO. Confirmo que, em todo o trabalho conducente à sua elaboração, não recorri a qualquer forma de falsificação de resultados ou à prática de plágio (ato pelo qual um indivíduo, mesmo por omissão, assume a autoria do trabalho intelectual pertencente a outrem, na sua totalidade ou em partes dele).

Mais declaro que todas as frases que retirei de trabalhos anteriores pertencentes a outros autores foram referenciadas ou redigidas com novas palavras, tendo neste caso colocado a citação da fonte bibliográfica.

Data e assinatura do estudante 04/09/20223

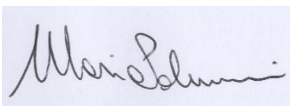

Maria Palmucci
24.11.2023 11:59:35
GMT+01:00

Dedication

I dedicate this work to all those who have helped and supported me in this long journey.

Thanks

Taking this path was a challenge for me and for my abilities, there were moments of discouragement, but my gaze towards the goal was always in front of me... ready to climb to the top. In this journey, I have to thank the support and appreciation, the patience in the face of my linguistic difficulties, which Professor Laura Pérez has always given me. I can't stop thanking the teacher who has been with me since 2005, thanks to him I have never stopped being curious about the world of feet and together we created this project, thanks doc UAM! I wouldn't be here if I weren't joined and supported by family, friends and above all by an understanding husband, biomechanics has been our cupid and her support in this project has been fundamental.

Epigraph

"Listen to your patient, he will tell you the diagnosis"

"Escucha a tu paciente, él te dirá el diagnóstico"

William Osler, 1849-1919

Summary

In pediatric podiatry clinics it can happen that a child presents with unidentified ankle pain, sometimes post-trauma, other times idiopathic. the diagnostic suspicion of a talar osteochondral lesion must in these cases be taken into consideration, sometimes the diagnosis for these patients arrives after months and months. The therapeutic protocol provides after an initial conservative treatment of about 6 months, in case of failure, a surgical treatment. This sample population underwent the intervention of biological reconstruction of the osteochondral lesion with the AMIC technique in arthroscopy, a technique widely used in adults, less so in the pediatric population. This project aims to study the biomechanical structure of these feet because it is essential both for purely scientific purposes but above all to reduce recurrences, ankle discomfort, which is why this sample was evaluated through a biomechanical clinical examination, evaluation forms such as the Foot Posture Index, AOFAS - hindfoot score, Foot Function Index after surgery to evaluate the health status and biomechanics of these feet. The results are

The sample, albeit small, reflects the niche of this pathology, and the data are comforting as the patients are doing better, all have biomechanics compatible with a moderately pronated foot, except for a few cases where overpronation is notable.

Keywords: pediatric, osteochondral lesión, AMIC, biomechanic

Abstract

Ankle pain in children is often underestimated and pointed to sprain trauma. In reality, it can often hide real talar osteochondral lesions which, if not treated adequately, limit the patient's daily life. The literature shows that even minimal biomechanical alterations on an osteochondral lesion cause increasing damage to the ankle joint over time. The aim of this study is the analysis of the biomechanical position of the feet of patients undergoing arthroscopic AMIC biological reconstruction of the talar osteochondral lesion in childhood. The subjects were evaluated with an accurate biomechanical, static and dynamic examination, they were subjected to baropodometric analysis and evaluation with the Foot Posture Index, Foot Function Index, AOFAS hindfoot.

The data of the study show how a foot with a pronated biomechanical position is correlated to a low AOFAS score and the correlation between the Foot Posture Index and the Foot Function Index highlights how a low Foot Function Index was found in patients with physiological/slightly pronated feet.

The study showed that pediatric osteochondral lesions occur in morphologically physiological or mostly pronated feet, however the sample size is small to establish a strong correlation. Surely it can be stated from the clinical history of the patients that the cause is often traumatic, with mainly sprain traumas, but there are also cases of atraumatic origin.

KEYWORDS: PEDIATRIC, OSTEOCHONDRAL LESION, AMIC, BIOMECHANIC

Índice

Index of figure

Index of table

Índice de Anexos

Listas

Abreviaturas

ACI: Autologo Chondrocyte Implantation
AITFL anterior inferior tibiofibular ligament
AL anterolateral
AM anteromedial
AMIC autologus matrix-induced chondrogenesis
AOFAS: American Orthopaedic Foot and Ankle Society's- ankle-hindfoot scale
AP: anterior-posterior
ATFL anterior talofibular ligament
ATFLi inferior anterior talofibular ligament
ATFLs superior anterior talofibular ligament
ATTL Deep anterior tibiotalar ligament
ATTs superficial anterior tibiotalar ligament
CFL calcaneofibular ligament
CKC closed kinetic chain
cm: centimeter
cm2: square centimeter
CMC Chondrocyte-matrix complex
CNS : central nervous system
CoP: centre of pressure
CT computed tomography
DPTTL posterior deep tibiotalar ligament
EVA: Ethylene-vinyl acetate
FDL flexor digitorum longus
FFI: Foot Function Index
FHL flexor hallux longus
FPI foot posture index
GAG glycosamminoglycans
GRF: Ground reaction forces
IM intermalleolar ligament
IP:interphalangeal joint
IRCS: International Cartilage Repair Society
ITFL tibiofibular interosseous ligament
LIMJA longitudinal axis midtarsal joint
M1: first metatarsal
M2: second metatarsal
M3: third metatarsal
M4: fourth metatarsal

M5: fifth metatarsal
mm:millimeters
MRI magnetic resonance imaging
MSCs multipotent stem cells
MTJ midtarsal joint
MTPJ metatarsophalangeal joint
NCSP: neutral calcaneal stance position
OCL: ostehocondral lesion
OKC Open Kinetic Chain
OLT: osteochondral lesion of talus
P1 proximal phalangeal
P2 intermidiate phalangeal
P3 distal phalangeal
PB: peroneus brevis
PGA polyglycolic acid
PITFL posterior inferior tibiofibular ligament
PL: peroneus longus
PLLA polylactic acid
PT posterior tibial
PTFL posterior talofibular ligament
PTFL posterior tibiofiluar ligament
PTTL Deep posterior tibiotalar ligament
PTTs superficial posterior tibiotalar ligament
R1: First ray
RCSP: resting calcaneal stance position
ROM: range of motion
ST subtalar
T tesla
TC tibiocalcaneal ligament
TCL Deep tibiocalcaneal ligament
TFIL tibiofibular intermalleolar ligament
TFTL tibiofibular transverse ligament
TNJ talonavicular joint
TNL tibionavicular ligament
TSL tibiospring ligament
TTJ tibio-talar joint or ankle joint
TW: toe walking

Symbols

>: greater than

<: less than

≥: greater than or equal to

±: plus/minus

≤ - Less than or equal

% - Percentage or relative frequency

Acronyms

CESPU: Cooperativa De Ensino Superior Politécnico Universitário

ESSVA: Escuela Superior de Salud de Vale de Ave

HPUB: Hospital Podológico Universitario Universidad de Barcelona

UB: Universidad de Barcelona

1 Introduction

This paper includes what was learnt during the internship period of the academic year 2021/2022 from March 7 to July 8 2022. It lasted 20 weeks of internship, 32 hours per week and a total of 630 hours. The second year of the CESPU Master Degree in Pediatric Podiatry was made possible thanks to the ERASMUS scholarship which made me attend the Podiatric Hospital of the University of Barcellona (HPUB).

The second year was splitted in CESPU lessons and HPUB clinical practice, supervised by Dr. Laura Perez Palma, head mistress of Pediatric Podiatry department and Master Degree in Pediatric Podiatry of the University of Barcelona. On this occasion I attended and actively took part in the medical examinations, clinical picture and therapeutic recommendation, together with Pediatric teachers of the Department of HPUB Pediatric Podiatry. Moreover, in Italy, I have attended the orthopedic clinic of Dr. Umberto Alfieri Montrasio, pediatric and adult foot and ankle Surgeon of the specialized unit of the foot and ankle USPeC of IRCCS Galeazzi-Sant'Ambrogio Hospital of Milan.

During the clinical practice, I was able to admire the clinical procedure implemented by HPUB and once in Italy I applied it to the theoretical knowledge learnt in the lesson.

The second part of the year was addressed to study and clinical cases evaluation of pediatric patients follow-up after the surgery of biological reconstruction with AMIC technique in arthroscopy for talar osteochondral lesions. The study has provided a precise revision of the scientific literature, the writing of an evaluation of clinical record for these patients, the statistical analysis of collected data and in the end, a recommendation of therapeutical record. The bibliography has been introduced according to the 7 edition of APA rules.

2 Professional internship

The professional clinical part of this internship has been attended in the University Podiatric Hospital of Barcelona with the shadowing of teachers from the Pediatric Podiatry department during medical visits.

2.1 Barcelona

The organization consists of:

- a waiting room with a reception where the patient is welcomed by relevant staff
- Podiatric rooms for the biomechanical analysis including the following equipment: an examination bed, a baropodometric footplate, a podoscope, desk with PC and two chairs in order to welcome the patient and the companion, clinical evaluation equipment: goniometer, plumb bob, pelvimetry
- chiropodist rooms, equipped in order to perform podiatry treatments
- surgery room
- Radiology room to take the foot x-ray with a Radiology technician
- Lab: for the orthotic plantar treatment
- A room dedicated to detect footprints with plaster cast
- Rooms and departments

In the pediatric lab, during the clinical evaluation to students of 3 and 4 degree of the university and the students of Pediatric Podiatry Master too, they became players of the podiatric medical visit. Starting from welcoming and getting the patient comfortable, the second step is the medical records fill in and anamnesis and in the end the clinical evaluations for the patient. Generally, the clinical scan begins with an evaluation on the medical table with the patient in supine and then prone position followed by an evaluation in orthostatic and lastly an analysis of gait or run. After that, the teacher, in consultation with students, asks to show up the diagnostic hypothesis according to a clinical reasoning which is a result of the evaluations. Once discussing the clinical case, the step forward is to recommend a treatment protocol. Back to the room with the patient, he is informed of the clinical diagnosis and the following therapeutic protocol. If a plantar or silicone orthosis or further instrumental tests are required (for example a radiography or a podiatric treatment), they will be implemented in the same session.

During the internship in Barcelona, I had the opportunity to attend as a volunteer with Dr. Laura Perez Palma the clinic of Fundació d'Osteopatia de Barcelona (FOB) c/ Consolat de mar, 45 2º planta, where I had the chance of evaluating very complex clinic cases both for the purely foot disease and the environmental context to which children belong with and the ethnicity. This is a Learning and Service Project (APS) in the degree course, it falls within the line of didactic innovation and active learning methodologies. The aim of the project is to strengthen students in their learning process in direct contact with reality, at the service of both institutions and their users, as well as enhance their commitment as future social service professionals. Thanks to this clinic, I had the opportunity to test the importance of the cultural habits of the patient and the capability of getting in touch and communicating with the patient and their parents. The clinical evaluation consisted of a clinical record collection, often already provided by osteopath colleagues, a clinostat scan in pronate and supine position, an evaluation in orthostatism and finally a gait analysis. Later, together with Dr. Perez Palma, we discussed the clinical case and suggested a treatment protocol.

2.2 Italy

During my internship in Italy at the foot and ankle orthopedic clinic, I was given the opportunity to independently manage the clinic, but under the careful observation of Dr. Alfieri Montrasio. The clinical evaluation was differentiated based on the patient's age. For patients under 7 years old, a suitable setting for their age was created before the visit, with carpets, toys, and colors, in order to make the child feel comfortable and free to move around. For this pediatric population under 7 years old, the medical history was taken separately between the podiatrist, orthopedist, and parent, without the presence of the child to avoid boring them. Subsequently, the young patient was called in for the examination, initially allowed to play freely on the carpet. Then they were asked to remove their shoes, socks, pants, and sometimes even the diaper (if it was hindering their mobility). The examination continued with an analysis of their movements on the carpet, walking, and coordination of play with a ball. Then it proceeded with the analysis on the examination table in different positions. As for patients above 7 years old, the evaluation protocol applied was the traditional one, which involved welcoming the patient and their parents, collecting medical history, analyzing the patient (without shoes, socks, pants, and sometimes even shirt) in open kinetic chain and subsequent closed kinetic chain in standing and walking positions.

During this Italian internship from November 2021 to December 2022, I evaluated 128 pediatric patients, ranging from 0 to 18 years old, including 73 males and 55 females. For patients under 7 years old, a suitable setting for their age was created before the visit, with carpets, toys, and colors, in order to make the child feel comfortable and free to move around. For this pediatric population under 7 years old, the medical history was taken separately between the podiatrist, orthopedist, and parent, without the presence of the child to avoid boring them. Subsequently, the young patient was called in for the examination, initially allowed to play freely on the carpet. Then they were asked to remove their shoes, socks, pants, and sometimes even the diaper (if it was hindering their mobility). The examination continued with an analysis of their movements on the carpet, walking, and coordination of play with a ball. Then it proceeded with the analysis on the examination table in different positions. As for patients above 7 years old, the evaluation protocol applied was the traditional one, which involved welcoming the patient and their parents, collecting medical history, analyzing the patient (without shoes, socks, pants, and sometimes even shirt) in open kinetic chain and subsequent closed kinetic chain in standing and walking positions.

2.2.1 Observation/intervention

During this Italian internship from November 2021 to December 2022, I evaluated 128 pediatric patients, ranging from 0 to 18 years old, including 73 males (57%) and 55 females (43%). (fig.1 -2)

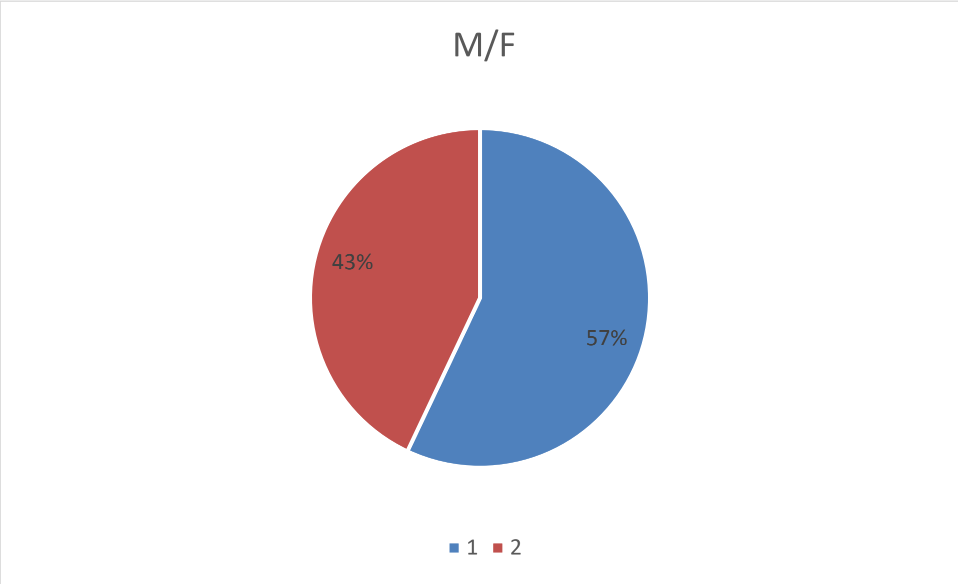

Figure 1. representation with a pie chart of the percentage of males and females of the pediatric population of the Italian internship.

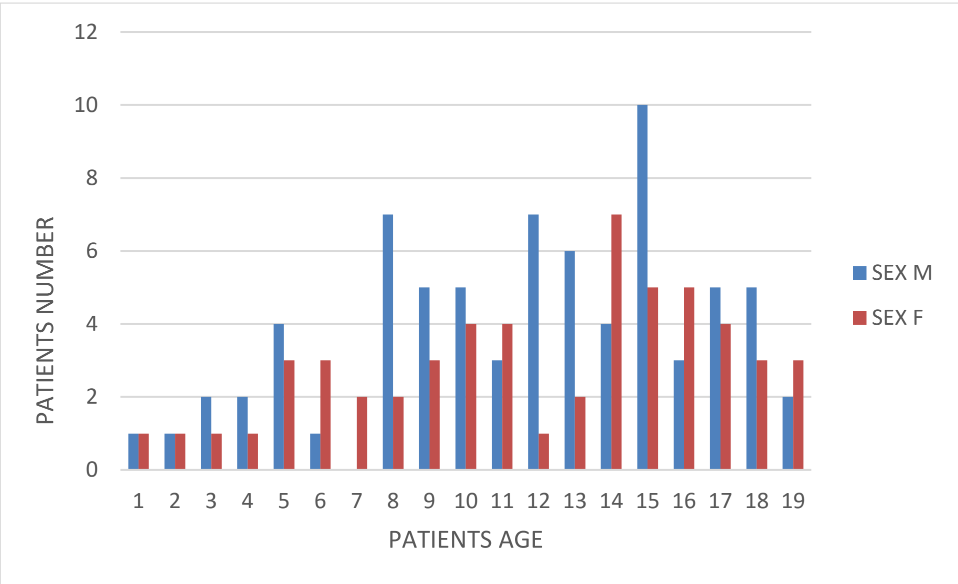

Figure 2. representation of the distribution of males and females divided by age in the pediatric population of the Italian internship.

Clinical evaluations reported the following results in incidence of found diseases/paramorphisms (fig.3):

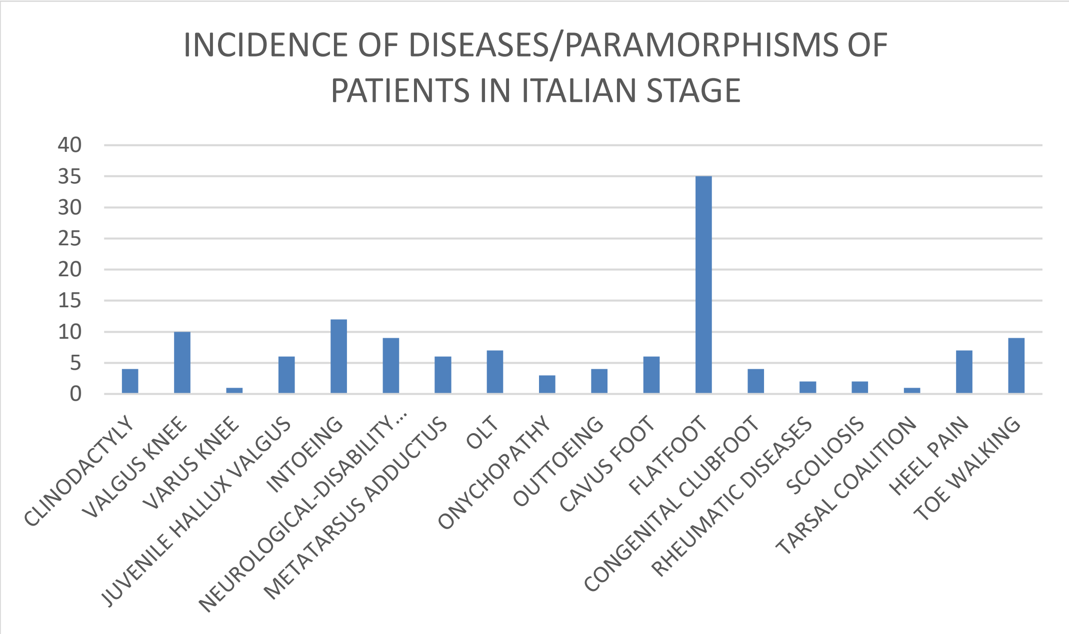

Figure 3: Incidence of diseases/paramorphisms of patients in Italian internship

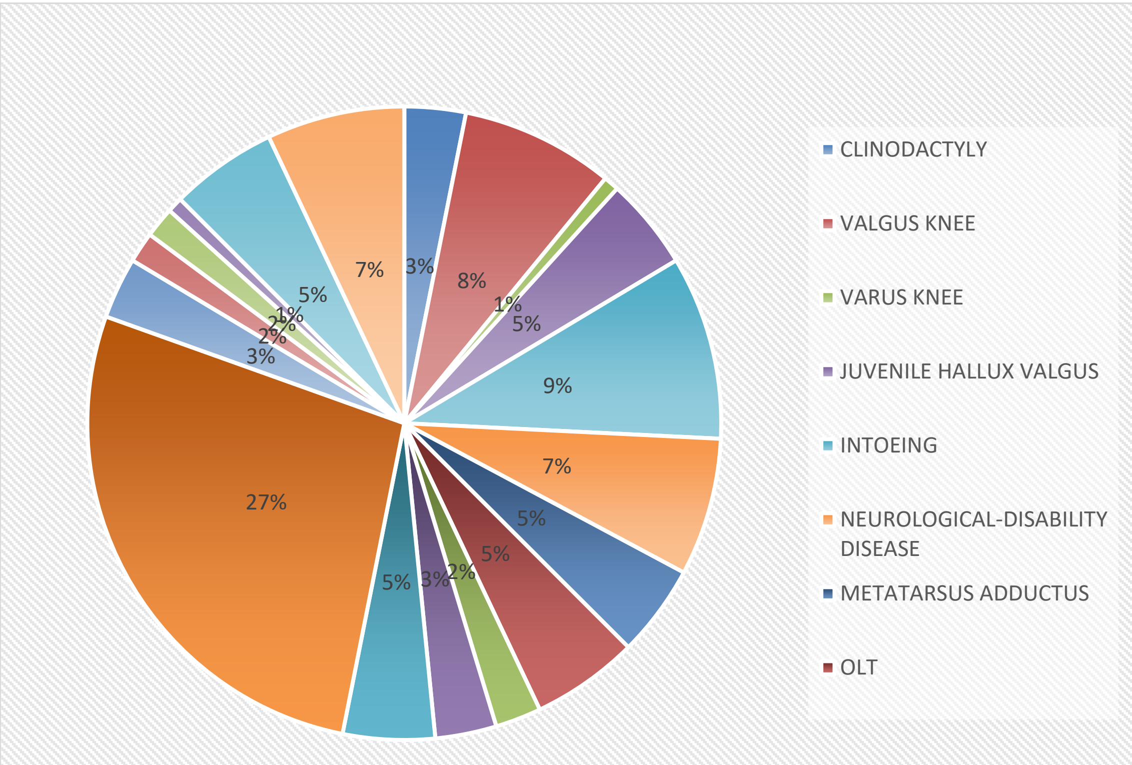

Figure 4: Incidence in percentage of diseases/paramorphisms of patients in Italian internship

According to the diagrams (fig. 4) , the highest rate of disease is the pronate flat feet with 27%, followed by in-toeing with 9%, valgus knee with 8%, toe-walking and neurological-disability disease with 7%. Lastly, with lowest percentages, metatarsus adductus, heel pain, cavus foot, talar osteochondral lesions, juvenile hallux valgus 5%, congenital clubfoot outcomes, clinodactyly, outtoeing 3%; scoliosis, tarsal coalition, onychopathy 2%, varus knee, rheumatic diseases 1%.

2.3 Clinical case 1

The reason for the visit: feet pain after training, the patient was already examined by foot orthopedic with surgical suggestion.

Anamnesis:

Male of 16 years old, 4 months, 73 kg weight, 177 cm height, foot size 42-43

Born of natural childbirth, born weight 3.3kg, 53 cm height

No crawling, beginning of independent walking at the age of 12 months

At the age of 6, affected by non-Hodking lymphoma.

First orthopedic examination when he was 14 years old for asymptomatic flexed hallux:

diagnosis of bilateral cavus foot and recommendation for use of orthotics with supinator wedge to hindfoot, medial arch support, pronator wedge to forefoot, without any particular relief(fig.5)

Figure 5. Posterior view of the patient resting on orthotic insoles according to orthopedic indications

Age of 15.5 appearance of pain while restarting sport activity (basketball 4-5 times per week)

Exploration at open kinetic chain

- inspection
    - plantar hyperkeratosis at 1th and 5th metatarsal head bilateral foot

- unperceivable bilateral flexed hallux
- palpation
  - dysmetria: there are not any dysmetrias after pelvic push manoeuvre
  - hip: physiological intra-extra rotation 45°-45°
  - knee: patella in line with zenith, unperceivable extra rotation of right patella
  - foot:
    - Silfverskiöld test: reduced dorsiflexion of the ankle joint with the knee extended, recovers with the knee flexed bilaterally
    - No pain on digital pressure of the Achilles tendon bilaterally
    - No pain on digital pressure of the plantar fascia and heel bilaterally
    - No pain on digital pressure of the sinus tarsi bilaterally
    - Reduced inversion of the subtalar joint bilaterally
    - No pain during mobilization of the subtalar joint; midtarsal and Lisfranc joints
    - No pain on the piano test
    - No pain on digital pressure of the metatarsal heads
    - No pain on toe's immobilization
    - ROM reduced dorsiflexion of IP joint right hallux
- Normal muscular tests
- From forefoot to rearfoot: valgus rigid forefoot 9° left (fig.6), 8° right (Kirby sec: lateralized axis)

Figure 6. valgus rigid forefoot 9° left in neutral position

<u>Exploration in seat position:</u>

- Negative Thomas test

<u>Exploration in closed kinetic chain:</u>

- orthostasis
  - absence of support of the big toe on the ground
  - on the sagittal plane: accentuated prominence of the base of the 5th metatarsal
  - RCSP 5° left, 4 °right inverted
  - Navicular drop on the left: -0.4, on the right: -0.3
  - No ligament laxity
  - Active maximum pronation test 1/3 (compared to maximum supination 2/3) (fig.7)

7.a Max pronation 7.b RCSP 7.c max supination

Figure 7. vision of the execution of the test of max active pronation compared with the maximum active supination 7.a active maximum pronation, 7.b RCSP relaxed calcaneal stance position, 7.c active maximum supination

  - Adam test positive
  - Squat test positive
  - Stairs test: negative
  - Jack test positive
  - Colemann test negative (fig.8)


figure 8: performing Coleman's test on left foot

- Modified Coleman test for valgus forefoot: positive (fig.9)


figure 9: performing modified Coleman's test on left foot

- FPI: -7 sx, -9 dx (table 1)

Table 1: Foot Posture Index of the clinical case 1

FPI					
Talar head palpation	talar head palpable on lateral side/but not on medial side	talar head palpable on lateral side/slightly palpable on medial side	talar head equally palpable on lateral and medial side	talar head palpable on medial side/slightly palpable on lateral side	talar head palpable on medial side/but not on lateral side
	-2	-1	0	1	2
right		-1			
left		-1			
Curves above and below lateral malleoli	curve below the malleolus either straight or convex	curve below the malleolus concave, but flatter/more shallow than curve above the malleolus	both infra and supra malleolar curves roughly equal	curve below the malleolus more concave, than curve above the malleolus	curve below malleolus markedly more concave, but than curve above the malleolus
	-2	-1	0	1	2
right	-2				
left		-1			
calcaneal inversion/eversion o	more than an estiamted 5°inverted (varus)	between vertical and an estimated 5° inverted (varus)	vertical	between vertical an estimated 5° evrted (valgus)	more than an estimated 5° everted (valgus)
	-2	-1		1	2
right		-1			
left		-1			
Bulge in the region of talo-navicular jont	markedly concave	slightly, but definitely concave	area of TNJ flat	bulging slightly	bulging markedly
	-2	-1	0	1	2
right	-2				2
left		-1			2
medial arch height	arch high and acutely angled towards the posterior end of the medial arch	arch moderately high and slightly acute posteriorly	arch height normal and concentrically curved	arch lowered with some flattening in the central portion	arch very low with severe flattening in the central position - arch making ground contact
	-2	-1	0	1	2
right		-1			
left		-1			
abduction/adduction of the forefoot on rearfoot (too-many-toes)	no lateral toes visible. Medial toes clearly visible	medial toes clearly more visible than lateral	medial and lateral toes equally visible	lateral toes clearly more visible than medial	no medial toes visible. Lateral toes clearly visible
	-2	-1	0	1	2
right	-2				
left	-2				

- Static (figure 10) and dynamic (figure 11-12-13) baropodometric examination with FDM Zebris platform

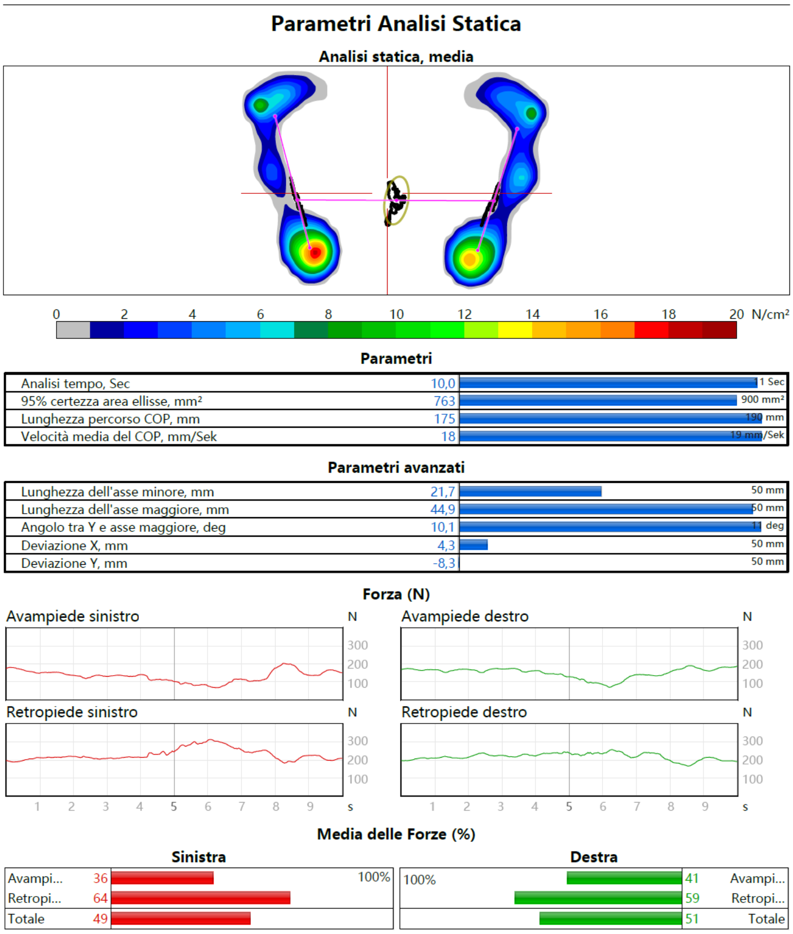

Figure 10. Static baropodometric examination with patient in RCSP with FDM Zebris platform

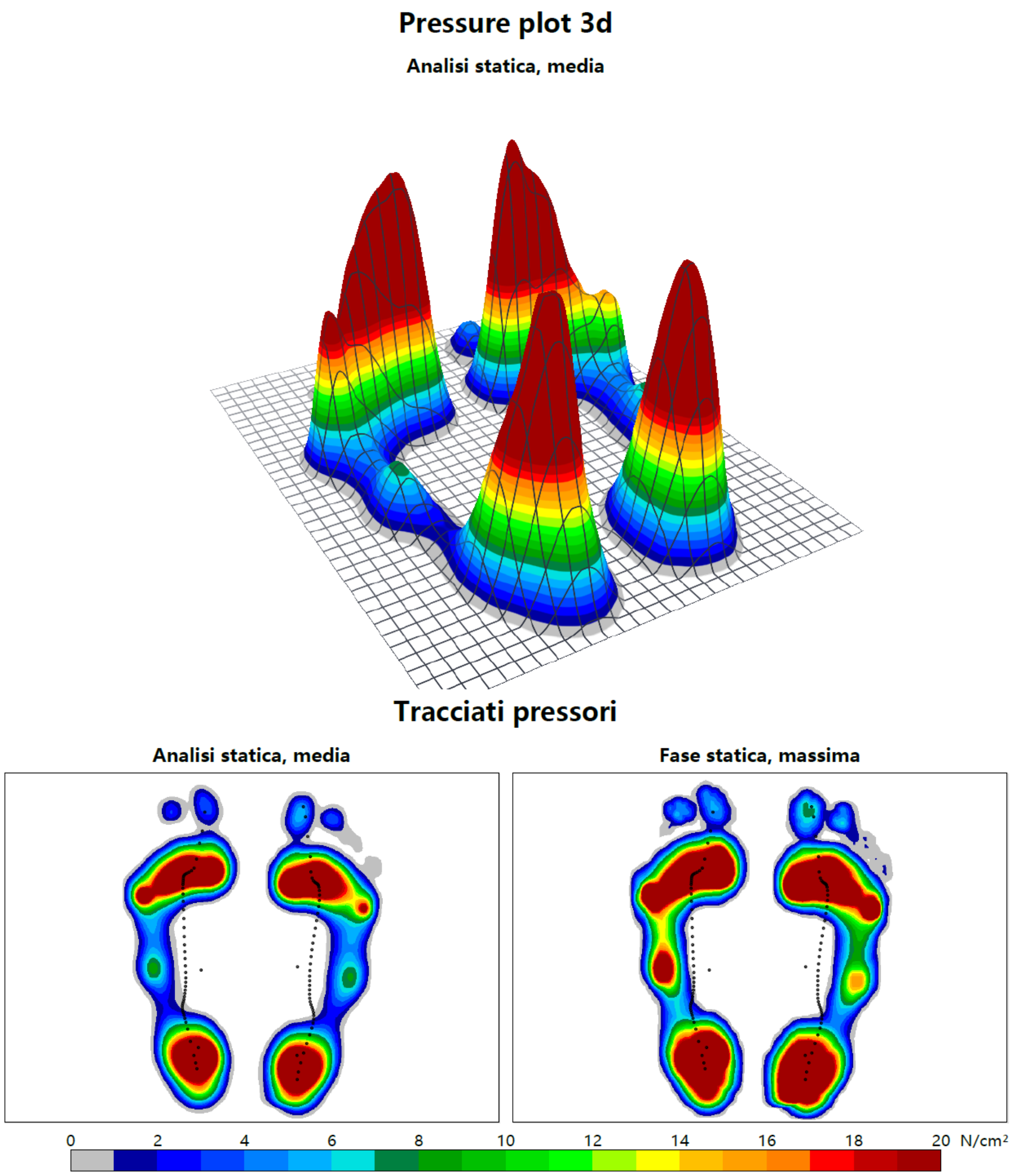

Figure 11: dynamic baropodometric examination with FDM Zebris platform

Analisi COP

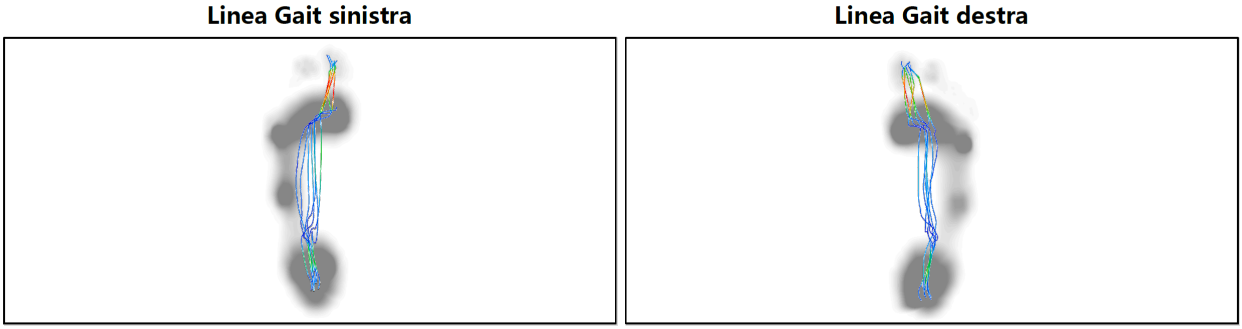

Gait line length, mm	L	244,3±11,0	400 mm
	R	251,9±4,5	
Tempo di contatto, Sec	L	0,99±0,05	3 Sec
	R	1,00±0,02	

Forza e pressione

Curve pressorie

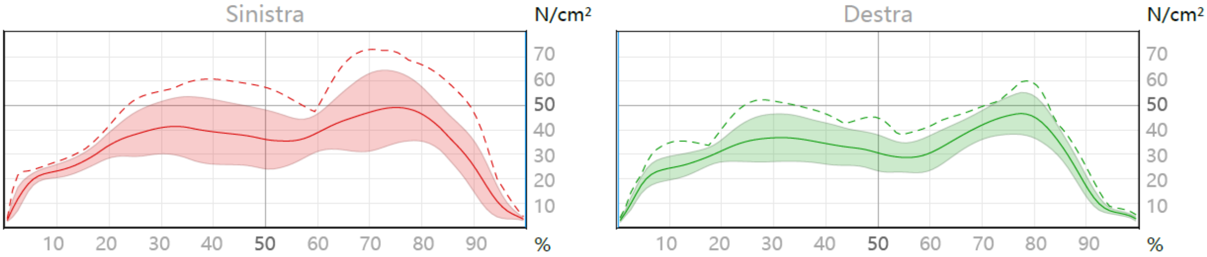

Curve di forza

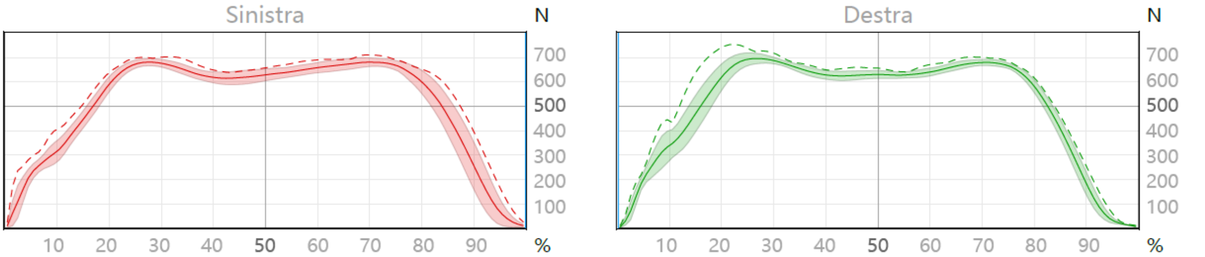

Parametri della forza

Forza massima1, N	L	682,0	800 N
	R	696,7	
Tempo forza massimale1 (t1), %	L	27	100%
	R	26	
Forza massima2, N	L	681,5	800 N
	R	680,7	
Tempo forza massimale2 (t2), %	L	70	100%
	R	70	

Figure 12: dynamic baropodometric examination with FDM Zebris platform. note the butterfly curve of both the right and left foot

3 Zone - curve di forza

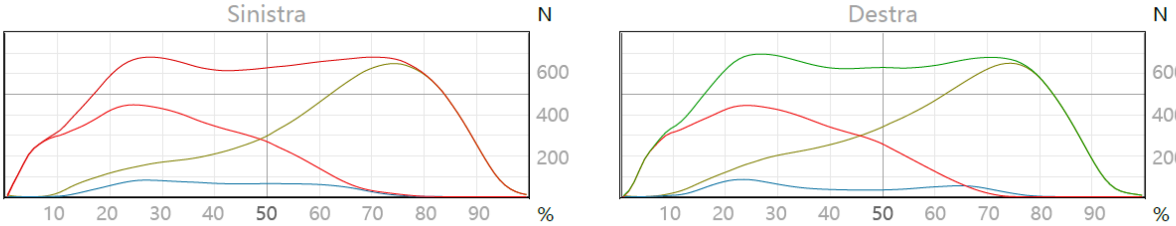

Variazione di carico

Tempo di cambio tallone/avampiede, Sec	L	0,46±0,07	0.6 Sec
	R	0,43±0,06	
Tempo di cambio tallone/avampiede, %	L	46,4±8,9	100%
	R	43,6±7,1	

Forza massima, N

Avampiede	L	668,0±23,9	800 N
	R	657,5±24,4	
Mesopiede	L	90,6±84,9	
	R	98,9±45,2	
Tallone	L	463,4±42,6	
	R	460,9±35,7	

Massimo della pressione, N/cm²

Avampiede	L	50,9±14,5	80 N/cm²
	R	47,6±8,6	
Mesopiede	L	9,9±9,0	
	R	8,8±3,8	
Tallone	L	42,6±12,2	
	R	40,1±8,2	

Tempo forza massimale, % fase statica

Avampiede	L	71,5±3,0	100%
	R	72,2±1,4	
Mesopiede	L	30,6±17,2	
	R	30,2±14,8	
Tallone	L	23,2±3,1	
	R	19,8±4,4	

Figure 13: report of dynamic baropodometric examination with FDM Zebris platform. note the time of change rearfoot/forefoot of both the right and left foot

<u>Dynamics</u>:

1° rocker: Heel strike is lateral and there is reduced pronation of the subtalar joint, with early contact of the first metatarsal head followed by detachment, absence of support from the big toe during the second rocker, excessive supination that continues during the third rocker with lateral propulsive push, reduced shock absorption and load absorption phase.

Reduced step angle and distance between heels <5cm.

<u>Evaluation</u>:

Bilateral supinated cavus foot.

<u>Proposed treatment</u>:

- functional orthotic therapy (fig.14) with 4mm polypropylene plantar orthotic, neutral post, lateral stabilization with 60-shore EVA, intrinsic correction for bilateral forefoot valgus, 3mm expertene at the forefoot level, and 4mm Poron in the heel bilaterally.

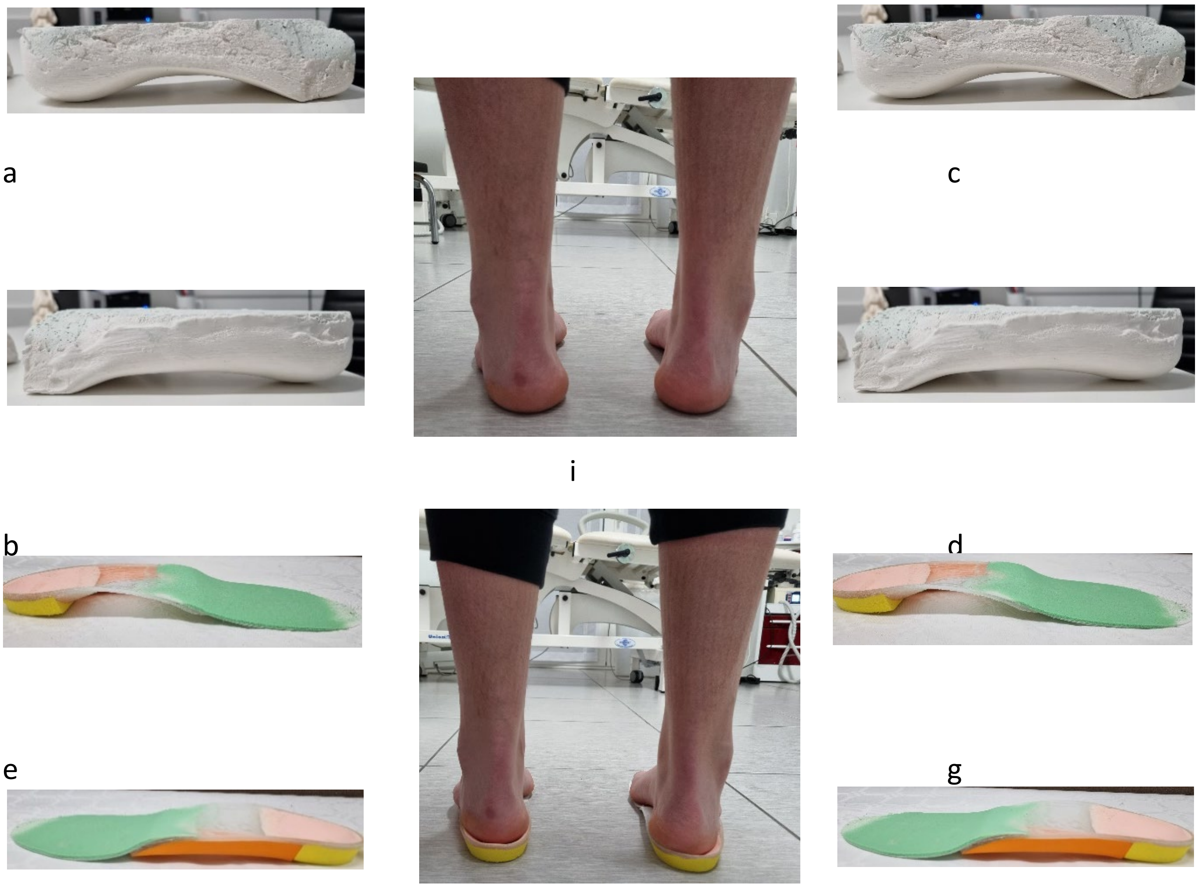

a c i b d e g f l h

Figure 14: functional orthotic therapy of clinical case 1. Medial (a) and lateral (b) view plaster cast with intrinsic valgus forefoot correction left foot; medial (c) and lateral (d)

view plaster cast with intrinsic valgus forefoot correction right foot. Medial (e) and lateral (f) view of functional orthotic of left foot and medial (g) and (lateral (h) view of functional orthotic of right foot. 14.i RCSP, 14.l Posterior view of the patient resting on functional orthotic

Observations: the plantar orthotic therapy was gradually introduced first in daily life and after approximately 3 weeks in sports activities. After about 4 weeks, the patient reported the disappearance of pain and expressed the need to "never take them off" due to a feeling of instability in the absence of orthotics. The parents were satisfied as they were not convinced by the proposed surgical treatment, which they considered too aggressive

2.4 Clinical case 2

The reason for the visit:

visit suggested by osteopath for a not clear feet

Anamnesis:

Male of 3 years old, 18 kg weight, 99 cm height, foot size 29

Italian Mother and Egyptian Father

Born of natural childbirth at 38 weeks, born weight 4.1kg, 52 cm height

Normal Apgar score when he was born

Slight respiratory problem during the following hours and for this reason he was admitted to the hospital for one week

Bronchial Asthma treated with cortisone for preventive measure

Less crawling, beginning of independent walking over the age of 18 months

Orthopedic examination: physiological flat feet

1^visit

Exploration at open kinetic chain

- Inspection
    - 2nd toe slightly dorsiflexed bilaterally
- Palpation
    - Asymmetry: no asymmetry noted after pelvic thrust maneuver
    - Hip: 70° left hip internal rotation, 65° right hip internal rotation
    - Foot:
        - Silfverskiöld test: negative
        - Good range of motion in the ankle joint bilaterally
        - No pain on digital pressure of the Achilles tendon bilaterally
        - No pain on digital pressure of the plantar fascia and heel bilaterally
        - No pain on digital pressure of the sinus tarsi bilaterally
        - No pain during mobilization of the subtalar joint; midtarsal and Lisfranc joints
        - No pain on digital pressure of the metatarsal heads
        - No pain during finger mobilization
    - Muscle strength testing within normal limits

Exploration in sitting position:

- W pattern

Exploration in closed kinetic chain (fig. 15:

 a  b

Figure 15.a : dorsal view in RCSP, 15.b: posterior view in RCSP

- Standing position (fig.16):

- Navicular drop: 1.7cm left , 2.2cm right
- Negative Jack test
- Negative heel rise test
- Severe supination resistance test bilaterally
- Jumping on both feet performed
- Jumping on one foot performed, but still uncertain
- Foot Posture Index (FPI) (table2) : Left and right: 11

Table 2: Foot Posture Index of the clinical case 2

FPI					
Talar head palpation	talar head palpable on lateral side/but not on medial side	talar head palpable on lateral side/slightly palpable on medial side	talar head equally palpable on lateral and medial side	talar head palpable on medial side/slightly palpable on lateral side	talar head palpable on medial side/but not on lateral side
	-2	-1	0	1	2
right					2
left					2
Curves above and below lateral malleoli	curve below the malleolus either straight or convex	curve below the malleolus concave, but flatter/more shallow than curve above the malleolus	both infra and supra malleolar curves roughly equal	curve below the malleolus more concave, than curve above the malleolus	curve below malleolus markedly more concave, but than curve above the malleolus
	-2	-1	0	1	2
right					2
left					2
calcaneal inversion/eversion o	more than an estiamted 5°inverted (varus)	between vertical and an estimated 5° inverted (varus)	vertical	between vertical an estimated 5° evrted (valgus)	more than an estimated 5° everted (valgus)
	-2	-1	0	1	2
right					2
left					2
Bulge in the region of talo-navicular jont	markedly concave	slightly, but definitely concave	area of TNJ flat	bulging slightly	bulging markedly
	-2	-1	0	1	2
right					2
left					2
medial arch height	arch high and acutely angled towards the posterior end of the medial arch	arch moderately high and slightly acute posteriorly	arch height normal and concentrically curved	arch lowered with some flattening in the central portion	arch very low with severe flattening in the central position - arch making ground contact
	-2	-1	0	1	2
right					2
left					2
abduction/adduction of the forefoot on rearfoot (too-many-toes)	no lateral toes visible. Medial toes clearly visible	medial toes clearly more visible than lateral	medial and lateral toes equally visible	lateral toes clearly more visible than medial	no medial toes visible. Lateral toes clearly visible
	-2	-1	0	1	2
right					1
left					1

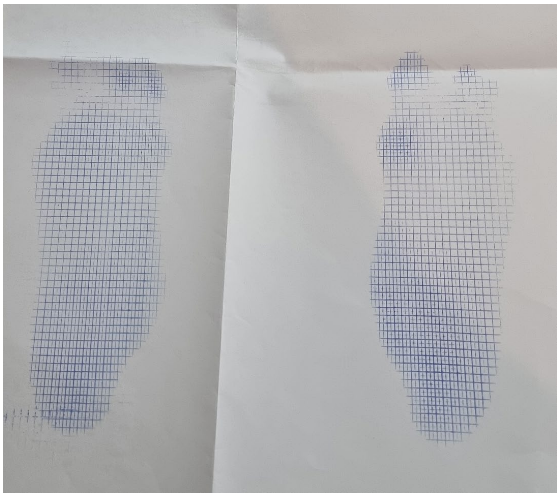

Figure 16. 2-dimensional imprint of the patient's plantar support made with an ink plantograph

Dynamics:

- clumsy run (fig.17)

figure 17: freeze frame anterior view of the patient's clumsy running

- Good coordination in ball-game
- Walking on the heels performed
- Walking on tiptoes performed (fig.18) , the heel is not inverted and often give up by lay down the foot and close even more step angle

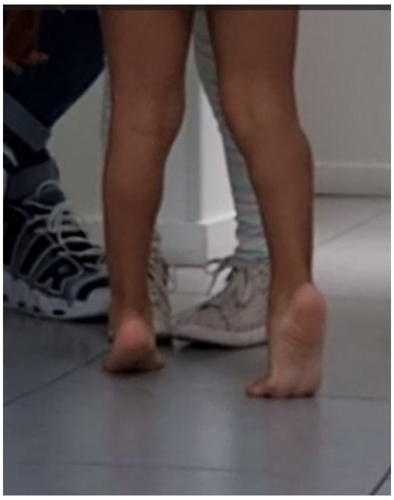
figure 18: freeze frame posterior view of the patient's Walking on tiptoes performed

- Difficulty in walking on the external side (fig.19)

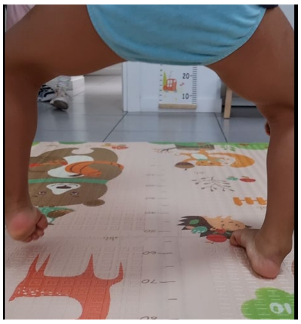
figure 19:freeze frame of posterior view of difficulty in walking on the external side

- Walking on the sagittal plane (fig.20) : during the second rocker, inversion of the curve of the medial longitudinal arch.

Figure 20: freeze frame of walking on the sagittal plane during the second rocker, inversion of the curve of the medial longitudinal right (a) and left(b) arch

- Walking on the frontal plane (fig.21): heel contact centered-medially with slippage of the adipose pad under the lateral aspect of the heel.

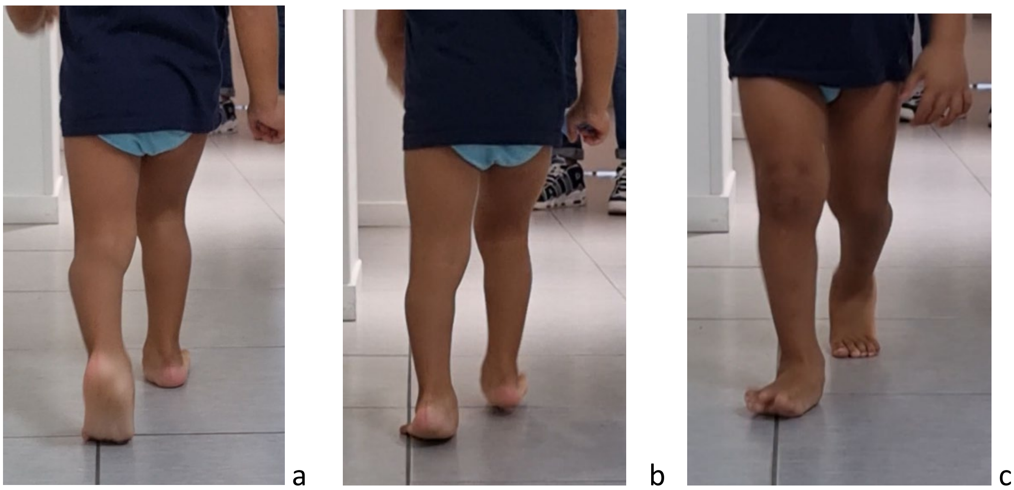

Figure 21: freeze frame of walking on the frontal plane. 21.a heel contact centered-medially with slippage of the adipose pad under the lateral aspect of the right heel. 21.b

preparation of the heel contact of the right heel and posterior view of the pronated left foot. 21.c freeze frame of anterior view of the 1^rocker of the right foot

Evaluation:

Suspicion of vertical talus

Proposed treatment:

- After consulting with a pediatrician, perform weight-bearing X-rays of both feet (AP and lateral projections) to study the talus.
- Apply bilateral positional taping on the 2nd toe using kinesiotape.
- Use shoes with a square toe, laced, with a high and wide toe box, and strong and sturdy construction.
- At daycare, use closed shoes or non-slip socks, avoid slippers.
- Avoid sitting in a W position.
- Orthopedic evaluation of the foot

Observations:

vertical talus is often associated with syndromes; however, during the assessment, the patient was cooperative, participating, answering questions, playing, and speaking simultaneously. They could count, and I did not detect any suspected additional cognitive deficits

follow-up visit:

At 3 and 4 months years old , weight 19kg, height 102cm, shoe size 27

Engages in swimming twice a week.

Medical history: the mother reports that lately the child does not want to move, sits at the park, is seen stumbling more frequently, and falls often.

Non-weight-bearing foot X-rays were taken (fig.22)

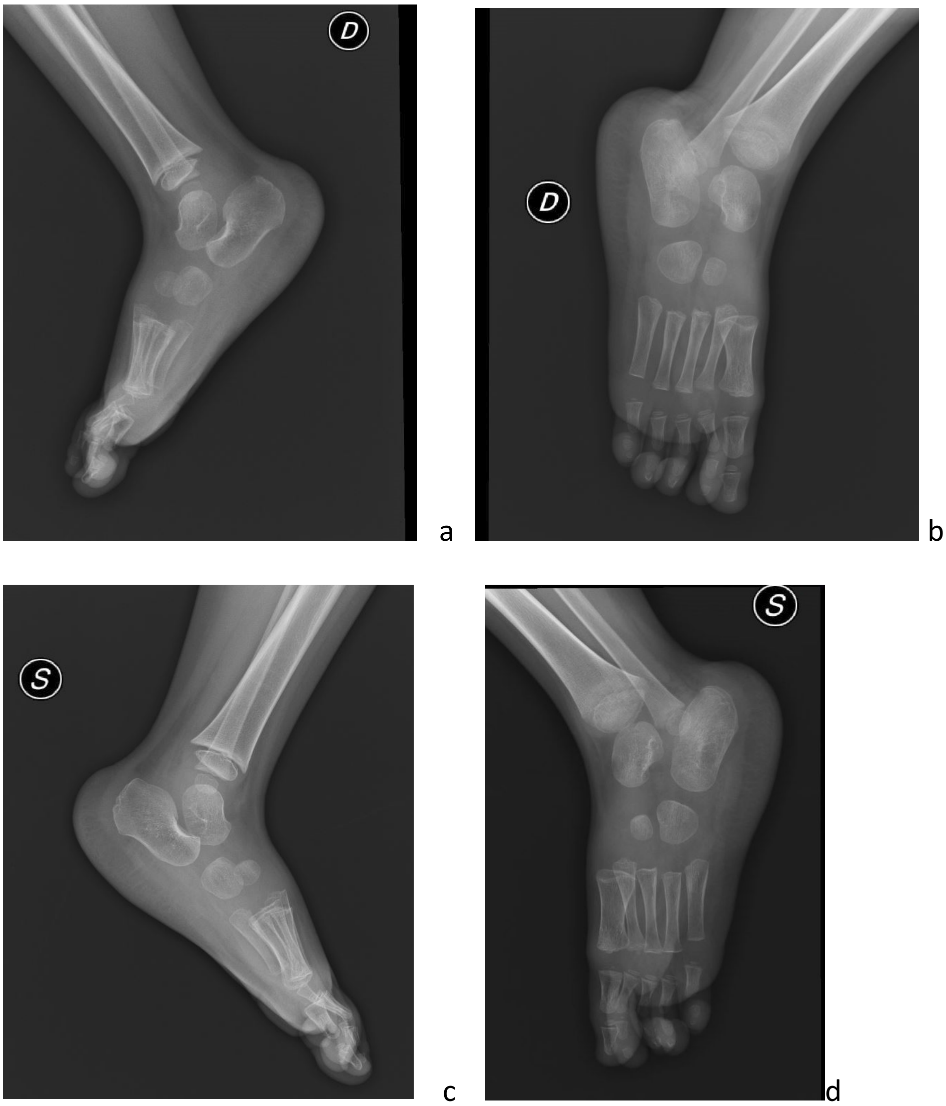

Medical report:

Bilateral talus study

RX-rays left foot

RX-rays right foot

No evident focal morphostructural alterations are observed in the investigated skeletal segments. Articular relationships are preserved. Class I dose according to Article 161, paragraph 6 of Legislative Decree 101/2020

Figure 22. Non-weight-bearing foot X-rays . 22.a-b right foot, 22.c-d left foot

Exploration in open kinetic chain

- Inspection:
    - Slightly dorsiflexed 2nd toe bilaterally.
- Palpation:
    - No asymmetry observed after pelvic thrust maneuver.
    - Hip: 70° left hip internal rotation, 65° right hip internal rotation.
    - Foot:
        - Silfverskiöld test: Negative.
        - Good range of motion in the bilateral ankle joint.
        - No pain on digital pressure of the Achilles tendon bilaterally.
        - No pain on digital pressure of the plantar fascia and heel bilaterally.
        - No pain on digital pressure of the sinus tarsi bilaterally.
        - No pain during mobilization of the subtalar joint, midtarsal joint, and Lisfranc joint.
        - No pain on digital pressure of the metatarsal heads.
        - No pain during finger mobilization.
- Muscle strength testing within normal limits.

Exploration in sitting position:

- W-sitting position.

Exploration in closed kinetic chain:

- Orthostasis (fig.23):

Figrue 23.a posterior view in RCSP, 23.b: dorsal view in RCSP, 23.c medial view in RCSP of the left foot, 23.d medial view in RCSP of the right foot

- Navicular drop: 1.7cm left, 2.2cm right
- RCSP 12° left , 13° right everted.
- Negative Jack test (fig.24)

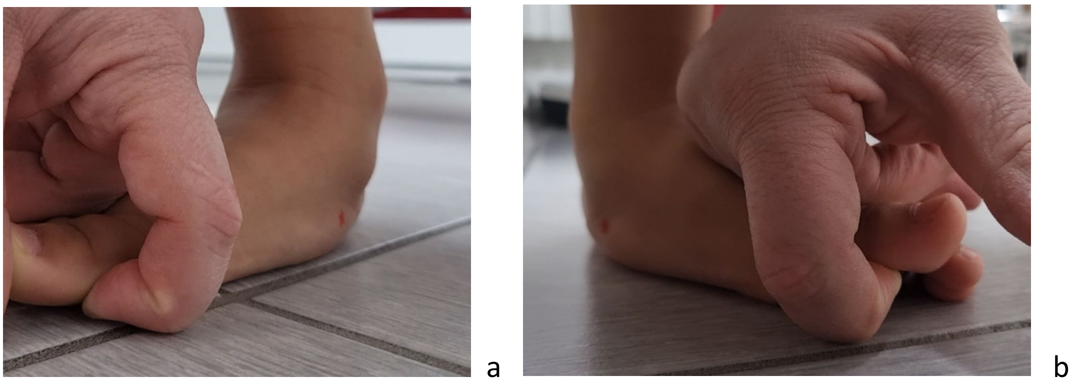

Figure 24 Negative jack test of the right (a) and left (b) foot

- Uncertain heel rise test.
- Severe supination resistance test bilaterally.
- Jumping on both feet performed.
- Jumping on one foot performed, but still uncertain.

- Reduced heel contact and increased midfoot contact (fig. 25)
- Foot Posture Index (FPI): Unchanged at 11 compared to previous assessment.

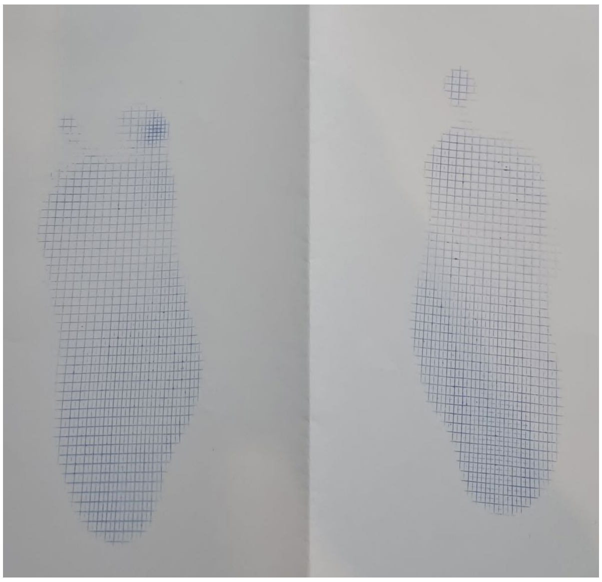

Figure 25. 2-dimensional imprint of the patient's plantar support made with an ink plantograph

Dynamics

- clumsy run
- Good coordination in ball-game
- Walking on the heels performed
- Walking on tiptoes performed (fig.26), the heel is not inverted and often give up by lay down the foot and close even more step angle

 a  b

Figure 26. a-b freeze frame posterior view of the patient's Walking on tiptoes performed

- Difficulty on walking on the external side, flexes knees and loses balance

Figure 27: freeze frame anterior view of difficulty in walking on the external side

- Walking on the sagittal plane during the second rocker shows inversion of the medial longitudinal arch curve.
- Walking on the frontal plane (fig. 28): Center-medial heel contact with slippage of the adipose pad under the lateral aspect of the heel.

 a  b

Figure 28: freeze frame of walking on the frontal plane. 28.a anterior view, 28.b posterior view

<u>Evaluation:</u>

Suspicion of vertical talus, worsening of gait.

<u>Proposed treatment:</u>

- Consult with a pediatrician for weight-bearing X-rays of both feet (AP and lateral projections) to study the talus.

- Continue with bilateral positional taping of the 2nd toe using kinesiotape.
- Use shoes with a square toe, laced, with a high and wide toe box, and strong and sturdy construction.
- At daycare, use closed shoes or non-slip socks, avoid slippers. Avoid sitting in a W position.
- Orthopedic evaluation of the foot.

<u>Observations:</u>

vertical talus is often associated with syndromes; however, during the assessment, the patient was cooperative, participating, answering questions, playing, and speaking simultaneously. They could count, and I did not detect any suspected additional cognitive deficits.

Weight-bearing X-rays are required. (fig.29)

<u>Telematic consultation</u>

Subsequently the mother sent the x-rays in charge

a

b

c

d

Figure 29 Weight-bearing X-rays: LL view of the right (a) and left (b) foot; AP view of the right (c) and left (d) foot

The patient was examined by 2 different pediatric orthopedic teams who confirmed the diagnosis of vertical talus, but did not assess the motor difficulties and limited themselves to indicating orthotics with medial vault support and then towards the age of 9 "we'll see" ...she is now awaiting a visit to the Rizzoli orthopedic institute in Bologna, where I was able to discuss the case and they will evaluate any procedures, they agree with me that this foot cannot tolerate medial vault support.

2.5 Clinical Case 3

<u>The reason for the visit</u>:

right heel pain (fig.30), especially during plantar flexion, limping, request for a biomechanical consultation while awaiting surgery


a


b

Figrue 30 a-b: site of pain indicated by the patient

<u>Anamnesis:</u>

female of 13 years old and 10 months, 60 kg weight, 168 cm height, foot size 40

Born of cesarean section childbirth two weeks in advance, born weight 3.220kg, 48 cm height

Less crawling, beginning of independent walking over the age of 13 months

Ankle instability in inversion, various diagnostic investigations, but no diagnosis made. On August 26, 2022, during vacation while playing in the water with an inflatable mattress, the patient experienced a strong pain in the right ankle. Subsequently, on the beach, they had pain and difficulty walking. At the local emergency department, the diagnosis was tendonitis. Upon returning from vacation, at the emergency department of the hospital in Monza, the diagnosis was osteochondritis dissecans of the talus (fig.31-32-33)

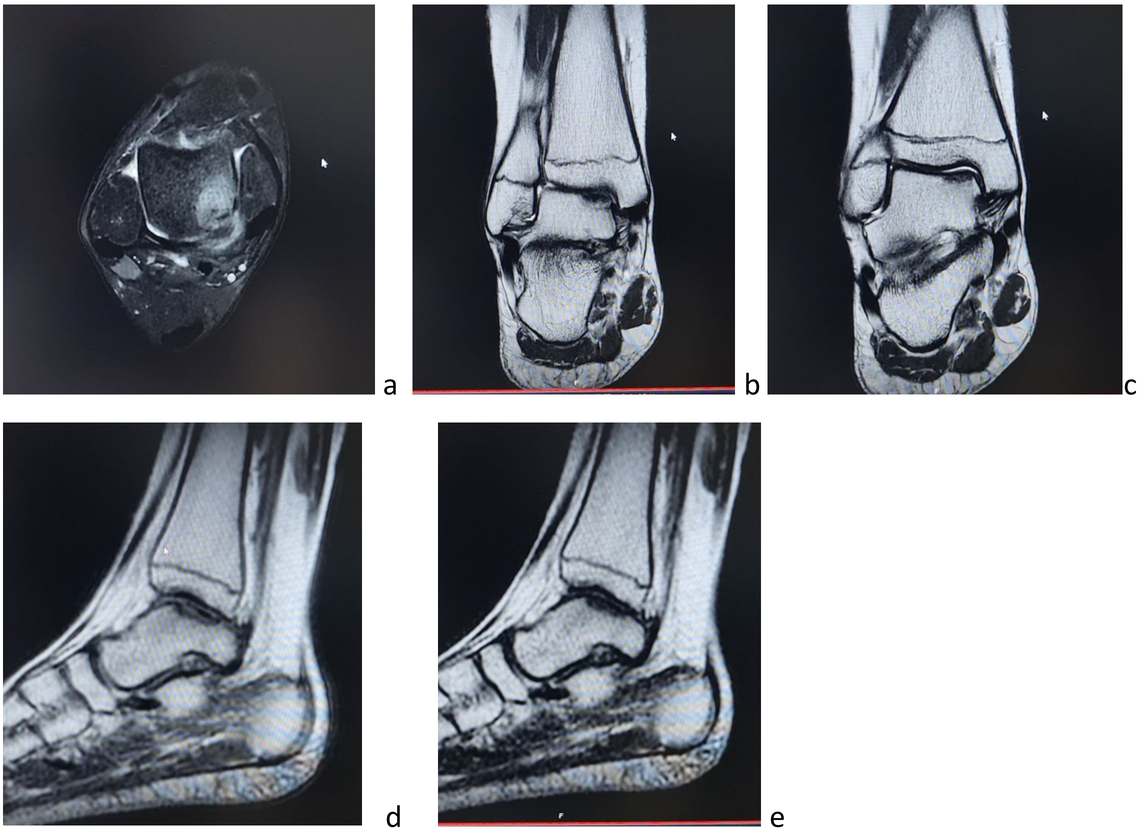

Figure 31: MRI. 31.a coronal view, 31.b-c frontal view, 31 d-e lateral view

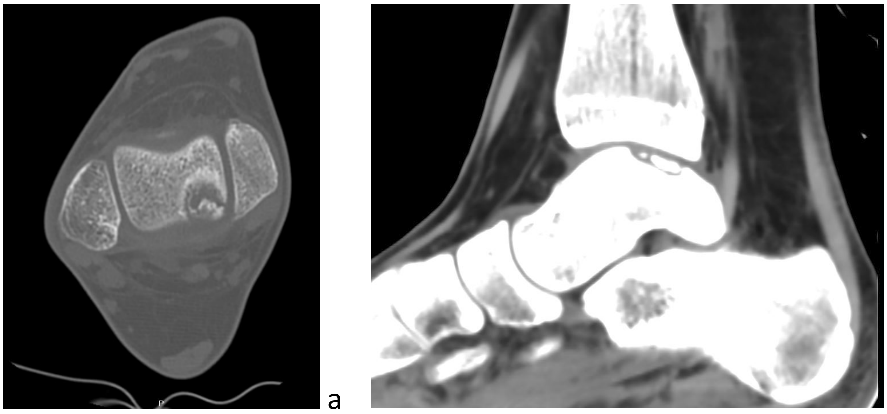

a b

Figure 32. CT. 32-a coronal view, 32-b lateral view

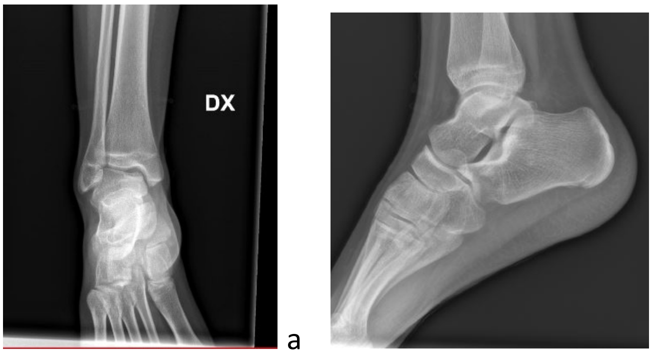

a b

Figure 33 Non-weight-bearing foot X-rays . 33-a anterior view, 32-b posterior view

Exploration at open kinetic chain

- Inspection:
    - nothing to report.
- Palpation
    - No noticeable asymmetries after pelvic thrust maneuver.
    - Knee: Intermalleolar distance approximately 8.5cm.
    - Foot:
        - Silfverskiöld test: reduced dorsiflexion at the talo-crural joint with the knee extended, recovers with knee flexed bilaterally.
        - No pain upon palpation of the Achilles tendon bilaterally.
        - No pain upon palpation of the plantar fascia and heel bilaterally.
        - Pain upon palpation of the medial and lateral talar sinus on the right side.

- No pain during mobilization of the subtalar, midtarsal, and Lisfranc joints.
- No pain upon palpation of the metatarsal heads.
- No pain during digit mobilization.

  - Muscle strength tests within normal limits.
  - Forefoot-rearfoot relationship: flexible forefoot valgus 6° on both sides.

Sitting position exploration:

  - Legs crossed.

Orthostasis (fig. 34)

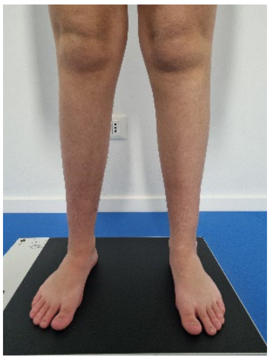 a  b

Figure 34.a anterior view in RCSP, 34.b: posterior view in RCSP

- Ligamentous laxity according to the Beighton score: 7 out of 9. (fig.35)

 a 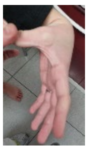 b

Figrue 35: ligamentous laxity of the hand

- Intermalleolar distance: 11cm.
- Navicular drop: 0.3cm on the left, -0.4cm on the right.
- RCSP: 5° of eversion on the left, 6° of eversion on the right.
- Maximal active pronation test: 2/3.
- Jack test positive.
- Heel raise test negative (fig.36) , painful at the right ankle when flexing the knee

Figure 36: freeze frame of heel raise test

- FPI (table 3) : 1left, 3 right

Table 3: Foot Posture Index of the clinical case 3

FPI					
Talar head palpation	talar head palpable on lateral side/but not on medial side	talar head palpable on lateral side/slightly palpable on medial side	talar head equally palpable on lateral and medial side	talar head palpable on medial side/slightly palpable on lateral side	talar head palpable on medial side/but not on lateral side
	-2	-1	0	1	2
right				1	
left			0		
Curves above and below lateral malleoli	curve below the malleolus either straight or convex	curve below the malleolus concave, but flatter/more shallow than curve above the malleolus	both infra and supra malleolar curves roughly equal	curve below the malleolus more concave, than curve above the malleolus	curve below malleolus markedly more concave, but than curve above the malleolus
	-2	-1	0	1	2
right			0		
left			0		
calcaneal inversion/eversion o	more than an estiamted 5°inverted (varus)	between vertical and an estimated 5° inverted (varus)	vertical	between vertical an estimated 5° evrted (valgus)	more than an estimated 5° everted (valgus)
	-2	-1	0	1	2
right					2
left				1	
Bulge in the region of talo-navicular jont	markedly concave	slightly, but definitely concave	area of TNJ flat	bulging slightly	bulging markedly
	-2	-1	0	1	2
right			0		
left			0		
medial arch height	arch high and acutely angled towards the posterior end of the medial arch	arch moderately high and slightly acute posteriorly	arch height normal and concentrically curved	arch lowered with some flattening in the central portion	arch very low with severe flattening in the central position - arch making ground contact
	-2	-1	0	1	2
right			0		
left			0		
abduction/adduction of the forefoot on rearfoot (too-many-toes)	no lateral toes visible. Medial toes clearly visible	medial toes clearly more visible than lateral	medial and lateral toes equally visible	lateral toes clearly more visible than medial	no medial toes visible. Lateral toes clearly visible
	-2	-1	0	1	2
right			0		
left			0		

<u>Dynamics (fig.37):</u>

1st rocker: Uncertain heel strike on the right side, with predominant inversion contact, but immediately followed by an excessive speed of pronation that extends into the 2nd rocker phase. On the left side, physiological heel contact with predominant supination loading on the left

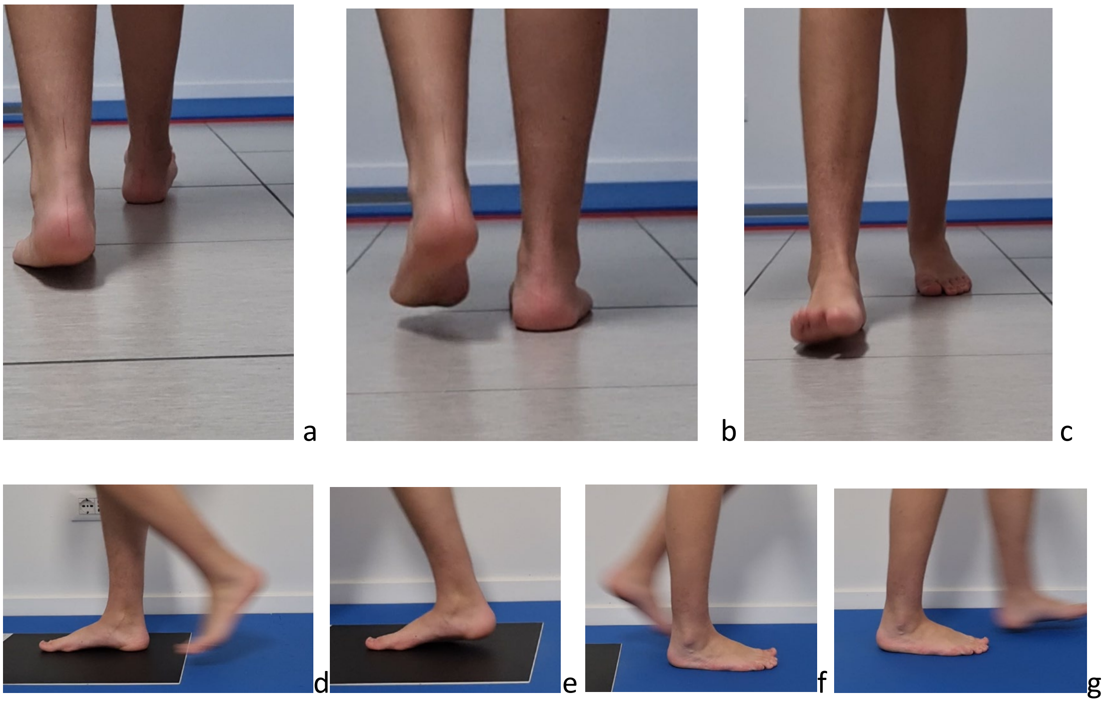

Figure 37: freeze frame of walking on the frontal plane (a-b anterior view) (c posterior view) and sagittal plane (d-e-f-g).

Evaluation:

large osteochondral lesion of the talus in the posterior-medial quadrant in a loose foot.

Proposed treatment:

awaiting biological reconstruction using the AMIC technique. Shoes with laces to be tied and untied, providing support around the heel.

Observations:

the patient's ligamentous laxity and recurrent ankle sprains during pediatric age may be the cause of the current problem. Since there was no specific trauma reported but repeated asymptomatic sprains, the osteochondral talus lesion may have been exacerbated by these continuous injuries on a foot with congenital ligamentous laxity and inadequate muscular control, especially considering that the patient has not engaged in sports activities for years

3 Seminars

3.1 SEMINAR Professor Liliana Avidos 06.2022

Professor Liliana Avidos held a seminar to discuss functional equinus of the tibiotalar joint and teach us about the exploration and treatment of a clinical case. In general, the joints that have greater movement in the sagittal plane are more involved in postural control. Firstly, it was explained what is meant by functional equinus of the tibiotalar joint, which refers to a tibiotalar joint in which the range of motion (ROM) in dorsiflexion is present but is not sufficient during closed kinetic chain activities. Functional equinus of the tibiotalar joint can be partially compensated. The Silfverskiöld test can be used to evaluate the end feel and determine if it is bony, soft, or elastic. In 2010, Bubckley proposed a classification for functional equinus of the tibiotalar joint: stage 1 with dorsiflexion ROM <10° without compensation, stage 2 with dorsiflexion ROM <5° with compensation. When a patient has biomechanical toe walking (TW), walking on tiptoes itself is already a compensation. Ground reaction forces (GRF) are very high at the forefoot during toe walking, inducing a dorsiflexor moment. During TW gait, only the forefoot rocker is present, there is an increase in cadence, monopodal support is reduced because the center of pressure (CoP) is already anterior, therefore the controlateral foot strike is anticipated, and the step becomes short and quick. The compensation of proximal or distal joints depends on anatomical morphology, functional activities, and joint mobility (the one with the greatest range of motion) and depends on the individual's constitution. Some equinus ankles compensate proximally with hyperextension or knee recurvatum. At a higher level, compensation can occur in the pelvis with flexion and anterior tilt, and finally, lumbar hyperlordosis with dorsal kyphosis. At the distal level, the main compensation comes from the dorsiflexion ROM of the midtarsal joint (MTJ) and the talonavicular joint (TNJ) (Arnow, Diaz-Doran, Sullivan et al., 2006). In these feet, plantarflexion of the talus is less than pronation, leading to subluxation of the TNJ and dorsiflexed TMTJ.

The three forms of manifestation of functional ankle equinus are:

1. non-significant compensation: deficit in heel strike, metatarsal overload, hopping gait

2. proximal compensation: knee recurvatum and pelvic flexion, lumbar hyperlordosis and dorsal kyphosis.

3. distal compensation: navicular-cuneiform dorsiflexion with midfoot hypermobility, abduction, signs of overpronation or flatfoot.

The causes of this problem include:

- anatomical anomaly of the soleus muscle in the myofibril: fewer sarcomeres, smaller elastic area.
- origin in the central nervous system (CNS): "more powerful flexor muscles, dependent on intrauterine position, less secure children have the stimulus to seek the safest position, the position of pregnancy, in these children, there is a greater voluntary flexor action" (hypothesis from an article).
- delay in corticospinal axis maturation.

It is essential to emphasize that functional equinus of the ankle is not a pathology but a dysfunction:

- the therapies to be adopted in childhood are diverse:
- muscle stretching.
- triceps inhibition with botulinum toxin (subtherapeutic dose to inhibit the response)
- Achilles tenoplasty
- Ankle-foot orthosis when it does not reach 90°
- Foot orthoses

Based on cost (not just economic) and risk/benefit. In the musculoskeletal view, the heel counter is considered negative, but from a neuromotor perspective, the heel counter is a positive stimulus because muscles are more relaxed when in contact with the heel, improving sensory input. Generally, a stiffer material is preferred for the heel counter, with EVA being the best option. In 2011, a study with gastrocnemius biopsy highlighted that excessive muscle effort in toe walking (TW) leads to permanent concentric shortening of the triceps.

Neuromotor concept:

- the somatosensory system (highly represented in the plantar aspect of the foot) is reduced when the foot is unloaded, compromising proprioception. As a result, there is no vestibular control of posture (oscillations in TW gait).

- The vestibular system (vestibulospinal) is highly represented in the heel. If there is no contact with the heel, the main stimulus is not active, leading to a greater feeling of insecurity and increased flexor muscle contraction. Stimulation of the somatosensory representation of the heel activates the antigravity muscles, leading to the inhibition of extensor muscles in TW gait.

From a therapeutic perspective, accommodating the heel by providing greater support leads to improved somatosensory activation, increased vestibular activation, enhanced antigravity muscle activity, resulting in a reduction of equinus and improved postural control.

Alongside TW gait with a definite neurological etiology, the term "idiopathic toe walking" is an umbrella term that includes all situations not attributable to a specific cause. The seminar allowed me to connect the theory of functional equinus with clinical realities observed during the internship, where there was a concomitant sensory deficit in children with hyperactivity, dyslexia, etc. This enables the clinician, when proposing a therapeutic protocol, to consider not only the biomechanical aspect but also the functionality of the ankle and the compensatory mechanisms created.

3.1.1 SEMINAR Professor Liliana Avidos 06.2022 – TIBIAL MORPHOLOGY

Professor Liliana Avidos conducted a seminar discussing tibial morphology and its influence on foot biomechanics. The degree of tibial inclination affects the bio and pathomechanics of the foot. However, literature supporting this is limited and mainly focused on femoro-tibial morphology and tibial inclination in the frontal plane. Deformity in the transverse plane, with femoral adduction, accompanies hip and tibial internal rotation. If the tibia does not follow the movement of the femur or viceversa, it can lead to trauma or subluxation. In the frontal plane, the femur and tibia can have distinct movements. Pure genu valgum (from coxa vara and femoral adduction) leads to increased load on the medial side, further away from the axis of the subtalar joint (STJ). If the weight force is further away from the ST axis, increasing the external moments of pronatory forces, there will be greater pronation, especially with the frontal plane component of eversion and increased Fick angle.

The physiological inclination of 4-6° varus of the tibia allows the heel to contact the ground during the first rocker phase while the pelvis is still in external rotation. This contact with the heel creates the first pronatory moment due to the ground reaction forces (GRF) on a rigid surface. However, on a soft surface, part of the force is absorbed, resulting in higher energy consumption and a lesser useful force component. The question often arises as to why pronation is so frequent. In the presence of an unyielding surface, the degree of pronation of the subtalar joint (ST) must compensate for at least 4-6° of tibial varus. If the tibia has greater varus, then the pronatory moment will be greater. This pronation of the ST joint requires internal rotation of the lower limb, resulting in knee valgus and lateral patellar overload, sometimes leading to lateral subluxation of the patella. During foot pronation, the varus tibia internally rotates due to the force vectors, resulting in compression. On the other hand, when the foot does not have a residual pronatory motion to compensate for tibial varus, the ground reaction forces (GRF) produce an external pronatory moment that generates eccentric flexor forces, leading to stress fractures of the tibia or medial tibial stress syndrome, for example. This behavior can also be explained through the piezoelectric effect of the bone: force on the bone generates a negative charge at the flexion point and a positive charge at the tension/stretching point. The negative charge leads to an osteoblastic reaction, while the positive charge leads to an osteoclastic reaction, resulting in fractures from lateral to medial.

The podiatrist can modulate the GRF through plantar orthotic therapy in such a way that it is varus-inducing before the navicular bone and then reduces.

3.2 Seminar: April 1st and 2nd, 2022 are the Catalan Podiatry Conference

I was offered the opportunity to attend the XXVI Catalan Scientific Conference on April 1st and 2nd, 2022 in Barcelona. On this occasion, there was an extensive session on pediatric foot conditions, with the participation of experts in the field of podopediatrics.

The main theme was digital deformities and their possible podiatric treatments. Another topic addressed was congenital clubfoot in the population of Sri Lanka. This presentation allowed me to expand my knowledge in this area, considering that with globalization, our podiatry clinics are becoming increasingly diverse and require a more global understanding of the incidence of certain pathologies within different ethnic groups.

4 TUTORIAL GUIDANCE

I conducted 7 official face-to-face tutorials and numerous tutorials via e-mail or online meetings, most of which helped me in the final stages of my internship to establish the methodology to follow for my final master's project. The tutorial guidance was provided by Professor Manuel Portela, Dr. Liliana Avidos, and Dr. Laura Pérez.

They were instrumental in helping me focus on the work and resolve any doubts that arose during its development. Communication with the tutors for supervision was both face-to-face and via email.

I would like to emphasize their availability and the support they provided during the planning and execution of the tutorials.

4.1 OTHER TRAINING ACTIVITIES:

During the completion of this Master's degree, I had the opportunity to participate in various training activities outside the university environment. I was involved in the TCIO Pediatric Osteopathy Master's program in Milan, which showcased interdisciplinary collaboration between pediatric osteopaths, neuro-psychomotor technicians specializing in developmental stages, and podiatrists. This opportunity enriched my knowledge in the field of pediatric osteopathy. In the spring of 2022 and subsequently in 2023, I had the opportunity to deliver oral presentations to podiatry students at the Medical-Technical School in Lugano on the podopediatrics module. I also attended a course by Dr. Sandra Lorenzi, a dermatologist, which included a session dedicated to nail pathologies in children. This course was an important source of enrichment in the field of pediatric dermatology. Finally, since the spring of 2023, I have been attending a pediatric orthopedics update course at the Rizzoli Hospital in Bologna. All these experiences have allowed me to enhance and explore pediatric podiatry from a broader perspective that extends to other areas.

5 Biomechanical foot assessment in pediatric patients post intervention with arthroscopic AMIC tecnique for osteochondral lesion.

Next, we are going to develop the theme chosen for carrying out the research work. In this case, the theme is the Biomechanical foot assessment in pediatric patients post intervention with arthroscopic AMIC tecnique for osteochondral lesion.

5.1 PUBLISHED LITERATURE REVIEW AND FUNDAMENTALS ON THE DISEASE STATUS OF OSTEOCHONDRAL LESIONS AND THERAPY/TREATMENT

The first historical description of ankle cartilage injury can be attributed to Monro in 1737, ((Monro A., 1737)), who described the removal of free osteochondral bodies of traumatic origin from the ankle. However, it was König ((Konig F., 1887)) in 1887 who first mentioned osteochondral defect of the talus, describing with the following words "osteochondritis dissecans" to refer to damage to the articular cartilage and subchondral bone of the femoral condyle, resulting in the formation of an intra-articular loose body. Subsequently, in 1922, Kappis (Kappis M., 1922) identified a similar lesion at the talus level using the same term, but it was only later that the term "osteochondritis dissecans of the talus" was replaced with "osteochondral lesion of the talar dome" (OLT) by Kouvalchouk and Watin Augouard. (Kouvalchouk JF, Schneider-Maunoury G, Rodineau J, Paszkowski A, 1990). Over time, various terms and definitions have been used, and until a few years ago, there was no consensus on the terminology to describe ankle cartilage injuries. The real problem lies in the poor quality of evidence from studies on the treatment of these lesions. Most studies have a level of evidence IV and short-term follow-up. For this reason, the International Consensus Meeting on Cartilage Repair of the Ankle was held in 2019, where the leading international experts in the field came together to define the appropriate terminology. The experts reached a consensus on the definition of several terms, and the one most relevant to this work is the definition of osteochondral lesion of the talus (OLT), which refers to the combination of both bone and chondral damage, involving both the cartilage and subchondral bone.

This injury is mainly caused by one or more traumatic events, however an idiopathic condition should exist too.

In the beginning the insufficiency consists only of cartilage damage caused by shear forces, with the subchondral bone intact. However, bone contusion as a result of high-impact forces can lead to a defect. Ankle injuries often result in osteochondral lesions with subchondral cysts. According to the International Consensus Meeting on Cartilage Repair of the Ankle (Murawski et al., 2022), subchondral cysts are deep lesions compared to the chondral surface and adjacent to the subchondral plate of the lesion. These subchondral cysts are characterized by their consistency, presence or absence of communication with the joint, depth/dimensions, presence or absence of a bony rim surrounding the cyst, and location. These cysts are often associated with persistent deep ankle pain, limiting ankle mobility.

OLTs are predominantly located in the anterolateral or posteromedial area of the talar dome. Normally, lateral OLTs are less deep, oval-shaped, and caused by shear forces. On the other hand, medial lesions are deeper, cup-shaped, and usually have an etiological mechanism consisting of torsional impact forces and axial load.

Even today, the scientific literature is still searching for better explanations of the etiology and prevention of these OLTs because it is still not understood why some progress to persistent pain and bone edema, while others remain asymptomatic and non-progressive. Understanding this mechanism more thoroughly will help prevent and reduce the management costs of this condition and allow for early detection. Too often, the clinical history of pediatric patients with OLTs presents a significant delay in diagnosis, as the pain and other symptoms are often mistaken for simple ankle sprains or alignment defects. As supported by podiatrist A. Evans (Evans, 2020), pain in pediatric patients should never be underestimated but requires the clinician's strong anamnestic skills and proper clinical reasoning to enable a rapid and effective functional assessment for appropriate therapeutic management.

In order to achieve this, it is essential to start with basic science and an understanding of the anatomical and biomechanical characteristics of the ankle.

5.1.1 ANATOMY AND BIOMECHANICS

The ankle joint, or tibio-talar joint (TTJ), is a congruent and dynamic joint composed of three bones (tibia, fibula, and talus), collateral ligaments, syndesmotic ligaments, and tendons of the surrounding muscles. This joint efficiently dissolves compression, shear, and rotational forces encountered during the gait cycle and adapts to body weight and ground reaction forces (GRF). The articular surface provides intrinsic stability under static conditions, while load and dynamic stability are ensured by ligaments and the balance of muscle forces.

From this, we can infer the mechanical efficiency of the ankle and its relative resistance to primary osteoarthritis. At the same time, we can evaluate any cartilage or ligament injuries, malalignments caused by trauma or inflammatory diseases, which can lead to joint degeneration.

Tibio-talar joint (TTJ) is composed of talus trochlea and talus joint with the tibial plafond, forming the upper part of the ankle joint. Medially, it articulates with the surface of the tibial malleolus, while laterally it articulates with the fibular malleolus. This configuration forms the articulation between the body of the talus and the tibiofibular mortise (Fig. 38).

Figure 38: anatomical formulation of TT joint

The malleoli's articular facets are parallel and correspond to the respective medial and lateral articular facets of the talus. From an anatomical point of view, the tibial plafond is concave in the anteroposterior direction, with a slight medial elevation in the proximal direction. This implies that the surface is slightly oblique from distal lateral to proximal medial, allowing for greater congruence with the trochlea of the talus. The angle between the longitudinal axis of the tibia and the tibial plafond is approximately 93° (with variations due to anatomical differences, such as females having a slightly lower inclination compared to males) (Inman VT, 1976). The tibial plafond is wider posteriorly, and sometimes the posterior margin articulates with the third malleolus, also known as Destot's malleolus (De Palma L, Santucci A, Falcioni D, 2014). A sagittal crest corresponding to the groove of the talus divides the tibial plafond into two convex surfaces in the transverse plane (Fig. 39).

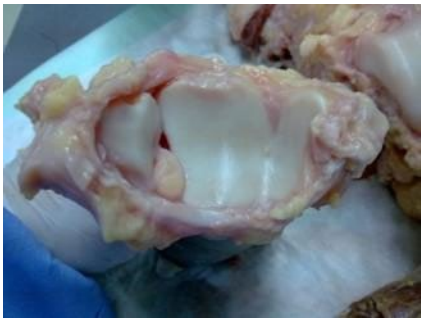

Figure 39: anatomical formulation of tibiofibular mortise

The tibiofibular mortise, also known as the bimalleolar fork, is stabilized by several ligaments, including the distal tibiofibular interosseous ligament (ITFL), the anterior inferior tibiofibular ligament (AITFL), the posterior inferior tibiofibular ligament (PITFL), the tibiofibular intermalleolar ligament (TFIL), and the tibiofibular transverse ligament (TFTL). These ligaments stabilize the tibiofibular syndesmosis, which influences the stability of the talus trochlea. Another crucial structure is the interosseous membrane, which stabilizes the tibiofibular joint by transmitting loads between the tibia and fibula. In fact, complete sectioning of the interosseous membrane reduces the load transferred to the fibula by 30% (Skraba JS, 1984; Vukicević S, Stern-Padovan R, Vukicević D, 1980). Membrane lesions larger than 5mm can create ankle instability in both the transverse and sagittal planes at the tibiofibular joint (Van den Bekerom MP, Mutsaerts EL, 2009).

The talus is composed of the head, neck, and body or dome (Hintermann B, 2005). The talus has a cone shape with a smaller medial radius and a larger lateral radius. The surface is wider anteriorly and concave in the transverse direction, divided into two asymmetric surfaces by a groove with an axis from postero-medial to antero-lateral, and convex in the antero-posterior direction. The medial and lateral margins converge asymmetrically into a narrow posterior process that in some cases can include the os trigonum. The medial articular facet has a comma-shaped form and is smaller in surface area compared to the circular-shaped lateral facet. The talar trochlea has a greater width anteriorly (28-32mm) than posteriorly (20-25mm). (fig.40)


Figure 40: anatomical formulation of talar dome

Biomechanical studies (Niladri Kumar Mahato, 2012) have shown that as the weight force on the upper surface of the talus increases, the medial inclination of the neck increases, and the talus "compresses." Despite being a bone with a small surface area, it is capable of accumulating and dissipating load equally, as supported by various authors (Niladri Kumar Mahato, 2012).

The stability of the ankle joint is determined by the articular geometry as well as the complex ligamentous and capsular structures of the ankle.

The ankle joint capsule (De Palma L, Santucci A, Falcioni D, 2014) attaches anteriorly at the neck of the talus and posteriorly at the transition point between hyaline cartilage and cortical bone. It is taut and thickened laterally and medially, while it is lax and thin anteriorly and posteriorly, with the presence of two recesses (anterior and posterior). The synovial membrane fully lines the joint capsule and is reinforced by the adjacent ligamentous structures, with no interruption, by the extensor, flexor, and peroneal tendon retinacula that originate fibrous expansions inserting into the joint capsule (Vega et al., 2020).

The stability of the ligamentous complex is provided by the medial collateral ligament, also known as the deltoid ligament, which has a triangular shape. The function of this medial complex is to stabilize the medial side and prevent valgus tilt of the talus and its external rotation. The anterior and posterior components limit the ventral and dorsal sliding of the talus (Hochschild J, 2003). In the literature, there are several anatomical descriptions of this ligamentous complex. The most recent proposal by Caine and Dalmau-Pastor (Cain & Dalmau-Pastor, 2021) in 2021 suggests that the ligamentous complex originates from the medial malleolus, particularly from the two colliculi (anterior and posterior) separated by an intercollicular groove, and inserts at the talus, calcaneus, and navicular bone in a delta-shaped pattern. The anatomical variations of this complex are infinite, and often the absence of a specific bundle results in intrinsic ankle instability. However, the main classification divides the complex into two layers: superficial and deep, separated by adipose tissue. The superficial layer has a fan-shaped and thin but extensive structure, while the deep layer is shorter and thicker. In detail, the superficial layer is composed of the following ligaments:

- Tibionavicular ligament (TNL)

- Posterior deep tibiotalar ligament (DPTTL)

- Tibiospring ligament (TSL)

There may be three additional ligaments that can vary: superficial anterior and posterior tibiotalar ligaments (ATTs-PTTs) and tibiocalcaneal ligament (TC).

In particular, the TN ligament originates from the anterior portion of the tibial colliculus and inserts on the dorsomedial surface of the navicular bone, with an oblique course in a plantar-anterior direction. It is the thinnest and longest ligament, located at the most anterior part of the superficial layer of the deltoid ligament.

The TS ligament also originates from the anterior portion of the tibial colliculus and inserts on the superomedial aspect of the spring ligament (also described as the tibio-ligamentous complex), providing medial stability along with the spring-deltoid complex. The PTTs-ATTs ligament originates from the posteromedial portion of the anterior colliculus and the medial surface of the posterior colliculus, inserting on the posteromedial tubercle of the talus.

The TC ligament originates from the medial portion of the anterior tibial colliculus and inserts on the medial border of the sustentaculum tali and the superomedial part of the spring ligament.

The deep layer consists of:

- Deep posterior tibiotalar ligament (PTTL)

- Deep anterior tibiotalar ligament (ATTL)

- Deep tibiocalcaneal ligament (TCL), which is not always present

The PTTp ligament originates from the intercollicular groove, anterior surface of the posterior colliculus, and the upper segment of the posterior surface of the anterior colliculus. It has an intra-articular band that inserts on the posteromedial tubercle of the talus and an extrasynovial band that inserts posteriorly on the talus.

The ATTp ligament originates from the tip of the anterior colliculus and the anterior part of the intercollicular groove, inserting on the medial surface of the talus distal to the anterior segment of the talus articular surface in a comma-shaped pattern.

While the superficial layer of the deltoid ligament provides resistance to talar tilt and external rotation, the deep layer stabilizes the TT joint against plantarflexion, preventing talar tilt in valgus and limiting external rotation.

This concept had already been supported in the past by Close et al. (CLOSE, 1956), and later Siegler et al. (Siegler S, Block J, 1988) highlighted the tibiospring ligament as being highly resistant to tensile force.

Several cadaver studies have provided more consistent and detailed descriptions of the ligament bundles. In a meta-analysis by Yammine K. (Yammine K, 2017), the prevalence of components of the deltoid ligament was highlighted, particularly the consistently present components of TN, TS, PTTp. Some peculiarities were also noted, such as TN being the longest and thinnest, TC being the thickest and providing stabilization in supination/inversion in case of lateral collateral ligament injuries, and PTTp being the shortest.

The vascular supply to the deltoid complex is provided by three extraosseous sources (Haynes JA, Gosselin M, Cusworth B, McCormick J, Johnson J, 2017): the medial tarsal artery, anterior tibial artery, and posterior tibial artery, as well as two intraosseous sources from the origin of the ligament at the medial malleolus to its insertion on the medial surface of the talus.

In summary, the medial ligament complex is an essential static stabilizer of the medial part of the ankle joint (TTJ), and its injury can lead to the displacement or tilting of the talus within the ankle mortise (CLOSE, 1956). Within the deltoid complex, the superficial layers provide resistance against external rotation and valgus stress of the ankle and hindfoot, while the deep layer resists ankle eversion and abduction of the talus (Boss AP, 2002). This is important during the gait cycle, as any injury to the deltoid complex affects not only the medial longitudinal arch but also the tibial rotation and foot inversion-eversion (Golano P, Farineas O, 2004; Grath GB, 1960; Vadell AM, 2012).

On the other hand, there is the lateral collateral ligament (Hochschild J, 2003), composed of three bundles: anterior talofibular ligament (ATFL), posterior talofibular ligament (PTFL), calcaneofibular ligament (CFL). The function of this ligament is to prevent excessive ankle inversion, and it is more prone to injury due to its anatomical weakness compared to the contralateral side.

The PTFL ligament is approximately 5-8 mm thick, 30 mm long, and 5 mm wide. It originates from the medial surface of the fibula and runs medially in a horizontal direction towards the posterior aspect of the talus. This ligament originates from the medial surface of the lateral malleolus from the lowermost segment of the digital fossa.

Due to the presence of multiple bundles, it does not insert into a specific area and runs horizontally across the lateral and posterior surfaces of the talus. The short transverse and intermediate fibers insert into the lateral surface of the talus in a groove along the postero-inferior border of the articular surface of the lateral malleolus, while the long fibers are directed postero-medially and insert into the posterior surface of the talus. The medial fibers insert into the postero-lateral tubercle, trigonal process, or os trigonum (if present) and contribute to the formation of the floor for the flexor hallucx longus groove (FHL).

The uppermost fibers of the posterior segment on the medial side are continuous with the superficial tibio-talar ligament, forming the posterior intermalleolar ligament. It is an intracapsular ligament but extrasynovial, well-vascularized by vessels from the fossa originating from the talus and the fibula.

The ATFL ligament originates from the anterior portion of the lateral malleolus, just lateral to the articular cartilage of the malleolus, and inserts distally to the articular surface of the talus. Its center is located 18mm proximal to the subtalar joint (ST). This ligament is flat, approximately 15-20mm long, 6-10mm wide, and 2mm thick, and can be considered an intra-articular ankle reinforcement. It runs medially to the fibula at an inclination of approximately 45° towards the talus in the transverse plane. Recent studies by Vega et al. (Vega et al., 2020) have shown that the ATFL ligament is divided into two bundles: the superior anterior talofibular ligament (ATFLs) and the inferior anterior talofibular ligament (ATFLi), separated by fibrofatty tissue and a small-diameter artery that runs through the gap. The ATFLs is an intra-articular ankle structure with a distinct origin from ATFLi, as it originates from the anterior surface of the fibula just above the insertion of the ATFLi bundle.

From its fibular insertion, with the ankle in a neutral position, the ATFLs bundle runs anteriorly and horizontally to attach to the neck of the talus, closing onto the articular surface of the talus dome. From dynamic observations, the ATFLs becomes lax with ankle dorsiflexion and taut with plantarflexion, resulting in an increased median distance between the insertions in plantarflexion compared to dorsiflexion (Vega et al., 2020).

The ATFLi bundle is extra-articular, closely related to the lateral part of the capsule of the ST joint, of which its insertion area is found to be a part. The ATFLi and CFL ligament share a fibular origin located on the anterior part of the malleolus, proximal to the tip of the fibula, and just below the fibular insertion of the ATFLs. From this common origin point, the ATFLi runs parallel to the ATFLs and extends anteriorly towards the neck of the talus, just below the insertion of the ATLFs. The distance between the insertions of ATFLi remains unchanged during ankle movements as it is an isometric ligament. The ATFLi and CFL ligament are connected by arcuate fibers that join the lower border of ATFLi and the anterior border of CFL. The arcuate fibers originating from the ATFLi and the lateral part of the talus are directed posteriorly and distally, forming an arc to unite the anterior border of the CFL ligament and the lateral part of the calcaneus, thereby creating an intrinsic reinforcement to the joint capsule of the ST joint (Golano P, Vega J, de Leeuw PA, Malagelada F, Manzanares MC, Götzens V, van Dijk CN, 2010).

The CF ligament has a cylindrical shape, is deep to the peroneal tendons, located beneath the tendon sheath, and superficial to the joint capsule. The CF ligament is 2.5 times stronger than the ATFL ligament, approximately 20-30mm long, 4-8mm wide, and 3-5mm thick. It originates from the anterior border of the fibula, just below the ATFL ligament, and inserts onto the small tubercle located posteriorly to the lateral surface of the calcaneus. It is a biarticular ligament, as it allows for movements of dorsiflexion/plantarflexion and inversion/eversion and contains fibers of the talocalcaneal ligaments.

With the ankle in a neutral position and from its fibular origin, the CF ligament runs obliquely plantarly and posteriorly to insert onto the posterior aspect of the lateral surface of the calcaneus. The CF ligament becomes horizontal in plantarflexion and vertical in dorsiflexion without any change in length between these two positions (Vega et al., 2020). The position of the talus changes the angle between the CF ligament and the longitudinal axis of the fibula: it becomes lax in valgus and taut in varus, which explains its injuries even in the absence of dorsiflexion movement of the TTJ joint (Vega et al., 2020). With the study by Vega et al. (Vega et al., 2020), the term lateral fibulotalocalcaneal ligament complex was introduced, precisely because of its anatomical and functional connection. This complex also clinically explains those traumas that create microinstability (another term introduced by the authors, Vega et al., 2020), caused by the isolated trauma of the ATFLs, which could progress to chronic instability following repeated traumas, involving the ATFLi and/or occasionally the CF ligament.

Therefore, we can summarize the behavior of the ligaments in the lateral compartment in relation to the movement of the TTJ joint in the following table (Table 4).

TTJ	Dorsiflexion	Neutral	Plantarflexion
ATF - higher - lower	 SLACK TENSE	HORIZONTAL	 TENSE SLACK
PTF	max TENSE	SLACK	SLACK
CF	TENSE (VERTICAL)	TENSE (OBLIQUE)	TENSE (HORIZONTAL)

Table 4. Summarized table of ligaments' behavior in the lateral compartment, related to the movement of the TTJ joint.

According to Johnson and Marklof (1983) (Johnson EE, 1983), most of the changes in the ligaments occur in plantarflexion. According to Hollis et al. (1995) (Hollis JM, Blaiser RD, 1995), inversion and dorsiflexion movements increase when the CF and ATF ligaments are sectioned.

The intermalleolar ligament (IM) has four bundles: one at the tibial level, one at the medial process of the talus, one at the lateral process of the talus, and one that runs in the tarsal direction, at the level of the tarsal tunnel in the septum separating the posterior tibial tendon from the flexor digitorum longus. During plantarflexion, the IM ligament becomes less tense and approaches the transverse ligament. This IM ligament can cause posterior impingement, highlighting its important posterior stabilization of the ankle.

According to the meta-analysis by Yammine K. (Yammine K, 2017), the anterior and posterior tibiofibular ligaments control the movement of the fibula relative to the tibia within the syndesmosis. The deltoid ligament has anterior bundles with reduced stiffness compared to the posterior bundles and is involved later in the containment of excessive rotation of the ST joint. The TN ligament contributes to the high degree of freedom of movement along with the shape of the articular surfaces. The lateral compartment, specifically the ATF ligament, shows an increase in tensile strength during loaded ankle movement and contains the talus in plantarflexion. From the meta-analysis (Yammine K, 2017), it is evident that the deltoid ligament can be injured in traumatic movements such as ankle eversion, but also in ankle inversion associated with significant tibial external rotation. Therefore, the deltoid ligament not only stabilizes the medial compartment but also contributes to the stabilization of the lateral compartment.

Some authors (De Palma L, Santucci A, Falcioni D, 2014) include the lower tibiofibular joint, i.e., the distal joint between the tibia and fibula, in the ankle joint complex. It is an amphiarthrosis, not covered by hyaline cartilage, consisting of the articular surface of the tibia and fibula, a fibrous capsule, and the anterior, posterior, and interosseous tibiofibular ligaments. The tibial articular surface, or fibular notch, has a truncated triangular shape proximally and is concave antero-posteriorly, while the fibular surface is convex and complementary to the tibial surface, with dense connective tissue anteriorly and partly fibro-adipose tissue posteriorly. Proximally, the lower tibiofibular joint articulates with the distal part of the interosseous membrane and distally with the talotibiofibular joint. There is a small synovial recess that originates from the TTJ joint, extending a few millimeters between the articular surfaces, and occasionally there may be cartilage covering in this area. This synovial recess extends anteroposteriorly for 10-15mm, approximately 2mm wide, and 4-25mm high (De Palma L, Santucci A, Falcioni D, 2014). This joint has a significantly reduced range of motion, and the only movement is the transverse displacement of the fibula, which can move closer to or away from the tibia during dorsiflexion/plantarflexion of the TTJ joint, allowing constant adherence and congruity of the bimalleolar clamp to the talus trochlea, aided by the distal tibiofibular ligaments.

The anterior tibiofibular ligament (ATFL) (Kelikian AS, 2011) is a flat fibrous sheet that originates from the longitudinal tubercle of the anterior border of the fibular malleolus in front of the upper segment of the talus articular surface and the lower segment of the anterior border of the fibular diaphysis. The fibers are directed upward and medially and insert onto the anterolateral tubercle of the tibia; some reach the anterior surface of the distal tibia. The ATFL can be divided into two or three bands and may be multifascicular. It is supplied by vessels from the peroneal artery.

The posterior tibiofibular ligament (PTFL) (Kelikian AS, 2011) has two components: superficial and deep.

The superficial component of the PTFL originates from the posterior margin of the tubercle above the digital fossa of the lateral malleolus and extends distally to the upper part of the posterior margin of the fossa and proximally to the ridge that separates the lateral and medial surfaces of the fibula posteriorly. The fibers are directed upward and medially, and the main insertion is on the posterolateral tibial tubercle. The remaining fibers continue their course and insert onto the distal tibia and may reach the lateral border of the groove for the posterior tibial tendon. The deep component is the transverse ligament. This ligament is thick, strong, and conoid in shape with a twist in its fibers. It originates from the posterior fibular tubercle located above the fossa and the upper segment of the fossa. The fibers are directed upward, medially, and posteriorly. At the posterior margin of the tibial articular surface, the fibers change direction and become horizontal or transverse. This ligament inserts into the lower part of the posterior margin of the tibial articular surface and reaches the medial margin of the tibial malleolus, providing the strongest attachment. The transverse ligament descends below the posterior tibial margin and forms a true posterior lip that deepens the tibial articular surface. The posterior half of the medial surface of the lateral malleolus lacks an articular surface but is filled by the transverse ligament, which makes contact with the surface of the talus and leaves its imprint as a triangular smoothed facet on the posterior half of the lateral edge of the superior talus surface.

The interosseous ligament (Kelikian AS, 2011) is a reddish ligament composed of a dense mass of short fibers mixed with adipose tissue and vessels. These fibers form an arch over the underlying synovial recess and may be perforated in some specimens. The ligament originates from the anterior-inferior triangular segment of the medial aspect of the distal fibular diaphysis. This area of origin is higher anteriorly and lower posteriorly, and the fibers insert onto a similar corresponding area on the lateral surface of the distal tibia. The fibula is in contact with the tibia only through a tiny crescent-shaped articular surface lined with cartilage, which is continuous with the articular surface of the lateral malleolus. A semilunar cavity is present above this tibiofibular interline and is proximally bounded by the concave base of the interosseous ligament. The anterior segment of the cavity corresponds to the synovial recess previously described, communicating with the ankle joint through the linear opening. This synovial recess is approximately 1cm high. The posterior part of the semilunar cavity is smaller and occupied by a reddish synovial fringe that originates only from the fibular surface and descends into the ankle joint between the fibula and the lateral surface of the talus. In dorsiflexion, the synovial fringe withdraws into the cavity, while in plantarflexion, it descends into the TTJ joint.

The interosseous membrane is continuous with the apex of the interosseous ligament. The anterior fibers are oblique, directed downward and laterally, while the posterior fibers are almost vertical.

5.1.2 BIOMECHANICS

The ankle, apparently, could be described as a biomechanically simple joint since it is a hinge joint with cylindrical articulating surfaces, one concave and the other convex, providing good congruence and allowing wide angular movements. (Root M, Orien WP, 2001)

Several authors have studied the biomechanics of the ankle joint (TTJ) since the 1950s. Close and Iman (Close JR, 1952) described the TTJ as a cone-shaped joint with its apex directed medially and having a single fixed axis of motion with one degree of freedom. Later, Barnett, Napiere, and Hicks described three distinct axes based on the curvature of the trochlea talus of the TTJ (Barnett C, 1952). This finding contradicted the previous explanation as it did not account for the translation that the tibia undergoes at the level of the trochlea talus. In 1976, Inman (Inman VT, 1976) described a single axis of motion located on the transverse plane passing through the centers of the malleoli. It subtends an angle of 20-30° with the knee axis and 84° with the foot axis on the transverse plane. On the frontal plane, it forms an 80° angle with the longitudinal axis of the tibia. This concept was maintained until 1977 when Root et al. (Root M, Orien WP, 2001) described a triplanar axis with one degree of freedom, directed from posterior-lateral-plantar to anterior-medial-dorsal, inclined 8-12° on the transverse plane and 12-18° on the frontal plane. This results in a triplanar motion of pronation-supination, with the sagittal plane motion of dorsiflexion-plantarflexion being predominant. Several authors continued the research to find the best description of the ankle joint's movement and axis, leading to the four-bar linkage model proposed by the Bolognese school (Leardini A, O'Connor JJ, Catani F, 1999; Leardini A, O'Connor JJ, 2014).

The described model includes two functional units, tibiofibular mortise and talus-calcaneus, rotating relative to each other through inextensible linear segments without resistance, represented by ligaments CFL and TCL. The four-bar linkage scheme involves: 1. The ligament CFL (segment AB), 2. The ligament TCL (segment CD), both without resistance. The line connecting the distal insertions of the ligaments CFL and TCL (segment BC) stabilizes the ankle's plantarflexion-dorsiflexion motion through bars 1 and 2, while bars 3 and 4 create a shifting motion of the axis. This better accounts for the possibility of tibia or talus, in OKC or CKC, sliding on each other. The motion between the polycentric and polyaxial trochlea is defined by a combination of rolling and sliding movements, with rotation determined by the more anterior fibers of the ligaments TFL and CFL. Leardini et al. (Leardini A, O'Connor JJ, Catani F, 1999) pointed out that during sagittal plane motion, the fibers of the ligaments TFL and CFL are isometric. As a result, the instantaneous center of rotation shifts from posterior-inferior to anterior-superior. Moreover, anatomical studies by Sarrafian (Kelikian AS, 2011) suggest that the tibia only covers 2/3 of the talus trochlea in any position, making the ankle joint poorly congruent and rotating around a variable center of rotation. Consequently, we can conclude that the TT joint has a dorsiflexion-plantarflexion motion combined with sliding, resulting in a triplanar motion with a predominance in the sagittal plane.

Clinically, the minimum range of motion of the ankle joint is important in adults, which on average varies from 10° of dorsiflexion to 15° of plantarflexion (Hintermann B, 2005) with the knee extended, the Subtalar joint (STJ) in a neutral position, and the midtarsal joint (MJ) at the end of pronation on the longitudinal axis (LMJA). The minimum 10° of dorsiflexion is necessary during the second rocker phase of the gait cycle to allow the tibiofibular mortise to advance by sliding on the trochlea talus; otherwise, compensatory actions such as excessive pronation or early heel lift occur to compensate for the lack of passive dorsiflexion in the TT joint. During the first rocker phase, approximately 20° of plantarflexion is required to allow the heel contact and forefoot loading, and during the third rocker phase to enable the foot to lift off the ground (Perry J, 2010; Valmassy RL, 1996). Several studies have demonstrated the ROM of the TT joint, summarized as an average of 35° of plantarflexion and 26.5° of dorsiflexion, while information on other planes of movement is limited and not recent, as these studies do not specify if the motion is isolated to the TT joint or includes other articulations.

Factors influencing the ROM of the TT joint include age, which reduces ROM as one gets older, and sex, as there is a reduction in dorsiflexion in females and a reduction in plantarflexion in males (Hintermann B, 2005; Root M, Orien WP, 2001). Anatomically, bony blocks occur due to contact between the posterior tubercle of the talus and the posterior margin of the tibia, limiting plantarflexion, while contact between the anterior portion of the trochlea talus and the distal surfaces of the tibia and fibula restricts dorsiflexion. Additionally, tension from the ATFL ligament and the anterior fibers of the deltoid ligaments (TN, TS, ATTs-PTTs) limits plantarflexion, while the posterior portion of the deltoid ligament and the PTF ligament limit dorsiflexion. Muscular factors also influence the ROM, as tension from extensor muscles limits plantarflexion, while tension from the triceps sural limits dorsiflexion (Valmassy RL, 1996).

The ROM of the TT joint should be distinguished between the situation of Open Kinetic Chain (OKC), where dorsiflexion of the TT joint is accompanied by foot abduction and eversion, and plantarflexion is associated with foot adduction and inversion, and the situation of Closed Kinetic chain (CKC), where dorsiflexion of the TT joint is accompanied by leg intrarotation and foot abduction, and plantarflexion is associated with leg extrarotation and foot adduction (Hintermann B, 2005; Valderrabano V, Hintermann B, Nigg BM, Stefanyshyn D, 2003; Valmassy RL, 1996).

The stability and integrity of the ankle joint are provided by soft tissues and the geometry of the joint surfaces, contributing to 30% of rotational stability and 100% of inversion/eversion stability (De Palma L, Santucci A, Falcioni D, 2014). Otherwise, situations of overload may occur, leading to potential cartilage and joint damage. The anteroposterior stability of the ankle during the gait cycle and its resistance to shear forces are due to the bony constraint and ligament complex. Some authors have demonstrated that during weight-bearing in the gait cycle, the TT joint undergoes anteroposterior shear forces equivalent to 70% of body weight (De Palma L, Santucci A, Falcioni D, 2014).

The resistance to compressive forces is directly related to the subchondral bone tissue of the tibia and talus. Some studies have shown that removing the subchondral plate reduces tibial compressive force resistance by 30-50%, and if further sections are made more proximally, this reduction can increase up to 90%. On the other hand, the talus seems to have higher resistance due to the presence of trabecular lines near the upper cortex of the talar neck. However, removing this part increases stress on the talus spongy bone significantly (De Palma L, Santucci A, Falcioni D, 2014). The area of highest tibial force is located in the posteromedial zone, which acts as a pivot, whereas the risk of overload occurs more commonly in the anteromedial zone, which is less robust. The forces transmitted to the distal tibia are eccentric and distributed along the cortical rim, with over 90% of the force being absorbed within the distal tibial cortex. A normal ankle has a contact surface of approximately $12cm^2$, with the tibiotalar contact area (a) representing about $7cm^2$ and the mediolateral contact areas (b) about $5cm^2$. The contact surface increases from plantarflexion to dorsiflexion, while forces decrease proportionally. The medial and lateral malleolar facets have more contact during dorsiflexion.

In the clinical evaluation of ankle mobility in OKC, the Silfverskiöld test (Silfverskiöld N, 1924) is performed. The patient is in a supine position, and the tested leg is flexed at the hip and knee. The degree of dorsiflexion is measured with the knee extended and then with the knee flexed, applying moderate pressure from below. The point of pressure application is at the level of the second metatarsal (M2) but can be applied to the entire forefoot. According to the author, gastrocnemius limitation occurs when dorsiflexion is negative or equal to 0° with the knee extended or when it normalizes with knee flexion with a minimum difference of 13°. Root (Root M, Orien WP, 2001) later specified that during dorsiflexion in the Silfverskiöld test, it is necessary to maintain the subtalar joint in a neutral position and the midtarsal joint at the end of pronation on the longitudinal axis (LMJM) to avoid false dorsiflexion due to subtalar and midtarsal pronation. According to Root (Root M, Orien WP, 2001), the test starts with dorsiflexion with the knee extended, and if the minimum 10° is not achieved, the knee is flexed while keeping the subtalar joint in a neutral position. The TT joint is pushed into dorsiflexion until the first resistance is felt, and normally, at least 10° is required. If, with the knee extended, the TT joint does not achieve these degrees of dorsiflexion, and it recovers movement with knee flexion, it indicates limitation due to the gastrocnemius muscle. If it does not recover with knee flexion, it might be the soleus muscle, and tension may be appreciated on the Achilles tendon or there may be a bone joint blockage.

Plantarflexion of the TT joint is measured in the same way, taking care to avoid supination of the subtalar joint.

Another important test for clinical evaluation of the TT joint in CKC is the Lunge test. The patient stands in an upright position with the calcaneus in a neutral position (NCSP) facing a wall. The patient is asked to step forward with one foot approximately 10 cm from the wall and flex the knee to bring it closer to the wall without lifting the heel off the ground, performing a lunge. The maximum distance between the foot and the wall without lifting the heel off the ground is measured, or an inclinometer is placed on the tibial tuberosity or 15 cm distal to the tibial tuberosity. In the Lunge test, a distance of less than 10cm or a tibial angle lower than 35-38° indicates a reduced ROM of the TT joint in dorsiflexion. This test is found to be repeatable with insignificant error (Silfverskiöld N, 1924).

5.1.3 ANKLE BIOMECHANICS IN THE GAIT CYCLE

The function of the foot is not only static but mainly dynamic, particularly during the gait cycle, which consists of a stance phase and a swing phase. The stance phase, comprising approximately 60% of the gait cycle, is divided into three subphases: the heel contact phase or heel rocker (about 15% of the stance phase), the midstance phase or ankle rocker (about 20% of the stance phase), and the propulsion phase or forefoot rocker (about 20% of the stance phase). More recently, J. Perry (Perry J, 2010) introduced the 4th rocker, or toe rocker, representing about 5% of the stance phase.

1st Rocker (or heel rocker): During the heel rocker phase, the foot and lower extremity act as accommodators/absorbers, needing to absorb the peak of the ground reaction force (GRF). To achieve this, certain conditions must occur: specifically, the lower extremity must internally rotate, the ankle joint contacts the ground in a neutral position with approximately 2-3° of plantarflexion, allowing the foot to make contact and aiding force absorption along with the knee. The TT joint gradually plantarflexes, controlled by the muscles in the anterior compartment, to allow the forefoot to contact the ground. The Subtalar joint contacts the ground in slight supination before pronating subsequently, and the Midtarsal joint (MTJ) must invert to enable forefoot contact from lateral to medial. The pronation of the STJ joint must be controlled through the activation of the Posterior Tibialis (PT), the Soleus muscle, and finally the Flexor Hallucis Longus (FHL), together with the Flexor Digitorum Longus (FDL) and gastrocnemius muscles, which decelerate the internal rotation of the limb. The first Metatarsophalangeal joint (MTP) dorsiflexes by about 25° to avoid tripping with the big toe, thanks to the activity of the pretibial muscles (Extensor Hallucis Longus and Extensor Digitorum Longus, which are already active), while the MTPJ1 is plantarflexed by about 10° (M1). This dorsiflexion of MTPJ1 tension the plantar fascia and raises the longitudinal arch, promoting foot contact with the inverted calcaneus. The foot, during this rocker, prepares to bear the body's weight, and the medial longitudinal arch lowers, allowing MTPJ1 to plantarflex and generate the inverse Windlass mechanism (through eccentric activity of the Tibialis Anterior and Extensor Hallucis Longus muscles).

2nd Rocker:

In the 2nd rocker, or ankle rocker, the foot is in a single-limb support position, serving as a rigid lever to stabilize the forefoot on the ground, allowing it to bear the entire body weight. (Fig. 41)

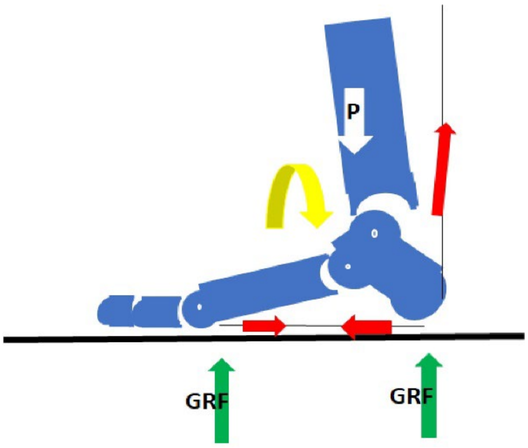

Figure 41: Diagram of forces during the midstance phase; the tension of the plantar fascia is highlighted in red below, and the tension of the Achilles tendon is shown above; the vertical component of the ground reaction force (GRF) is indicated, with maximum peaks on the heel and metatarsal heads.

The vertical component of the GRF decreases to about 75% of body weight and then increases again before the heel lifts off the ground. During this phase, the lower limb externally rotates, and the TT joint must passively dorsiflex by a minimum of 10°, preparing for the heel lift, which occurs around 35% of the stance phase. Often, the heel lift is anticipated, resulting in an extended time for the 3rd and 4th rockers. During this rocker, the soleus muscle functions eccentrically, storing energy. Simultaneously, the ST joint, starting from its maximal pronation position, must supinate to return to a neutral position at the end of this phase. The Achilles tendon begins to exert tension through the active contraction of the gastrocnemius and soleus muscles, which decelerate the anterior inertia of the leg and induce a significant moment of dorsiflexion on the MT joint.

At the same time, the plantar fascia, the short and long plantar ligaments, and the spring ligament produce a plantarflexion moment on the MT joint, increasing the longitudinal arch to counterbalance the dorsiflexion moments. This is achieved in association with the activation of the PT, FHL, FDL, and PL muscles, as well as the intrinsic foot muscles that adjust their tension based on demand. In this way, the MT joint is in sagittal plane equilibrium and can support the body weight. It is also supported by the "locking wedge" effect, achieved through compressive forces that sustain the load, along with the calcaneo-cuboid block and the inverse windlass mechanism.

The stabilization of the bones in the midfoot also occurs in the transverse plane, and it is achieved through the balance between the abductor force of the PL muscle and the adductor force of the PT muscle. During the second half of the midstance phase, the intrinsic muscles produce tension necessary for reciprocal stabilization of the metatarsal and midtarsal bones in the transverse and posterior planes.

In the ankle rocker, the stabilization of the first metatarsophalangeal joint (MTPJ1) is crucial since it is a necessary condition for normal propulsion before toe stabilization. The physiological stabilization of MTPJ1 requires a supinated position of the foot, a formula of "index minus," so that the base of M1 and the cuneiform can be positioned higher than the cuboid, allowing the PL muscle to exert a plantarflexion moment to stabilize the base of MTPJ1 against the ground reaction forces directed on the head of M1. During this phase, MTPJ1 moves from a neutral position to dorsiflexion of 21° during heel lift.

3rd Rocker:

During the 3rd rocker, or forefoot rocker, the leg continues to externally rotate, preparing for the weight transfer to the contralateral foot. The vertical component of the ground reaction force (GRF) reaches its peak, and the weight supported by the foot increases to about 125% of body weight. This peak is supported solely by the forefoot and toes, as the heel is lifted off the ground. The body weight is also shifted from the lateral side of the forefoot to the medial side. Once the heel is lifted, the weight is fully supported by the head of the fifth metatarsal (M5). Subsequently, the heads of the central metatarsals (M2-M3), along with the first toe, bear the majority of the body weight, shifting medially due to the action of the Peroneus Longus (PL) and Peroneus Brevis (PB) muscles. Finally, the weight is transferred to the contralateral foot with the final toe-off.

When the vertical projection of the body's center is over the metatarsal heads, the heel lifts off the ground. In this phase, the rounded profile of the metatarsal heads acts as a forefoot rocker, and the anatomical structure of the metatarsal heads facilitates rolling and allows the metatarsophalangeal joints to transition from an almost parallel position to the ground to a vertical position. The progression of the gait accelerates as the body's weight falls beyond the area of foot support. This is the moment when the greatest propulsive force is developed during the gait cycle. (Fig. 42)

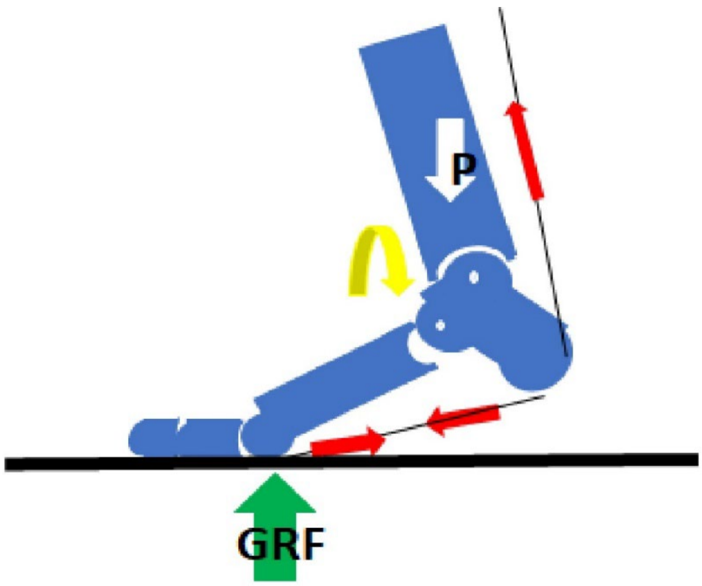

Figure 42: Diagram of forces during the propulsion phase; the tension of the plantar fascia is highlighted in red at the bottom, and the tension of the Achilles tendon is highlighted at the top. Additionally, the body weight corresponding to the ground reaction force (GRF) peak on the heel and metatarsal heads is indicated.

At heel lift-off, there is a sudden plantarflexion of the ankle (TTJ) of approximately 20°. This ankle unlocking serves to transfer the energy that was eccentrically accumulated in the triceps, allowing the limb to advance.

During heel lift-off, the forefoot must be stable on the ground, and the transverse head of the adductor hallucis muscle must activate to prevent the widening of the metatarsal fan caused by vertical, tensional, and shearing forces. At this moment, the foot must be in a supinated position, which, together with the passive windlass mechanism activated by the passive dorsiflexion of the first metatarsophalangeal joint (MTPJ1), promotes forefoot stability. Therefore, proper functioning of the MTPJ1 is necessary because, during the propulsion phase, the metatarsal continues to plantarflex, shifting the axis of rotation of the MTPJ1 dorsally and posteriorly, allowing P1 to slide over the head of M1 to achieve the required degrees of dorsiflexion. The big toe, being the last to lift off the ground, must be stable not only in the sagittal plane but also in the transverse plane, through the action of the adductors and abductors of the big toe.

The lesser toes, along with the big toe, are active during the propulsion phase and contribute to creating a rigid beam for the transfer of body weight to the contralateral foot.

Oscillation Phase:

During the oscillation phase, the foot does not support body weight, but adequate clearance is necessary. The leg continues to externally rotate, and the subtalar joint pronates in the first part, followed by supination to prepare for the inverted contact. The ankle joint (TT) continues to plantarflex during the early phase but rapidly transitions to dorsiflexion to maintain an appropriate distance from the ground during advancement and avoid tripping. During this phase, the first metatarsophalangeal joint dorsiflexes, again due to the action of the tibialis anterior and pretibial muscles, to lift the toes off the ground. This action causes an inclination of M1, which tensions the plantar fascia, elevates the arch, and activates the active windlass mechanism.

In conclusion, the ankle joint (TT) may seem simple, but it is actually very complex both anatomically and functionally in terms of biomechanics. To better understand ankle pathology, it is essential to comprehend the synergies among the different ligamentous, muscular, osseous, and capsular structures that come into play in the daily life of the ankle.

5.1.4 THE JOINT CARTILAGE

Articular cartilage is a tissue with unique biomechanical characteristics that allow joints to withstand mechanical stimuli without being damaged. This tissue covers the bony surfaces of all synovial joints; however, its composition and properties vary depending on the joint. Cartilage is composed of a single type of cell, chondrocytes, which produce the extracellular matrix in which they are trapped. Articular cartilage is neither vascularized nor innervated, so damage to it does not cause pain. The limited vascularity results in a scarcity of chondroprogenitor cells, which means that cartilage is unable to regenerate after an injury and tends to degenerate progressively.

There are different types of cartilage: Hyaline, Fibrous, and Elastic. Hyaline cartilage is composed of type II collagen, has a basophilic matrix, and is covered by perichondrium, which is a dense fibrous connective tissue that surrounds the cartilage. Chondrocytes are present in clusters or "isogenous groups" within hyaline cartilage. Fibrous cartilage, on the other hand, is formed by type I collagen and organized in thick bundles with an acidophilic matrix. It lacks perichondrium, and chondrocytes are arranged linearly. Elastic cartilage contains type II collagen and elastic fibers, which give it a yellowish color and opacity. It also has a perichondrium. Due to its high fibrous component compared to the cartilaginous matrix, it possesses strong elasticity and flexibility, which is why it is found in structures such as menisci, auricular cartilage, epiglottis, and larynx. (Peretti GM, Lombardo MDM, 2022)

With the exception of articular cartilage, other types of cartilage are covered by perichondrium. (Camarero-Espinosa S, Rothen-Rutishauser B, Foster EJ, 2016) The articular cartilage of interest is hyaline cartilage, which is present in the joints and growth plates. While the articular cartilage remains on the joint surfaces throughout an individual's life, the growth plate disappears at the end of skeletal maturation due to the fusion between the primary and secondary ossification centers. (Decker RS, 2017)

From a macroscopic point of view, articular cartilage is a white opalescent tissue that covers the surfaces of diarthroses (synovial joints), providing them with unique and particular mechanical properties, such as smooth sliding.

The function of cartilage is to resist compression and shear forces, transmit forces, cushion joint stresses, distribute peak loads over a larger surface area, reduce friction, and protect the subchondral bone. (Hunziker, 2002)

Articular cartilage has the role of supporting loads applied statically, cyclically, and repeatedly. Consequently, the macromolecules that make up articular cartilage, mainly collagen and proteoglycans, must be organized into a solid matrix capable of resisting such loads. (Chen Z, Yan F, 2016)

Hyaline cartilage is composed of the extracellular matrix, which consists of water, collagen, aggrecans/proteoglycans, non-collagenous glycoproteins, lipids, hyaluronic acid, and chondrocytes. The matrix is predominantly composed of water, accounting for approximately 70-80% of the cartilage's weight. It is more present in the superficial layers, increases with osteoarthritis, increases tissue permeability, decreases elasticity, and resistance to force. Collagen constitutes about 10-20% of the cartilage's weight, with type II collagen representing 80-95% of the collagen content. It forms a fibrillar structure and functions to create the framework of the cartilage, increasing tensile strength. The distribution of collagen is parallel at the superficial level, random at the central and vertical levels, and helps the cartilage resist two types of forces: compression and shear. Proteoglycans, which make up about 5-10% of the cartilage's weight, are macromolecules consisting of a protein core linked covalently to non-branched units of glycosaminoglycans (ILs), enriched with sulfate or carboxylic groups that increase the negative charge, attracting water. The most abundant proteoglycan is aggrecan, which is composed of chondroitin sulfate and keratan sulfate, bound to a hyaluronic acid backbone, concentrating negative charges within the cartilage. Other proteoglycans include decorin, biglycan, and fibromodulin, which stabilize the extracellular matrix together with collagen and increase resistance to compressive forces. This mechanism of increased resistance to compressive forces is due to water attraction by negative charges; this water accumulation swells the tissue and puts collagen under tension. Thus, during the application of compressive force, the negative charges repel each other and provide resistance to deformation. As water represents about 80% of the cartilage's weight, increasing deformation requires increasingly greater forces to deform a smaller percentage of the cartilage volume. (Roughley & Mort, 2014)

In cartilage, there are unique and highly specialized cells called chondrocytes, which make up less than 2% of the volume of adult cartilage. They are free cells that receive nutrients through diffusion from the synovial fluid and the underlying subchondral bone. Their primary function is to renew the extracellular matrix. Unlike bone, which undergoes defined tissue remodeling, cartilage undergoes molecular turnover. Chondrocytes produce enzymes that degrade the nearby extracellular matrix and replace the degraded molecules by secreting new ones, thus maintaining the architecture of the cartilage relatively unchanged. (Carballo CB, Nakagawa Y, Sekiya I, 2017)

During skeletal morphogenesis, mesenchymal cells differentiate into chondrocytes, which are responsible for producing and maintaining the extracellular matrix. Chondrocytes are highly sensitive to growth factors, interleukins, pharmacological molecules, matrix molecules, mechanical stimuli, and changes in hydrostatic pressure. For instance, IL-2 can lead to matrix degradation through a catabolic activity.

The histological structure of articular cartilage can be described as follows:

The lamina splendens does not have cellular components and serves to protect the cartilage and contribute to its resistance to shear forces. It also anchors macromolecules present in the synovial fluid.

The superficial or tangential layer contains small, flat chondrocytes with their major axis parallel to the surface. It occupies a relatively small space, about 10-20% of the cartilage thickness. This layer protects the cartilage from mechanical stress and resists shear forces due to a higher concentration of collagen, rich in fibronectin, and a lower concentration of proteoglycans in its extracellular matrix.

The transitional layer exhibits intermediate characteristics between the superficial and radial layers. It contains larger cells, a higher concentration of proteoglycans, and a lower presence of collagen.

The deep or radial layer constitutes approximately 30% of the cartilage thickness. It contains spheroidal chondrocytes arranged in columns (resembling growth plate cartilage), collagen fibers perpendicular to the articular surface, and a high concentration of proteoglycans.

The calcified layer, approximately 5-10% of the cartilage thickness, contains smaller chondrocytes with low metabolic activity. The collagen fibers are arranged radially but discontinuous compared to those in the subchondral bone. This layer is rich in type X collagen, which supports the structural integrity and mineralization of the cartilage. Additionally, it presents high concentrations of calcium. At the boundary between the deep layer and the calcified cartilage, there is a thin, undulating demarcation line called the tidemark. Its role is to transform shear forces into axial forces, transferring biomechanical stresses from the cartilage surface to the underlying bone. (Madry et al., 2010) This is necessary because bone and cartilage are biologically and biomechanically very different tissues and require a transition zone to distribute loads effectively. The presence of type X collagen fibers in the tidemark anchors the deep cartilage layer firmly to the calcified zone, neutralizing shear forces and preventing the separation of cartilage from the underlying bone.

Regarding cartilage injuries, they can be categorized as follows:

- Superficial lesions: These injuries may remain unchanged or progress over time. Chondrocytes can attempt to repair the lesion, but the healing process does not fully restore the biological and biomechanical characteristics of the original cartilage.

- Impact injuries: These injuries can lead to the apoptosis (cell death) of superficial cells within approximately three weeks, damaging the tidemark, which is the zone where the calcified cartilage connects to the subchondral bone. This type of injury also risks affecting the nourishment of the subchondral bone.

- Full-thickness lesions: These injuries can involve the subchondral bone and stimulate osteo-chondro-progenitor cells from the bone marrow to reach the injured area and attempt to repair it. However, the resulting tissue is fibrocartilaginous and does not possess the original cartilage's same characteristics.

Additionally, chronic micro-traumas from impacts can lead to thickening of the cortical endplate, the layer of bone tissue located beneath the calcified cartilage, weakening the tissue.

Currently, two widely accepted classifications for cartilage injuries in the literature are the International Cartilage Repair Society (ICRS) classification (Curl WW, Krome J, Gordon ES, Rushing J, Smith BP, 1997) and the Outerbridge classification (Slattery & Kweon, 2018). (fig. 43)

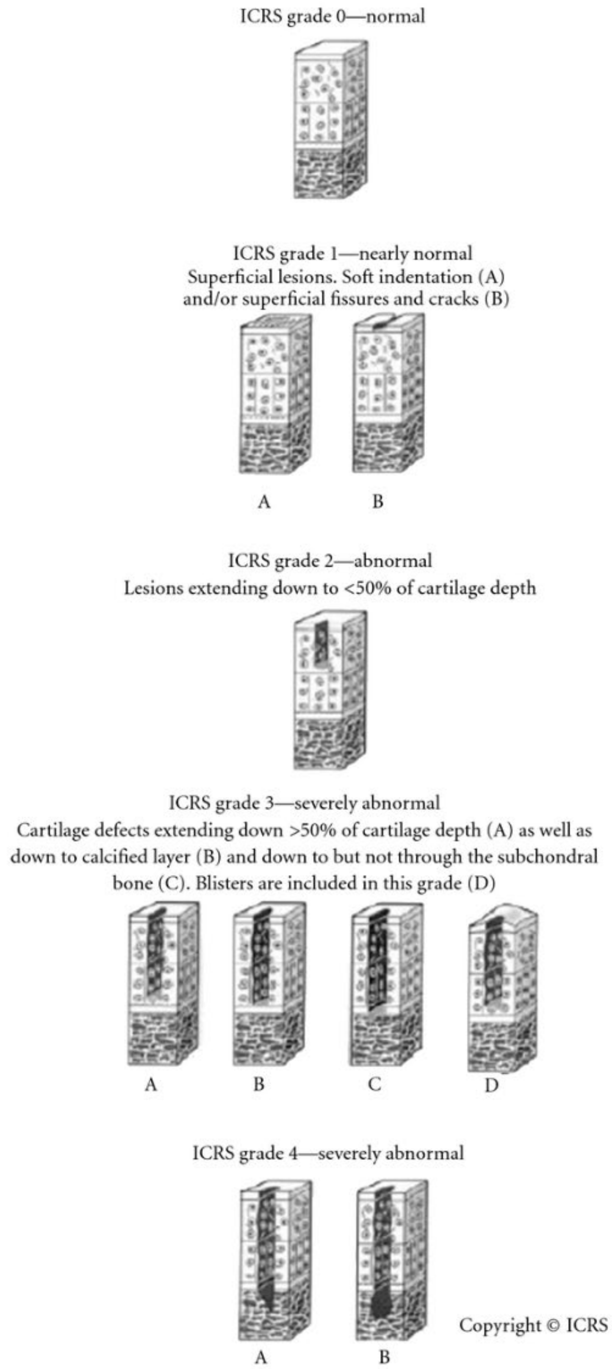

The International Cartilage Repair Society (ICRS) Cartilage Lesion Classification System. Reprinted with permission from the ICRS Cartilage Injury Evaluation Package (http://www.cartilage.org/).

Fig 43. International Cartilage Repair Society (ICRS) classification (Curl WW, Krome J, Gordon ES, Rushing J, Smith BP, 1997)

The Outerbridge classification divides cartilage lesions into 4 grades:

1. Grade 1 (I) - Softening of the cartilage.

2. Grade 2 (II) - Partial-thickness defect in the articular cartilage with fissures on the surface that do not reach the subchondral bone or exceed 1.5 cm in diameter.

3. Grade 3 (III) - Fissuring of the articular cartilage reaching the subchondral bone in an area with a diameter greater than 1.5 cm.

4. Grade 4 (IV) - Full-thickness lesion with involvement of the subchondral bone, regardless of size.

But what are the peculiarities of ankle cartilage compared to other joints?

An anatomical peculiarity of the ankle joint is its cartilage (Athanasiou KA, Niederauer GG, 1995), which is thicker on the tibial side (1.06-1.63 mm) and thinner on the talus side (0.94-1.62 mm), compared to the proximal joints of the knee (1.4-2.2 mm) and hip (1.7-2.2 mm). In women, the cartilage thickness is thinner (1.1 ± 0.28 mm) compared to men (1.35 ± 0.22 mm). This cartilage allows for better congruence between the joint surfaces, increases the contact area, and enhances load distribution. While this cartilage has a reduced tendency to develop primary osteoarthritis, it is more susceptible to developing secondary osteoarthritis.

The consistency of the cartilage (Millington SA, Li B, Tang J, Trattnig S, Crandall JR, Hurwitz SR, 2007) is hard, with greater thickness on the surface of the tibial plafond and thinner thickness on the malleolar articular surfaces. In the trochlear region of the talus bone, the cartilage thickness varies from thin to thick in the anteroposterior direction and has a softer consistency in regions with greater thickness in contact with the tibia, both on the tibial plafond and the medial malleolar surface. The surface layer of the articular cartilage of the talus bone has chondrocytes arranged parallel to the tissue and interconnected, with only 25% of chondrocytes found in single-cell configurations, unlike the knee where half of the chondrocytes in the femoral condyles and patellar groove are arranged in arches and clusters. Additionally, the distance between chondrocytes is significantly greater in the talus bone compared to the femoral condyles (Rolauffs B, Williams JM, Grodzinsky AJ, Kuettner KE, 2008).

At a biological level, the cartilage of the talus bone differs from the hip and knee (van Dijk et al., 2010). Chondrocytes in the talus bone have a greater capacity for proteoglycan synthesis and a higher percentage of water, resulting in different physical properties of this tissue: increased stiffness, greater matrix density, higher load resistance, lower permeability, and reduced susceptibility to mechanical insults (Cole et al., 2003; Huch et al., 1997; Juras et al., 2016; Kuettner & Cole, 2005).

According to some studies (Kuettner & Cole, 2005), it is believed that ankle cartilage has a greater capacity for repair compared to knee cartilage. The presence of a higher concentration of proteoglycans and water allows for greater stiffness and less permeability. This results in a denser extracellular matrix, providing greater load resistance and reduced susceptibility to mechanical damage (Treppo et al., 2000). Chondrocytes in ankle cartilage synthesize proteoglycans at a faster rate, leading to a greater capacity for repair (Kuettner & Cole, 2005). However, compared to knee chondrocytes, ankle chondrocytes are more sensitive to anabolic factors such as osteogenic protein-1 (OP-1) (Treppo et al., 2000). Ankle injuries have shown an upregulation of type II procollagen C-peptide and increased aggrecan turnover (epitope 836), both of which are markers of synthesis, compared to their counterparts in the knee (Cole & Kuettner, 2002). Furthermore, ankle chondrocytes are less sensitive to catabolic mediators, including fibronectin fragments and interleukin-1β (IL-1), both of which have been shown to inhibit proteoglycan synthesis (Aurich et al., 2002). The levels of matrix metalloproteinases (MMPs), enzymes responsible for degrading extracellular matrix proteins, also differ between ankle and knee joints (Mehana, 2019).

In normal ankle cartilage, the expression of matrix metalloproteinase-8 (MMP-8) mRNA was found to be non-detectable, while normal knee cartilage showed the presence of this MMP (Chubinskaya AS, Huch K, Mikecz K, Cs-Szabo G, Hasty KA, Kuettner KE, 1996).

The higher content of proteoglycans, along with a lower water content, provides greater stiffness and lower hydraulic permeability to ankle cartilage. As a result, the cartilage of the ankle is more rigid and resistant to compression, which may protect it from continuous microtrauma. The lack of a synergistic response of ankle chondrocytes to harmful compression and Interleukin-1 (IL-1) suggests that even with traumatic injuries, ankle cartilage is more resistant to the progression of degeneration. These findings demonstrate that the extracellular matrix plays a significant role in protecting ankle cartilage.

The ankle and knee are two joints with anatomical and biomechanical differences that seem to explain the different degenerative changes between the two joints. While the knee joint is relatively unstable, non-congruent, and partially stabilized by menisci, ligaments, and muscles with a mixed movement of flexion-extension and rotation, the ankle joint is more stable and congruent. The distal tibia, distal fibula, and dome of the talus bone, along with ligaments and the interosseous membrane, contribute to making this joint extremely stable, with triplanar movement, but predominantly in the sagittal plane of dorsiflexion-plantarflexion. The ankle, when subjected to high loads, becomes highly congruent, transmitting the body's weight from the tibia to the foot. The greater load on a smaller surface area of the ankle, compared to the knee, implies that there are differences that allow the ankle to resist high compression loads (Kempson GE, 1991).

Ankle cartilage has greater congruence, but the alteration of loads based on the reduction of the contact area is a unique feature. Some authors (de Vries et al., 2010; van Dijk et al., 2010) have shown that the average tibio-talus contact area is 4.4 cm^2, a reduced surface. The force exerted on healthy cartilage reaches 650N/cm^2, and during walking, the load is 3.9-5 times greater than body weight. This has highlighted that in the case of a reduced contact area, the load per cm^2 increases significantly. For example, if the talus shift is about 1mm, the load increases by 42% (a value still tolerated), but for a shift of 2mm, the load increases by 50%, and it begins to be intolerable, leading to tissue plasticity and overloading. Studies have shown that the load on the talus bone's trochlea is higher in the central, medial, and lateral zones. In cases of talus shift and joint instability with displacement of forces in the anteromedial direction, compression occurs medially, with shearing forces in the lateral zone. This can lead to more frequent chondral lesions at the medial and lateral levels, lateral instability, and displacement of loading forces in the anteromedial direction.

Current data suggest that there is not a single property, but rather numerous subtle differences between the cartilages and bones of the two joints, which may help protect ankle cartilage from progressive degeneration. Understanding these differences between the two joints could allow us to identify the active factors in the early stages of cartilage damage preceding the development of overt osteoarthritis. A method to reverse the effects of early pathological processes is to decrease the chondrocytes' response to catabolic factors and stimulate them to rebuild their matrix. Simulating the characteristics of ankle chondrocytes in different joints could facilitate the development of therapeutic strategies for early diagnosis and prevention of osteoarthritis.

How does osteochondral trauma happen?

The occurrence of osteochondral lesions (OLT) is most commonly triggered by trauma, which can result in several situations:

- Damage to the cartilage lining: this can lead to softening or fissures in the cartilage due to the forces applied to it, for example, in the case of a sprained ankle.
- Contusional damage to the subchondral bone: typically, this type of damage is progressive in nature.
- Avulsion of an osteochondral fragment: sometimes, this can occur in the case of an ankle fracture.

However, the exact mechanism behind the development of OLT is not yet completely clear and well-defined. In superficial lesions, cartilage dislamination is observed, while the subchondral bone remains intact. More intense traumas can involve the subchondral bone, resulting in contusions or microfractures. In more traumatic injuries, reparative properties can be altered, as water is forced out during loading in the damaged trabecular bone or around the detached fragment. Studies suggest that the increase in water in the subchondral bone and the increased pressure favor local osteolysis and the formation of subchondral cysts. The fluid hinders bone turnover and promotes necrosis, especially in an area with already limited vascularity.

In situations of a closed kinetic chain in the ankle, water is forced from the cartilage into the injured subchondral bone, with the diameter of the opening influencing the fluid pressure inversely.

The details of what happens in "bone bruises" or bone contusions are not yet fully known to science, but the evolving spectrum seems to vary from contusion to the detachment of an osteochondral fragment.

At the site of the cystic area, compact bone is formed, which reduces the pressure increase, compromising the support of the bone to the cartilage. This could be a possible cause of the detachment of the osteochondral fragment as it hinders repair.

Repeated traumas can lead to not only cartilage damage with an increase in the lesion's size but also damage to the subchondral bone, which is fundamental for supporting chondrocyte activity. When there is a lesion in the subchondral bone, the vascular supply to the cartilage, provided by vessels that penetrate its deep and calcified layers, is compromised. This is due to both the presence of the lesion and the reduced vascularization of the talus bone itself, leading to an alteration of the cartilage structure.

OLTs have difficulty in self-repair because chondrocytes have a limited tendency for mitotic activity, unlike full-thickness lesions, which can undergo a self-repair process aided by mesenchymal stem cells present in the subchondral bone marrow. These stem cells can migrate, proliferate, and differentiate under the control of SOX family transcription factors. At around two weeks into the process, these cells take on a spindle-shaped form, reflecting the fibrous nature of this fibrocartilage tissue. This new tissue does not have the same biomechanical properties as hyaline cartilage; it does not integrate with the pre-existing cartilage matrix and cannot even fill the lesion properly. This fibrocartilaginous tissue will then progressively evolve, losing chondrocyte components and leading to fibrosis and eventually arthritis.

The repair mechanism of the subchondral bone is not yet fully defined. After about two weeks, mesenchymal cells that come from the bone marrow differentiate into immature bone, recreating the damaged margins. If bone proliferation is excessive to the point of thinning the cartilage, the bone tissue can degenerate over time, leading to fibrillation, cell loss, and loss of type II collagen.

These reparative processes occur for lesions of small dimensions, but for large lesions, there is only a covering with a thin fibrocartilaginous layer. (Kraeutler et al., 2017).

5.1.5 EPIDEMIOLOGY AND ETIOLOGY

The true incidence of OLTs (Osteochondral Lesions of the Talus) is not describable because many remain unknown, both because they are often asymptomatic and due to the low rate of diagnosis among symptomatic cases. Among all osteochondral defects, those affecting the ankle represent about 4%, with the highest incidence occurring between the ages of 20 and 30. For this age group, the prevalence is male in 70% of cases and bilateral in 10%. (Vuurberg G, 2016).

The incidence of OLTs after an ankle sprain is reported to be 6.5%, and this value is likely underestimated as these injuries often go unnoticed. In the USA, over 2 million acute ankle sprains are estimated each year. Saxena et al believe that over 50% of cartilage injuries occur in patients with ankle sprains. Hintermann reports that even ankle fractures have a high incidence of OLTs, approximately 73%. In a retrospective study of active military personnel, around 27 OLTs were found per 100,000 people per year, with a significant high incidence of OLTs among siblings. (Woods K, Harris I, 1995) The literature questions whether there could be a correlation with congenital or hereditary factors; in fact, Statin identifies 1 Missense Mutation in the Aggrecan C-type Lectin Domain Of Chromosome 15 that leads to dominant OLTs. (Wodicka et al., 2016)

As of now, there is no certain data on the incidence of OLTs in the pediatric age group, except for the epidemiological study conducted in 2014 by J.I.Kessler et al. (Kessler et al., 2014), which investigated the incidence of OLTs in the pediatric age range (2-19 years). According to this study, ankle OLTs are twice as common as knee OLTs in this population. In contrast to previous data, this study highlights a higher prevalence of OLTs in females (1.6:1) and the most affected age group is 12-19, with a risk about 7 times higher than the 6-11 age group. The same study also revealed differences among ethnicities: non-Hispanic white individuals had over 50% higher risk compared to non-Hispanic whites and 6.3 times higher risk compared to African Americans.

The localization of OLTs is distinguished by those affecting: a) the talar dome: the most frequent and well-documented in the literature, predominantly affecting males, with various classifications and a preference for the postero-medial or antero-lateral area; b) the tibial plafond: less frequent, with limited literature, lacking its own classification, more common in the medial or centro-medial area, often appearing as cystic lesions; c) combined lesions (talar dome + tibial plafond): these have a high potential for progression and are considered pre-arthritic/degenerative lesions.

Frequency data regarding the localization of OLTs in the adult population are: 58% in the postero-medial zone and 42% in the antero-lateral zone. (Verhagen et al., 2003)

The 2014 study by Kessler et al. (Kessler et al., 2014) on the pediatric population showed that 71.8% of OLTs are in the medial zone, which is four times more common than lateral lesions. This was also confirmed by Carlson in 2020 (Carlson et al., 2020) and by Anastasio in 2023 (Anastasio et al., 2023), who highlighted the presence of medial lesions in 73% of the adolescent population and lateral lesions in 22.4%.

Unfortunately, the lack of data on possible asymptomatic or bilateral lesions due to the absence of imaging tests, as well as the varied terminology used until a few years ago to define this condition, has led to an undefined epidemiological picture of this pathology even today.

Trauma is the main cause, accounting for 93-98% of lateral OLTs and 61-70% of medial OLTs. Traumatic causes can be due to repeated microtraumas over time or an acute episode, such as an ankle sprain or fracture. However, not all patients present a history with traumatic etiology.

OLTs can be categorized into primary and secondary osteochondral lesions based on their etiopathogenesis. Primary osteochondral lesions of the ankle include all lesions with a non-traumatic etiology, characterized by necrotic evolution and chronic changes in the subchondral bone due to insufficient vascularization. This category was previously referred to as osteochondritis dissecans. Secondary osteochondral lesions encompass traumatic-based lesions, often resulting from sprains, fractures, chronic ankle instability, osteonecrosis, or malalignments. (Kon E, Viglione V, 2022)

Among the non-traumatic causes, ischemia leading to necrosis is well-known. Recent studies (Anastasio et al., 2023) have shown that the transition of vascularization from the perichondral area to the marrow cavity in adolescents is implicated in the formation of OLTs. This is supported by data indicating vascular regression in the epiphyseal cartilage during ossification, rendering the perichondral area more susceptible to OLTs in the pediatric population.

Other non-traumatic causes can be associated with endocrine issues or genetic factors. Additionally, the literature has identified identical OLTs among twins or siblings. (Woods K, Harris I, 1995) Regarding osteochondritis dissecans of the talus, the proportion that is related to a previous traumatic injury is not clear. (Bauer RS, Ochsner PE, 1987) In 1953, Roden et al. (Roden S, Tillegard P, Unanderscharin L, 1953) proposed that laterally localized osteochondritis dissecans on the talar dome had a traumatic etiology, while medial lesions were associated with non-traumatic causes. (Flick AB, Gould N, 1985)

In traumatic OLTs, 98% involve the lateral talar dome, and 70% involve the medial area. The prevalent mechanism is inversion and dorsiflexion, but acute traumas, repeated microtraumas, malalignments, and biomechanical alterations can also contribute. Kessler's study (Kessler et al., 2014) also suggests a post-traumatic cause, with pediatric patients in the study mostly participating in soccer, football, basketball, dance, and volleyball, which are similar to activities seen in the adult population.

Distortions of the ankle or chronic ankle instability are a significant cause of traumatic OLTs. When the ankle is inverted, the talar dome is compressed between the tibial plafond and the medial and lateral malleoli connected by syndesmotic ligaments. This compression can lead to cartilage fractures, delamination, or subchondral bone contusions. Cutting forces could also cause separation of the superficial cartilage layer, leading to lateral OLTs. Medial OLTs are often associated with plantarflexion of the ankle, anterior sliding force on the talus, inversion, and internal rotation of the talus on the tibia. (Berndt & Harty, 1959; van Dijk et al., 2010)

The position of osteochondral lesions in the talus has been described in correlation with traumatic mechanisms, with no significant differences between the adult and pediatric populations. To standardize the localization of talar dome lesions and analyze the frequency of affected areas, Raikin et al. (Raikin et al., 2007) created a grid system with nine distinct zones, numbered sequentially from anteromedial to posterolateral. Zone 1 corresponds to an anteromedial lesion, while Zone 3 represents an anterolateral lesion, Zone 7 indicates a posteromedial lesion, and Zone 9 denotes a posterolateral lesion.

Early OLTs often go unnoticed, and patients typically seek medical attention when ankle pain persists after a sprain. Patients may initially have a favorable clinical history, but they later develop increasing pain, swelling, stiffness, and a sense of blockage that worsens with weight-bearing. The exact mechanism producing these symptoms is not fully understood, but it's likely related to the focal loss of support in the talar dome or the continuous change in internal pressures triggering pain receptors, which are abundantly innervated in the subchondral bone. (Mach et al., 2002) These pain receptors are also stimulated by inflammation factors that lead to decreased pH and subsequent bone demineralization.

How does the damage occur?

The pathophysiological mechanism can be divided into three stages. In the first stage, or immediate stage, there is a destruction of the extracellular matrix, an increase in water content, alterations in collagen, and a decrease in proteoglycan aggregation. Subsequently, in stage 2, or acute phase, the actual damage to the extracellular matrix occurs with an altered chondrocyte response: there is an increased turnover of the extracellular matrix, coupled with elevated chondrocyte activity for continuous matrix repair. In the third stage, or chronic phase, there is a progressive depletion of the chondrocyte response due to prolonged elevated chondrocyte activity, altered cellular turnover, and progressive mechanical damage, all of which together result in a failure of the chondrocyte response. (Hendren & Beeson, 2009).

The chain of events involving mechanical or biochemical stress (aging, physical exercise), inflammatory oxidative stress, alterations in cartilage homeostasis (reduction of proteoglycans and aggrecans, reduction of low molecular weight proteoglycans like diglycans), degradation of the extracellular matrix, and loss of chondrocyte activity leads to a true osteochondral lesion.

More recently, a theory has emerged regarding the etiology of cystic formation in the subchondral bone following post-traumatic OLT: the articular-tibial bone tunnel (art-TBT), unlike the knee, has a high congruence of joint surfaces, causing synovial fluid to force its way into small ruptures in the subchondral bone, creating "cavities" or cysts in the spongy bone. In contrast to cartilage, the subchondral bone is rich in nociceptors that transmit the sensation of pain. Therefore, repeated high pressure of synovial fluid in the subchondral bone could explain the perceived pain in the patient. The channel connecting the subchondral bone plate with the cysts and the synovial joint could be evaluated using a CT scan. (van Dijk et al., 2010).

From a pathomechanical perspective, shear forces can cause superficial cartilage lesions without damaging the subchondral bone. However, after high-energy trauma or repeated microtraumas over time, the subchondral bone may become damaged. (Vellet AD, Marks PH, Fowler PJ, Munro TG, 1991).

5.1.6 CLASSIFICATION OF OSTEOCHONDRAL LESIONS

In the literature, various classification systems based on imaging are present to describe osteochondral lesions (OCLs), starting from the first classification proposed by Berndt and Harty in 1959 (Berndt & Harty, 1959; Pritsch M, Horoshovski H, Farine I, 1986). This initial classification was radiologically based and consisted of four stages:

1. Compression of the subchondral bone.
2. Incomplete detachment of the osteochondral fragment.
3. Complete detachment of the fragment without displacement.
4. Complete detachment and displacement of the fragment.

However, lesions that were not visible on X-rays went unnoticed (approximately 50%), including all cartilage lesions.

This classification remained in use until 1986 when Pritsch et al. (Pritsch M, Horoshovski H, Farine I, 1986) conducted a study comparing the Berndt and Harty classification with the arthroscopic appearance of the cartilage at the lesion site. With the advent of new instrumental techniques such as CT and MRI, new classifications followed. In 1991, Dipaola et al. (Dipaola JD, Nelson DW, Colville MR, 1991) proposed a classification that evaluated bone edema, cartilage integrity, and the presence of osteochondral fragments using MRI. This classification highlighted compatibility with arthroscopic findings and underscored the importance of MRI in the preoperative planning of osteochondral lesion treatment.

Subsequently, in 1993, the Berndt and Harty's classification was modified by Loomer (Loomer R, Fisher C, Lloyd-Smith R, Sisler J, Cooney T., 1993) with the addition of a fifth stage related to subchondral cystic lesions, visualizable through CT imaging. In 1995, the classification by Ferkel and Applegate based on arthroscopy was introduced, and it was later modified by Ferkel and Scaglione in 1996. All of these classifications reconsidered the presence of subchondral cysts and osteonecrosis.

Ferkel and Scaglione Classification: CT Features:

1. Subchondral cystic lesion with intact articular surface
2. A. Cystic lesion communicating with the talus dome
3. B. Open articular surface with overlying fragment
4. Non-displaced bone fragment
5. Displaced bone fragment

In 2012, Griffith (Griffith JF, Lau DT, Yeung DK, 2012) proposed an MRI-based classification that assessed the presence of bone marrow edema, integrity of the cartilage surface, and the remaining attachment or detachment point of the osteochondral fragment.

In addition to these instrument-based classifications, there are those based on arthroscopic analysis of the lesions, which consider the size of the lesion and the consistency of the tissue. The first one by Pritsch et al. (Pritsch M, Horoshovski H, Farine I, 1986):

Grade I: Intact, firm, and shiny cartilage.

Grade II: Intact but soft cartilage.

Grade III: Frayed (or worn) cartilage.

In 1995, Ferkel and Cheng (Cheng MS, Ferkel RD, Applegate GR, 1995) expanded this system to include chondromalacia and osteochondral lesions:

Grade A: Intact but soft and smooth cartilage.

Grade B: Empty cartilage.

Grade C: Fibrillations and fissures.

Grade D: Cartilage flap or exposed subchondral bone.

Grade E: Detached shiny fragment.

Grade F: Dislocated free fragment.

Taranow et al. (Taranow, W S, G A Bisignani, J D Towers, 1999) in 1999 used a dualistic approach with MRI for preoperative evaluation and then arthroscopy to stage and classify the final OCL.

In 2003, Mintz et al. (Mintz DN, Tashjian GS, Connell DA, Deland JT, O'Malley M, Potter HG, 2003) proposed a classification that combines arthroscopic and MRI evaluations, highlighting how, in cases of disagreement between the two analyses, MRI tends to underestimate the lesion.

In addition to the talar lesion classification systems, the International Cartilage Repair Society (ICRS) in 1997 (Curl WW, Krome J, Gordon ES, Rushing J, Smith BP, 1997) introduced a morphological classification for evaluating cartilage lesions based on depth and area of damage, which includes 4 grades and their respective subgrades (see table).

Grade 0: normal cartilage

Grade 1: Superficial lesion with:

1a: Chondral softening or presence of fibrillations

1b: Chondral softening or presence of fibrillations + tears or ruptures

Grade 2: Loss of chondral substance <50%

Grade 3: Lesion >50% depth.

3a: Lesion not extending to the calcified layer

3b: Lesion extending to the calcified layer

3c: Lesion reaching the subchondral bone, but not through it

3d: Fibrillating cartilage, "Blisters" type lesions

Grade 4: Lesion reaching the subchondral bone

4a: Lesion penetrates subchondral bone but not through full diameter, limited

4b: Lesion penetrates through full diameter into subchondral bone

There has been considerable debate in the literature regarding which instrumental evaluation is most specific for OCL: MRI, CT, or arthroscopy. All of these modalities are superior to clinical and radiographic examinations alone, but they are not statistically significant in identifying or excluding OCL. Arthroscopy has a sensitivity of 100% and a specificity of 97%, MRI has 96% sensitivity and 96% specificity, while CT has 81% sensitivity and 99% specificity.

For OCL of the talus, MRI tends to overestimate the size of the lesion, especially subchondral edema (K. B. Lee et al., 2008; Mintz DN, Tashjian GS, Connell DA, Deland JT, O'Malley M, Potter HG, 2003); furthermore, the MRI's inclination to detect subchondral changes compared to superficial lesions could result in the lack of detection of superficial defects (Oji DE, McCall DA, Schon LC, 2014).

Arthroscopy has the advantage of being able to directly identify a superficial OCL, but on the other hand, it is weak in potentially identifying a chondral lesion with intact superficial cartilage (Oji DE, McCall DA, Schon LC, 2014).

O'Neill et al. (O'Neill et al., 2010) emphasize the difficulty of identifying superficial OCLs in areas known for having a thin cartilage layer compared to other joints such as the knee.

However, the most widely applied classification in both clinical and scientific contexts is the one proposed by Prof. Giannini et al. (Giannini et al., 2005) in 2005, which primarily distinguishes between acute and chronic lesions, analyzing the characteristics of the articular surface and the dimensions, and providing an associated therapeutic algorithm. Acute OCLs are divided into two types, Type I and II, while chronic lesions are classified as Type 0, I, II, IIA, III (table 5).

Type of lesion	**Surface**	**Extension**	**Treatment**
Acute			
I	Damaged	$<1\ cm^2$	Débridement
II	Damaged	$\geq 1\ cm^2$	Fixation
Chronic			
0	Intact	any	Drilling
I	Damaged	$< 1.5\ cm^2$	Microfractures
II	Damaged	$\geq 1.5\ cm^2$	Cartilage replacement
IIA	Damaged	$\geq 1.5\ cm^2$, >5mm deep	Cartilage replacement and bone graft
III	Damaged		Osteochondral massive graft

Table 5: classification System fro osteochondral lesions of the talus (Giannini et al., 2005)

5.1.7 INSTRUMENTAL AND PHYSICAL EXAMINATION

The clinical evaluation of OCLs is challenging; often, these lesions remain unnoticed or are diagnosed belatedly, sometimes even years after the onset of symptoms. This is because the signs and symptoms are often of ambiguous specificity, frequently associated with other foot and ankle conditions or acute injuries, which can lead to them being overlooked.

Common symptoms typically include: pain in the ankle joint when bearing weight, swelling, and bruising (which usually resolve quickly). This is followed by chronic pain in the ankle joint when under stress during physical activities or on uneven terrain. Patients may experience a sensation of "locking" or "clicking," crepitus, instability, and limitations in the range of motion of the ankle. Pediatric patients often describe a feeling of needing to "pop" their ankle, but without success. The pain is usually localized around the ankle's malleolar region on the side of the lesion. In cases of postero-medial lesions, the pain may occur in the retro-malleolar Area. (Fig. 44-45)

Figure 44: zone of pain localized around the ankle region on the side of the lesion

Figure 45: pazient indicates zone of pain localized around the ankle region on the side of the lesion

From the literature, we have learned that OCLs can often be concealed after ankle fractures and may explain residual pain after acute trauma.

When should a suspicion of OCL arise? Certainly, when a patient reports chronic ankle pain while bearing weight and experiences functional limitations that are not always directly related to an acute traumatic event.

During the clinical evaluation, it is crucial to compare findings with the contralateral limb.

There are no specific maneuvers; frequently, tenderness upon digital palpation over the anterior joint line of the talo-crural joint is observed. To assess this, it's useful to begin the biomechanical evaluation from a position of plantarflexed TT joint at 35° and rotate the talus out of the mortise, evoking tenderness due to the exposed talar surface. Tenderness upon digital palpation of the lesion can be evoked: for antero-lateral lesions, the area around the antero-lateral dome is pressed with the ankle in plantarflexion, while for postero-medial lesions, the area posterior to the medial malleolus is pressed with the ankle in dorsiflexion.

Solely relying on clinical evaluation can make it difficult to specifically localize the lesion; at times, there might be posterior-medial tenderness caused by intra-articular effusion. Presence of a loose body in OCLs can often be associated with deep tenderness upon palpation of the anterior joint area. Another aspect to assess is the range of motion (ROM) of the talo-crural joint in dorsiflexion, often limited due to pain. Pain can also be evoked while dorsiflexing the ankle or during inversion.

At this point, the evaluation should continue with typical biomechanical aspects of a foot and ankle examination. Therefore, it's important to assess, using the Silfverskiöld test, if dorsiflexion limitation in the ankle is muscular or joint-related. During this maneuver and comparison with the contralateral foot, it's important to evaluate the end-feel of the potentially affected limb, as there's often tissue resistance. Assess the ROM of the talo-crural joint in plantarflexion, perform anterior and lateral drawer tests to assess ankle stability, and evaluate stress tests in inversion and eversion.

Subsequently, it's important to assess the mobility of the subtalar joint, including its ability to pronate and supinate. Sometimes, the ST joint is involved in protective postures and load avoidance due to pain from OCLs. This is followed by assessing the distal midtarsal, Lisfranc, and MTP joints.

From the OKC evaluation, move on to CKC analysis. Starting from the upright position, assess foot posture using the Foot Posture Index to determine if the foot is pronated or supinated. Clinical tests like the jack test, supination resistance test, maximum pronation test, single-leg stance test or heel rise test, and the Coleman test (for supinated feet) are performed, along with the squat test that often evokes pain due to dorsiflexion demand. Clinical evaluation cannot overlook gait analysis. During this examination, assess foot contact during the first rocker phase, which should normally occur with lateral heel contact. Analyze the timing of the stance phase; often, in the presence of OCLs, patients tend to avoid loading and prematurely lift the heel, reducing the duration of the first rocker and increasing the stance time during the third and fourth rockers compared to the healthy contralateral foot.

Once the clinician has a positive response to tenderness upon palpation of the talo-crural joint (indicating a suspicion of osteochondral lesion), further instrumental investigation is required.

Radiographic examination includes weight-bearing ankle X-rays in antero-posterior, lateral, Canale's oblique projection (15° foot pronation and 75° angulated projection to assess the joint space), Saltzman's projection at 20°, and sometimes lateral views with forced dorsiflexion or plantarflexion. Traditional radiography allows evaluation of loose bodies, but does not provide indications about subchondral bone contusions or other small lesions. However, it provides information about the anatomical and biomechanical aspects of the feet. For acute OLTs, radiographic evaluation is often difficult, but for chronic cases, transparency and possible cartilage depression can be assessed.

Computed Tomography (CT) allows analysis of bone morphology in multiple planes and can be requested to determine the exact degree of skeletal trauma. It also provides precise information about the position and size of detached fragments, mobile bodies, and osteochondral material. In the presence of OLT, it analyzes the vital part of the bone from the non-vital part, as well as the potential presence of loose bodies within the lesion. Unfortunately, this examination lacks assessment of surrounding soft tissues and is limited in visualizing solely cartilage lesions that are not displaced. However, it's crucial for preoperative planning and post-treatment follow-ups.

The gold standard, evidenced by A2, is Magnetic Resonance Imaging (MRI), which allows identification of subchondral bone edema, chondral damage, and other types of soft tissue lesions, even in mild and early stages. In the presence of intact cartilage surfaces, evaluation of deep layers involving subchondral bone is possible. MRI provides information about the size, composition, and stability of OLTs, which is essential for their classification and determining the most suitable therapeutic approach. T1 and T2-weighted MRI images analyze the talus, cartilage, and adjacent structures, including tendons and ligaments. T2-weighted sequences in particular evaluate the lesion and define the cartilage's state by highlighting its vitality and stability through interface fluid detection. Recently, biochemical imaging techniques such as T2 mapping have been added, allowing a qualitative evaluation of cartilage using a color-coded scale to assess GAG reduction, alteration of collagen architecture, and increased water content typical of a lesion. This technique has proven to be very useful for post-operative follow-up monitoring as well.

MRI sensitivity for cartilage lesions is 50% for 1.5 Tesla and 75% for 3 Tesla. A recent study (Patel et al., 2020) attempted to investigate if MRI results could predict instability of OLTs in the pediatric population and if there was a relationship between skeletal maturity and lesion stability. However, the only significant finding was that older age and thus more mature skeletal development were more predictive of unstable OLTs, without showing pathognomonic MRI signs. This is partly due to the immature skeleton, associated with stable lesions, having a greater potential for repair and spontaneous healing due to vascularization of the non-ossified cartilaginous epiphysis.

While CT provides precise dimensions of OLTs, compared to MRI which tends to overestimate them, a study by Anderson (Anderson IF, Crichton KJ, Grattan-Smith T, Cooper RA, Brazier D, 1989) showed that MRI is capable of identifying a higher number of lesions compared to CT.

5.1.8 TREATMENT

The treatment of OCL is complex, differing based on the stage of injury and needing personalization, relying on evidence for OCL and the individual characteristics of the patient and lesion to determine optimal treatment: age, body mass index (BMI), preoperative activity level, patient preference, lesion factors, prior failed treatments, morphological aspects of the lesion, and other ankle pathologies (alignment, stability, etc.).

Conservative treatment for ankle OCLs does not currently have a clear guideline in the literature; it aims to reduce pain through edema reduction, bone repair, and lesion healing with fibrotic tissue. Conservative treatment for acute OCLs involves initial functional rest for about 30 days, immobilization, or casting, which reduces synovial fluid entering the developing OCL, limiting damage to cartilage and subcartilaginous structures, reducing pain and synovial swelling. Partial weight-bearing is then initiated. Alongside rest, pharmacological therapy with pain relievers and NSAIDs, cycles of pulsed electromagnetic fields at home for at least 45 days (Benazzo et al., 2008; De Mattei et al., 2004) are used. Additionally, podiatric treatment for controlling foot biomechanics and correcting misalignments, infiltrative therapy with hyaluronic acid and autologous growth factors (platelet-rich plasma PRP) can be beneficial (Engebretsen et al., 2010; Mei-Dan et al., 2012).

Rehabilitative treatment, evidence A2, focuses on regaining active joint range of motion, followed by progressive loading with water rehabilitation and, for athletes, specific sports exercises and proprioception exercises. Conservative treatment includes well-defined follow-up to monitor the lesion and its potential progression using X-rays, MRI, and CT scans (D'Hooghe et al., 2018; Kon E, Viglione V, 2022).

This initial conservative therapeutic approach appears sufficient in the pediatric population, as demonstrated by Perumal (Perumal et al., 2007) and other authors (Lam & Siow, 2012) in pediatric cases of juvenile osteochondritis dissecans of grade II and III according to the Berndt and Harty classification. Heyse's study (Heyse et al., 2015) in 2015 on 67 children with juvenile osteochondritis dissecans of the talus showed excellent healing results with conservative treatment for grade I and II lesions according to the Berndt and Harty classification. The authors hypothesize that from grade III lesions onward, detachment from the bone creates a limitation to repair, and in such cases, conservative treatment can be a first step, potentially followed by surgical intervention.

Conservative treatment is applied within the first 6-12 months, and if symptomatic improvement does not occur, surgical treatment is considered. Surgical treatment is indicated when the lesion is symptomatic, conservative treatment has failed, or a fragment is present within the joint (Loomer R, Fisher C, Lloyd-Smith R, Sisler J, Cooney T., 1993).

Surgical approaches can be divided into three groups:

- Reparative techniques that remove damaged tissue and stimulate marrow precursor cells to promote repair. These techniques include debridement and abrasion, drilling, retrograde drilling, bone marrow stimulation/microperforations, reduction, and fixation.
- Reconstructive techniques involve autologous or allogeneic osteochondral grafts or fragments to repair the lesion. These include mosaicplasty and autologous and allogeneic osteochondral grafts.
- Regenerative techniques involve tissue engineering to use cells from the lesion site for regeneration, such as Autologous Chondrocyte Implantation (ACI) and autologous matrix-induced chondrogenesis (AMIC) (Dahmen et al., 2022; Stone, 1996).

To best explain surgical treatment, an algorithm is provided that differentiates based on the type of lesion according to the Giannini et al. classification for appropriate treatment (Giannini et al., 2005).

For the treatment of acute type I lesions with damaged articular surface $<1cm^2$, the treatment of choice is debridement, a cleaning of the damaged cartilage tissue using arthroscopic technique to reduce pain and repair the defect. These lesions often do not involve subchondral bone but can still be painful or associated with malleolar fractures requiring surgical treatment.

Acute type II lesions have intact cartilage, but the fragment is detached, with a size $\geq 1cm^2$, and the preferred treatment is fixation, involving reduction and synthesis of the fragment. If the osteochondral lesion and the fragment are $<1cm^2$, arthroscopic fixation is ideal; if not feasible, open surgery is considered. Resorbable screws or pins made of polyglycolic acid (PGA) or polylactic acid (PLLA), or metallic screws designed to sink into the cartilage, are preferred.

Following surgical treatment of acute lesions, an evidence-based A2 rehabilitation protocol is followed, including recovery of active joint range of motion, progressive loading with water rehabilitation, and for athletes, specific sport-specific and proprioceptive exercises. The protocol involves well-defined follow-up to monitor recovery using X-rays, MRI, and CT scans (D'Hooghe et al., 2018; Sullivan et al., 2017; Valderrabano et al., 2014).

In summary, acute OCLs present a challenge in diagnosing acute ankle injuries due to a lack of evidence in the literature, and there is no definitive recommendation for the use of arthroscopy in ankle fracture treatment. While there is ample documented evidence of a high incidence of OCLs in ankle fractures requiring open reduction and internal fixation, along with the ability of arthroscopic techniques to diagnose and treat lesions, there is no definitive evidence regarding the arthroscopic treatment of these lesions influencing short- and long-term clinical outcomes (Stone, 1996).

The treatment of chronic lesions is divided into stages 0, I, II, IIA, III according to the Giannini et al. classification (Giannini et al., 2005).

Chronic OCLs of type 0 are those lesions where the articular surface is intact. For this reason, Conti and Taranow (Conti & Taranow, 1996) proposed retrograde drilling arthroscopy in 1996. This involves retrograde milling of the subchondral bone without damaging the upper cartilage. Later, this technique was expanded by filling the osteochondral defect with cancellous bone graft or absorbable cements.

Treatment for chronic type I OCLs, lesions <1.5cm^2, involves microfractures or microperforations, aiming to recreate fibrocartilaginous tissue. Microfractures induce plate subchondral lesions that stimulate tissue repair by causing bleeding and releasing mesenchymal cells that are supposed to create fibrocartilaginous tissue, which has inferior mechanical properties compared to hyaline cartilage and is susceptible to deterioration over time (Natali S, Ruffilli A, Pintus EE, Luciani D., Cortese E., Buda R., 2017). Literature has shown the effectiveness of this technique on symptomatology and proper repair for lesions <1.5cm^2 (Giannini et al., 2001).

For chronic type II and IIA lesions, the indicated surgical technique is cartilage regeneration. Advances in bioengineering have led to evolving techniques such as mosaicplasty, osteochondral grafting, and autologous chondrocyte transplantation. A recent technique is the One Step method involving marrow concentration and a scaffold, performed arthroscopically. These techniques are suitable for lesions >1.5cm^2. For lesions with depth >5mm and extension >1.5cm^2, a spongy bone graft should accompany cartilage repair.

Chronic type III lesions with damaged articular surfaces, involving a large dome area and thick subchondral bone, are treated with allografts. Homologous osteochondral grafts (from a donor) replace specific joint portions with precision in recreating the shape and size of the damaged area.

The most described technique in literature for smaller OCLTs is microperforations. However, for lesions >1.5cm^2, the results of this technique are unsatisfactory. This led to the development of techniques implanting chondrocytes at the lesion site (Chi Zhang, You-Zhi Cai, 2016).

The earliest techniques in literature are two-step: ACI (Autologous Chondrocyte Implantation) and MACT. ACI, first described in 1994 by Brittberg et al., involves creating a culture of autologous chondrocytes suspended on a scaffold, which is then placed on the dome lesion. The original ACI and subsequent generations have proven more effective than microperforations in enabling repair. MACT, the second generation of ACI, uses a double-layered type I/III collagen membrane seeded with cultivated autologous chondrocytes. However, these techniques require two procedures, increasing operative risk and offering limited long-term cost-benefit (Chi Zhang, You-Zhi Cai, 2016; M Brittberg , A Lindahl, A Nilsson, C Ohlsson, O Isaksson, 1994).

The treatment approach has evolved into a one-step technique, such as the Chondrocyte-matrix complex (CMC), neonatal or juvenile cartilage tissue allografts, and the autologous matrix-induced chondrogenesis (AMIC) technique.

In our research study, we have adopted the AMIC technique, developed by Benthien and Behrens in 2005 (Behrens et al., 2006), which combines microperforations with the application of a two-layer natural type I and III collagen membrane derived from pigs (Chondro-Gide, Geistlich Pharma AG, Wolhusen, Switzerland). This membrane serves to protect and stabilize the blood clot resulting from subchondral bone microperforations. The non-porous layer ensures the clot remains near the lesion, while the porous layer allows multipotent stem cells (MSCs) to attach to collagen fibers, proliferate, and differentiate into chondrocytes. This membrane is absorbed within 6-24 weeks of implantation. A limitation of the microperforation-only technique is that the newly formed clot cannot withstand mechanical forces, causing stem cells and growth factors to be released into the joint rather than remaining at the lesion site (Y. H. D. Lee et al., 2014).

5.1.9 SURGICAL TECHNIQUE: AMIC PROCEDURE IN ARTHROSCOPY

The patient is positioned in a supine position, and a tourniquet is applied to the thigh. Standard arthroscopic landmarks are established: anteromedial (AM) portal, located medially to the anterior tibial tendon and superior to the joint line, being cautious of nearby saphenous vein and nerve; and anterolateral (AL) portal, situated medially to the lateral malleolus and lateral to the extensor digitorum longus tendon, taking care with the intermediate dorsal branch of the superficial peroneal nerve. Since identifying the latter nerve is challenging, it can be illuminated using the arthroscope inserted through the AM portal or by stretching the skin near the AL access point using a klemmer. To reduce the risk of injury during portal creation, normal saline solution is injected into the AM and AL locations to expand the spaces. Subsequently, the skin is incised, and the deeper layers are penetrated bluntly using a klemmer. The first phase of arthroscopy is performed with intra-articular water. Synovectomy is conducted using a Shaver size 4.5, and fibrous scar tissue is removed until a clear view of the ankle joint is achieved. Next, percutaneous placement of the Hintermann spreader (Integra Lifesciences, Plainsboro, NJ) is performed, and the lesion is identified with the foot positioned in equinus to anteriorize and expose the talus dome surface. Dissected and necrotic tissue at the base of the lesion is then removed using a dedicated curette until a site with regular margins suitable for treatment is obtained. Microperforations are created on the healthy subchondral tissue beneath the lesion using a Chondro Pick (Arthrex Naples, FL) across the entire area. The second phase is executed without intra-articular water. An arthroscopic cannula size 7 is placed, water is aspirated, the lesion area is dried with sponges, and maximum diameters and depths are measured using a graduated probe. If significant subchondral tissue loss (thickness >8 mm and presence of bone cyst) is observed, a cancellous bone graft is inserted. The graft is harvested from the calcaneus through an additional lateral incision, small portions are obtained, and they are placed within the lesion using the same cannula. A template of corrugated rubber (Penrose) is cut to define the shape and size of the osteochondral lesion. The membrane to be implanted is prepared with a slight underestimate of the template's size, as membrane humidification in the joint environment leads to minimal expansion (approximately 10-15%). The upper side of the membrane is smooth, more robust, and compact, providing better protection to the forming cartilage from mechanical stress during the rehabilitation and repair period. The lower layer is porous and rough, allowing mesenchymal stem cells (MSCs) from the subchondral circulation to adhere, proliferate, and produce new tissue. Subsequently, the Chondro-Gide membrane (Geistlich Surgery, Wolhusen, Switzerland) is inserted through the arthroscopic portal and carefully spread, ensuring it does not excessively protrude from the margins. The membrane is then secured along the lesion's perimeter with synthetic fibrin glue (Tissel, Baxter, USA), avoiding the area underneath, as this could impede the rise of MSCs. After 2-3 minutes, the Hintermann distractor is removed, normal ankle range of motion is checked, and the arthroscopic portals are sutured. The postoperative protocol involves crutch-assisted ambulation and non-weight-bearing on the operated limb for the first 21 days to prevent membrane mobilization. Subsequently, progressive full-weight-bearing ambulation is permitted for the following 21 days. From the 5th day onwards, the patient is encouraged to cautiously engage in active and passive mobilization of the ankle joint to avoid limitation of ROM. Low-impact sports (swimming, stationary cycling) are allowed after 6 weeks, and high-impact sports are permitted after 6 months.

The AMIC technique in arthroscopy offers several advantages: reduced postoperative recovery time, a lower number of intraoperative risks (such as infections, injury to the posterior tibial tendon, posterior tibial artery, or tibial nerve), non-invasiveness, and the possibility of performing additional procedures at a later time or repeating the original procedure. However, this technique also comes with limitations: the location of the lesion (for instance, very posterior lesions can be challenging to reach), the complexity of the technique which requires a steep learning curve for a specialized orthopedic surgeon experienced in foot and ankle surgery and proficient in arthroscopy. This technique has presented complications, although not in the pediatric context so far. In our experience, these complications include a recurrence of symptoms with a lack of osteochondral regeneration, possibly attributed to the patient's systemic condition (such as rheumatoid arthritis). Furthermore, technical errors have led to complications such as vascular injuries affecting collateral branches of the anterior tibial artery with a pulsating hematoma, necessitating vascular surgery intervention for hematoma evacuation and vessel ligature. Literature reports a certain percentage of complications, estimated at around 9%, including neurological injuries (49%), especially involving the superficial peroneal nerve, vascular injuries, tendon injuries, ligament injuries, skin injuries, cartilage injuries, infections, and instrument breakage.

In our study, pediatric patients underwent a biological reconstruction procedure using the AMIC technique in arthroscopy under general anesthesia.

5.2 METHODOLOGY

The retrospective study has been carried out upon a group of pediatric patients belonging to the Specialized Unit for Foot and Ankle at IRCCS Galeazzi-Sant'Ambrogio in Milan.

5.2.1 PRINCIPLES OF WHAT TO INCLUDE AND TO EXCLUDE

The study includes pediatric patients (≤18 years old) who underwent surgical biological reconstruction for large chronic osteochondral lesions (grade II, IIA according to Giannini) using the AMIC technique in arthroscopy, following the failure of conservative treatment. After the surgery, these patients underwent radiological follow-ups at 6 and 12 months and postoperative check-up visits at 1 month, 6 months, and 12 months post-intervention. Patients who underwent concurrent surgical procedures, those with autoimmune diseases, rheumatological conditions (rheumatoid arthritis), hemophilia, severe metabolic disorders, and oncological patients were excluded from the study.

5.2.2 SAMPLE

12 patients have been chosen, 9 girls and 3 boys

5.2.3 GOAL

The goal of the study is to evaluate the biomechanical alignment of the foot in patients who have undergone arthroscopic surgical biological reconstruction for large osteochondral lesions. The study aims to determine whether there is a correlation between foot positioning and both the incidence of the pathology and the outcomes of the procedure.

5.2.4 MATERIALS AND TECHNIQUE

All patients were evaluated by a single operator, MP, following a specific protocol. The protocol included:

Collection of Anamnestic Data: Patients' medical history was gathered, including information about any prior trauma, previous therapeutic interventions, sports activities before and after the surgery, and details about footwear worn in daily life and sports.

Completion of Evaluation Sheets:

- Foot Health Assessment: Italian Foot Function Index (17-Italian FFI) (Venditto et al., 2015).
- Biomechanical Alignment: Foot Posture Index (Gijon-Nogueron et al., 2019, 2020; Keenan et al., 2007; Loreti et al., 2023; Morrison & Ferrari, 2009; Redmond et al., 2006, 2008; Scharfbillig R, Evans AM, Copper AW,Williams M, Scutter S,Iasiello H,Redmond A, 2004).
- AOFAS Evaluation for Ankle and Hindfoot (Leigheb M, Janicka P, Andorno S, Marcuzzi A, Magnani C, 2016).
- Biomechanical Podiatric Assessment.
- Static and Dynamic Baropodometry Examination using FDM Zebris platform.

ITALIAN FOOT FUNCTION INDEX

Italian Foot Function Index (17-Italian FFI): The Foot Function Index (FFI) is a reliable outcome measure that assesses the conditions of the foot and ankle. The validated Italian version (17-Italian FFI) (Venditto et al., 2015) evaluates the effectiveness of treatment in patients with musculoskeletal disorders of the foot and ankle. It consists of three sections: a) "How severe is the foot pain," divided into 5 items. b) "How much difficulty did you have," divided into 9 items. c) "For how long have you had it," divided into 3 items. Each item is scored from 0 to 10, where 0 corresponds to "no pain" or "no difficulty" or "never," and 10 corresponds to "worst imaginable pain" or "difficulty requiring assistance" or "always." The total score is calculated as the patient's score divided by 170, multiplied by 100, resulting in a percentage. A lower percentage indicates no pain during daily life, while higher values indicate varying degrees of pain up to a maximum of 100%. FFI is considered a good Patient-Reported Outcome Measure (PROM) but is underutilized (Zwiers et al., 2018).

THE FOOT POSTURE INDEX

It is a scientifically validated method that allows describing the static position of the foot in the three planes of space, without a correlation with the dynamic behavior of the foot. It was described by Redmond et al. (Redmond et al., 2006; Scharfbillig R, Evans AM, Copper AW, Williams M, Scutter S, Iasiello H, Redmond A, 2004) and is based on a series of clinical measurements for each individual foot, which, when summed, provide a numerical value indicating a type of foot posture. Currently, the FPI has also been validated in the version (Loreti et al., 2023) in Italian. Additionally, recently, the FPI has been validated for the pediatric population (Gijon-Nogueron et al., 2019, 2020). The variables considered by the FPI can have a score ranging from -2 to +2, with 0 representing the neutral position, -2 indicating maximum supination, and +2 indicating maximum pronation. The six positions for collecting measurements are:

- Palpation of the head of the talus.
- Curves above and below the malleoli.
- Position of the calcaneus in the frontal plane.
- Talo-navicular prominence.
- ALI congruence.
- Abduction/adduction of the forefoot relative to the hindfoot.

In the pediatric population (ages 3-15), the reference values (Gijon-Nogueron et al., 2019, 2020) for describing the foot position are:

- At 3 years: -1 < Normal FPI < +11
- At 14 years: +3 < Normal FPI < +9 FPI ≤ -2 is considered abnormal and requires further evaluation.

For patients aged >15 years, the reference values for FPI-6 by Redmond (Redmond et al., 2008) are:

- FPI > +10: Highly pronated foot
- +6 < FPI < +9: Pronated foot

- 0 < FPI < +5: Physiological foot
- -4 < FPI < -1: Supinated foot
- -5 ≤ FPI: Highly supinated foot

AOFAS SCORE - ANKLE AND HINDFOOT EVALUATION

The American Orthopedic Foot and Ankle Society (AOFAS) scoring system for ankle and hindfoot outcomes (Kitaoka HB, Alexander IJ, Adelaar RS, Nunley JA, Myerson MS, Sanders M, 1994; Kitaoka HB, Alexander IJ, Adelaar RS, Nunley JA, Myerson MS, Sanders M, Lutter LD, 1997; Schneider & Jurenitsch, 1997) is the most commonly used scale for assessing pre- and post-therapeutic intervention outcomes. However, this scale does not fall under Patient Reported Outcome Measures (PROMS) (Zwiers et al., 2018) as it contains subjective items related to pain and function, while also having objective items for mobility and stability. Despite this, the AOFAS scoring system is still widely utilized within the scientific community and has been validated in Italian by the Leigheb et al. group (Leigheb M, Janicka P, Andorno S, Marcuzzi A, Magnani C, 2016).

The AOFAS SCORE consists of 9 items, with 1 item assessing pain with a maximum score of 40, 7 items for function with a maximum score of 50, and 1 item for alignment with a score of 10, for a total of 100 points. The AOFAS SCORE is considered excellent for scores >90, good between 80 and 89 points, fair between 70 and 79 points, and poor <69 points (Kitaoka HB, Alexander IJ, Adelaar RS, Nunley JA, Myerson MS, Sanders M, 1994; Kitaoka HB, Alexander IJ, Adelaar RS, Nunley JA, Myerson MS, Sanders M, Lutter LD, 1997; Schneider & Jurenitsch, 1997).

Except for FPI-6, which has been validated for the pediatric population, the other evaluation forms do not have specific references for this population. However, the choice to use these assessment forms is based on the literature research for comparable studies on the topic.

All patients underwent instrumental examinations including bilateral weight-bearing foot X-rays (AP and lateral projections), CT scans with a 16-slice scanner, axial scans followed by multiplanar reconstruction, and MRI with a 1.5T machine with a dedicated coil. MRI sequences included axial proton density-weighted fat-saturated, coronal proton density-weighted fat-saturated, and coronal T2-weighted turbo spin-echo (with slice thickness of 3mm). All examinations were evaluated by a musculoskeletal radiologist, and lesion dimensions were measured on both MRI and CT, including coronal length, sagittal length, depth, area, and ellipse formula. (fig. 46-47-48-49)

Fig. 46: X-Ray no-weightbearing in emergency room of a patient of ankle pain

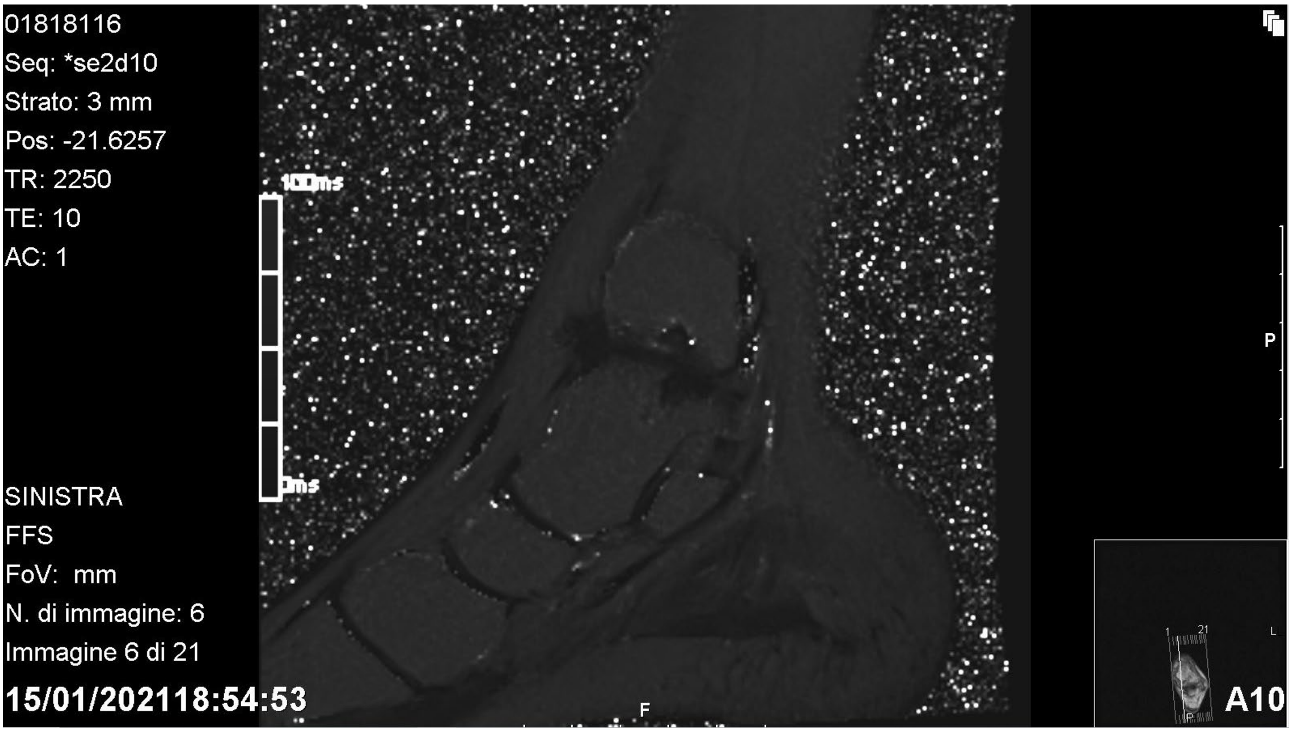

Fig. 47: MRI T2-mapping of OLT

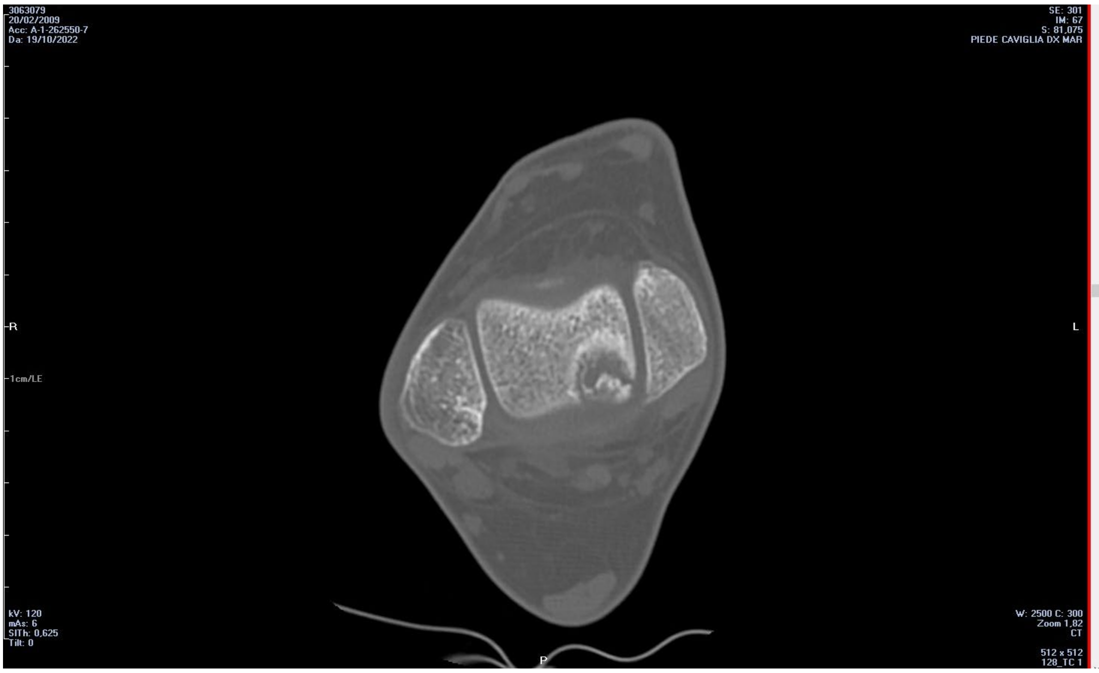

Fig. 48: CT scan in coronal plan of patient with OLT

Fig. 49 CT scan in frontal plane of a patient with OLT

THE PROTOCOL OF BIOMECHANICS EVALUATION

The biomechanical assessment was performed by a single operator, MP, a podiatrist with 15 years of experience. The tools used for the assessment included a pen, a goniometer, and an arthrogoniometer for rotation evaluation. The patient was asked to be barefoot and wear shorts or be without pants. The examination began with the patient lying supine, and the following evaluations were conducted (first on one foot and then on the contralateral foot):

- Skin inspection: Mapping of hyperkeratosis or nail deformities, if present.

- Evaluation of surgical scars, if any.

- Pelvic push maneuver.

- Assessment of lower limb length discrepancy.

- Hip range of motion assessment: especially intra- and extra-rotation at both flexed and extended knee positions.

- Patellar position assessment.

- Tibial torsion assessment.

- Sagittal plane ROM of the ankle joint and Silfverskiöld test (Silfverskiöld N, 1924).

- Pain assessment with digital pressure on the ankle joint interline.

- Pain assessment with digital pressure on the subtalar joint.

- ROM assessment of other foot joints: Subtalar, midtarsal , Lisfranc, metatarsals, metatarsophalangeal (MTP), interphalangeal (IP).

- Muscle strength assessment against resistance.

- Optional: Thomas test.

With the patient in prone position, perform the "pelvic rolling" maneuver and assess intra- and extra-rotation using the Rider’s test. Consider an optional thigh foot angle.

Flex the contralateral limb (position 4) to better assess the examined limb:

- Forefoot-rearfoot relationship assessment.
- Search for flat-spot or Kirby secondary axis.

Transition the patient to a relaxed upright position and assess the following parameters (variables based on the clinical case):

- Ligamentous laxity assessment using the Beighton score.
- RCSP (Resting Calcaneal Stance Position) assessment. (fig. 50)

fig. 50 Valuation of RCSP

- Navicular drop test.
- Navicular drift test if needed for highly abducted feet.
- Jack test.
- Hintermann test.
- Coleman and modified Coleman tests if the foot is supinated.
- Heel rise test (fig. 51) and one heel rise test.


fig. 51: heel rise test

- Supination resistance test.
- Maximum active pronation test. (fig. 52 a-b)

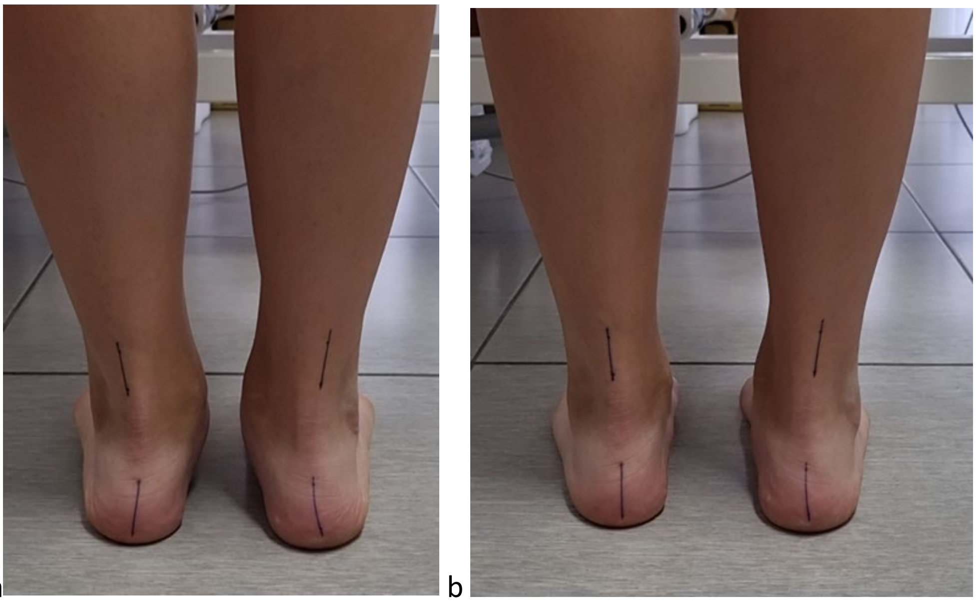

a b

Fig. 52 a: Maximum active pronation test, b RCSP

- Monopodal stance (fig. 53 a-b)

a b

fig. 53. a: monopodal stance on the right side, b: on the left side

- Lunge test (fig. 54)


fig. 54: Lunge test

- Bipodal (fig 55) and monopodal squat tests.

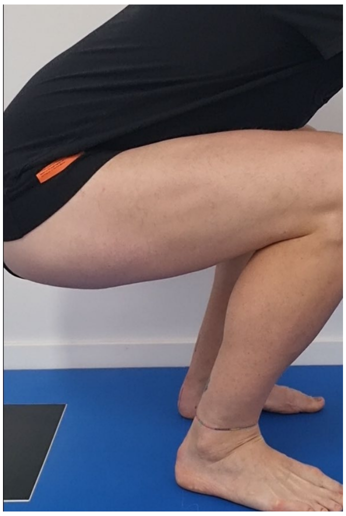
fig. 55 bipodal squat test

- Step test.

Afterward, observe the patient's gait in both the frontal and sagittal planes.

Heel Rise Test: With the patient standing in a relaxed upright position, they are asked to rise onto their toes as high as possible. This test is performed in both bipodal and monopodal stances. If the heel inverts due to the action of the tibialis posterior muscle during heel rise, the test is considered negative. If the heel remains stationary or in an everted position, the test is considered positive, indicating dysfunction of the tibialis posterior muscle.

Supination Resistance Test: The patient is in the RCSP while standing upright. The operator applies a downward force using the 2-3 fingers of their hand on the plantar aspect of the talonavicular joint to induce a supination movement. If the patient does not exhibit resistance, the test result is categorized as "soft." If there is moderate resistance, the result is categorized as "moderate." If the operator cannot generate a supination force, the test is considered "severe."

Maximum Active Pronation Test: The patient is in the RCSP position while standing upright. The operator instructs the patient to actively pronate both feet as much as possible without flexing or abducting the knees. Relative to the mobility of the subtalar joint, the heel may not evert further (indicating maximum pronation), evert to about one-third of its range of motion (ROM), or two-thirds of its ROM. While this test is not scientifically validated and lacks a universal interpretation, it is clinically useful for quantifying the foot's ability to pronate further (akin to a predictive value).

The collected data were analyzed using the IBM SPSS Statistics software by the same operator, MP.

5.3 RESULTS

Out of the 12 patients, only 9 participated in the podiatric evaluation, with 3 individuals not considering the study necessary. The sample consists of 7 females and 2 males. Among the 9 patients, 7 reported a traumatic cause for the onset of OLT (Osteochondral Lesion of Talus), while 2 had an idiopathic etiology. Four lesions were found in the left foot and five lesions in the right foot.

From the medical history, the time interval between the onset of pain and the diagnosis of OLT was reported for 9 patients as follows: approximately 12 months for 3 patients, around 24 months for 2 patients, approximately 35 months for 1 patient, about 48 months for 1 patient, and just a few months for the remaining 2 patients.

The distribution of the osteochondral lesion's location is as follows:

- Medial-posterior: 4 cases
- Medial-central: 1 case
- Medial malleolus: 1 case

Among these 9 patients, 6 were engaged in moderate-to-high level sports activities according to the provided figure 56:

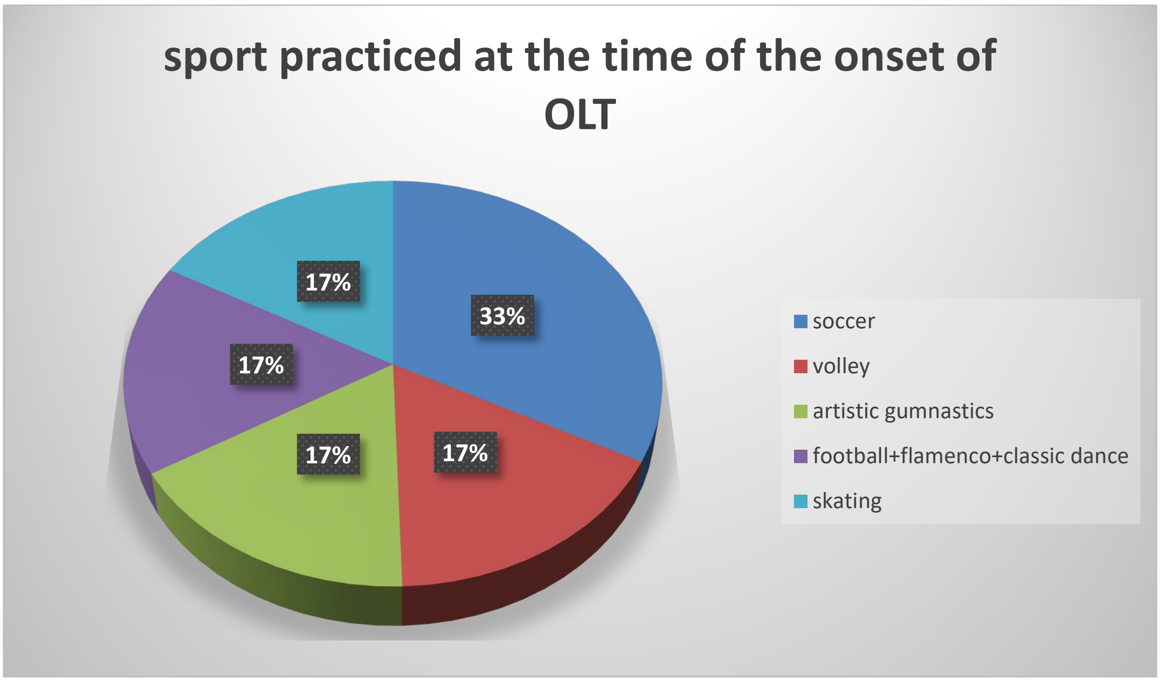

Figure 56: distribution of patient in sports activities

Only 5 patients underwent an initial conservative therapeutic treatment, which is described as follows:

- Post-sprain brace: 1 patient

- Post-sprain brace + crutches + instrumental manual physiotherapy (TECAR and magnetotherapy): 1 patient

- Physiotherapy: 1 patient

- Pre-existing plantar orthotic therapy: 1 patient

- Post-sprain brace + crutches + manual physiotherapy + plantar orthotic therapy: 1 patient

The average age at the time of surgical intervention for biological reconstruction using the AMIC arthroscopic technique is 15 years and 1 month, with the youngest patient being 13 years and 3 months old, and the oldest patient in the sample being 17 years old, all still in the stage of incomplete skeletal maturation. None of the patients experienced post-operative complications.

During the follow-up visits, the patients reported good recovery of the range of motion, no skin problems, and no signs of vascular or nerve injuries. After the surgery, none of the patients resumed their previous sports activities at the same level. Currently, 2 have completely stopped any sports activity, 1 continues the same activity as before, 3 have switched sports, and 1 patient has started engaging in sports. Meanwhile, 2 patients still do not participate in sports, but they do not report any limitations caused by the foot; on the contrary, all other patients who abandoned their previous sports reported that the foot could not bear the nearly professional workload, thus necessitating modifications in their habits. However, they do not currently feel limited.

The FPI-6 assessment shows that currently only 1 patient has both feet highly pronated (FPI-6 score of 8). One case involves a much more pronated foot (the operated foot) compared to the contralateral foot (FPI-6 scores of 8 vs. 5), and 1 case has bilaterally pronated feet, with one more point on the operated side (FPI-6 scores of 5 vs. 6). Additionally, 6 cases exhibit a normal FPI-6 score.

The AOFAS score for ankle and hindfoot ranges from a minimum of 84 to a maximum of 100 in our sample, with 4 patients achieving the maximum score. FFI values range from a minimum of 14 to a maximum of 20.

In the biomechanical assessment, notable aspects include 5 out of 9 patients having a negative Jack test, bilaterally. One patient tested positive on the Hintermann test. The navicular drop is positive for 1-1.5cm. One patient exhibits plantarflexion of the operated ankle's in the evaluation.

Through descriptive analysis performed using the IBM SPSS Statistics Editor, it can be observed that the collected data from the FPI, FFI, and AOFAS outcomes are fairly consistent with the age at which the patients underwent the intervention. (table 6)

STATISTICS						
	DISTANCE FROM INTERVENTION IN MONTHS	RIGHT FPI	LEFT FPI	FFI %	AOFAS REARFOOT	INTERVENTION AGE IN MONTH
N VALID	9	9	9	9	9	9
N MISSING	0	0	0	0	0	0
MEAN	49,11	3,11	3,11	15,89	93,33	182,00
MEDIAN	52,00	2,00	1,00	15,00	93,00	178,00
STANDARD DEVIATION	32,440	2,421	3,333	2,205	6,837	17,146
MINIMUM	8	0	0	14	84	159
MAXIMUM	104	8	8	20	100	204

Table 6: the collected data from the FPI, FFI, and AOFAS outcomes

Given the small sample size, it is necessary to perform correlations, both parametric (table 7) and non-parametric (table 8), between the variables.

		RIGHT FPI	LEFT FPI	FFI %	AOFAS REARFOOT
RIGHT FPI	Pearson correlation	1	,912**	,752*	-,720*
	Sig. (2-tailed)		<,001	,019	,029
	N	9	9	9	9
LEFT FPI	Pearson Correlation	,912**	1	,699*	-,687*
	Sig. (2-tailed)	<,001		,036	,041
	N	9	9	9	9
FFI%	Pearson Correlation	,752*	,699*	1	-,843**
	Sig. (2-tailed)	,019	,036		,004
	N	9	9	9	9
AOFAS REARFOOT	Pearson Correlation	-,720*	-,687*	-,843**	1
	Sig. (2-tailed)	,029	,041	,004	
	N	9	9	9	9

** Correlation is significant at the 0,01 level (2-tailed)
* Correlation is significant at the 0,05 level (2-tailed)

Table 7: parametric correlations analysis

From this analysis, it is evident that both FPI (Foot Posture Index) for both left and right feet are correlated with FFI (Foot Function Index). However, concerning the AOFAS (American Orthopaedic Foot and Ankle Society) score, there is a negative correlation with FPI, indicating that a higher AOFAS score is associated with a lower FPI value. It's worth noting that our sample has FPI scores ranging from 0 to 8, representing a spectrum from normal to highly pronated feet. In both correlations between FPI and FFI, as well as FPI and AOFAS, there is statistical significance indicated by a p-value of <0.05.

Moving on to non-parametric correlation analysis.(table 8)

			RIGHT FPI	LEFT FPI	FFI %	AOFAS REARFOOT
Spearman's rho	RIGHT FPI	Correlation Coefficient	1	,890**	,720*	-,728*
		Sig. (2-tailed)		,001	,029	,026
		N	9	9	9	9
	LEFT FPI	Correlation Coefficient	,890**	1	,787*	-,697*
		Sig. (2-tailed)	,001		,012	,037
		N	9	9	9	9
	FFI%	Correlation Coefficient	,720*	,787*	1	-,878**
		Sig. (2-tailed)	,029	,012		,002
		N	9	9	9	9
	AOFAS REARFOOT	Correlation Coefficient	-,728*	-,697*	-,878**	1
		Sig. (2-tailed)	,026	,037	,002	
		N	9	9	9	9
	** Correlation is significant at the 0,01 level (2-tailed)					
	* Correlation is significant at the 0,05 level (2-tailed)					

Tabel 8: non-parametric correlation analysis

A statistically significant correlation between FPI and FFI has been confirmed, as well as a statistically significant negative correlation between FPI and AOFAS.

Next, an examination was conducted to determine if there is a correlation between the etiology and the outcome of the intervention. (table 9)

Hypothesis Test Summary				
	Null Hypothesis	Test	Sig. [a.b]	Decision
1	right FPI distribution is the same on Etiology_ricod categories	Mann-Whitney U test with independent samples	,667[c]	Retain the null hypothesis
2	Left FPI distribution is the same on Etiology_ricod categories	Mann-Whitney U test with independent samples	,667[c]	Retain the null hypothesis
3	FFI% distribution is the same on Etiology_ricod categories	Mann-Whitney U test with independent samples	,500[c]	Retain the null hypothesis
4	AOFAS Rearfoot distribution is the same on Etiology_ricod categories	Mann-Whitney U test with independent samples	,889[c]	Retain the null hypothesis

a. the significance level is ,050
b. Asymptotic significances are displayed
c. the exact significance is displayed for this test

Table 9: correlation between the etiology and the outcome of the intervention analysis

For all variables (FPI, FFI, and AOFAS), when compared with the etiology, a statistically non-significant difference was observed, as well as for gender. (table10)

Hypothesis Test Summary				
	Null Hypothesis	Test	Sig. [a.b]	Decision
1	right FPI distribution is the same on Gender_ricod categories	Mann-Whitney U test with independent samples	,667[c]	Retain the null hypothesis
2	Left FPI distribution is the same on Gender_ricod categories	Mann-Whitney U test with independent samples	,500[c]	Retain the null hypothesis
3	FFI% distribution is the same on Gender_ricod categories	Mann-Whitney U test with independent samples	,222[c]	Retain the null hypothesis

4	AOFAS Rearfoot distribution is the same on Gender_ricod categories	Mann-Whitney U test with independent samples	,333[c]	Retain the null hypothesis

a. the significance level is ,050
b. Asymptotic significances are displayed
c. the exact significance is displayed for this test

Table 10: correlation between gender and the outcome of the intervention analysis

At this point, the analysis continued by evaluating whether there is a correlation between the location of the lesion and the outcome scores, as well as the type of foot. (table 11)

LOCATION OF THE LESION		RIGHT FPI	LEFT FPI	FFI %	AOFAS REARFOOT	DISTANCE FROM INTERVENTION IN MONTHS	INTERVENTION AGE IN MONTH
LATERAL	N VALID	1	1	1	1	1	1
	N MISSING	0	0	0	0	0	0
	MEAN	5,00	8,00	18.00	85,00	21,00	200,00
	MEDIAN	5,00	8,00	18.00	85,00	21,00	200,00
	MINIMUM	5	8	18	85	21	200
	MAXIMUM	5	8	18	85	21	200
MEDIAL	N VALID	7	7	7	7	7	7
	N MISSING	0	0	0	0	0	0
	MEAN	3,00	2,71	15,86	93,57	56,29	159
	MEDIAN	0	0	14	84	8	174,00
	MINIMUM	0	0	14	84	8	159
	MAXIMUM	8	8	20	100	104	204
	STANDARD DEVIATION	2,646	3,147	2,268	6,579	33,614	17,525

TIBIAL	N VALID	1	1	1	1	1	1
	N MISSING	0	0	0	0	0	0
	MEAN	2,00	1,00	14,00	100,00	27,00	191,00
	MEDIAN	2,00	1,00	14,00	100,00	27,00	191,00
	MINIMUM	2	1	14	100	27	191
	MAXIMUM	2	1	14	100	27	191

Table 11: correlation analysis between the location of the lesion and the outcome scores, as well as the type of foot.

These data do not indicate variability but rather descriptive considerations. For instance, patients with lesions in the medial talus have a high average AOFAS score (93.57), while those with lateral lesions have a score of 85, and patients with tibial malleolus lesions have a score of 100. Another interesting aspect to describe for medial talus lesions is the low average FPI score, an indicator of physiological feet.

The results of the outcomes were compared with the time elapsed since the surgery (table 12), yet this analysis did not reveal statistically significant differences.

			Distance From Intervention In Months	FFI %	AOFAS REARFOOT
Spearman's rho	Distance From Intervention In Months	Correlation Coefficient	1	-,139	,044
		Sig. (2-tailed)		,722	,911
		N	9	9	9
	FFI%	Correlation Coefficient	-,139	1,000	-,878**
		Sig. (2-tailed)	,722		,002
		N	9	9	9
	AOFAS REARFOOT	Correlation Coefficient	,044	-,878**	1,000

		Sig. (2-tailed)	,911	,002	
		N	9	9	9
	** Correlation is significant at the 0,01 level (2-tailed)				

Table 12: the results of the outcomes were compared with the time elapsed since the surgery

5.4 DISCUSSION

The limited sample size and lack of comparison data in the literature can be considered limitations of the study. At the same time, the anamnestic data align with what has been reported in the literature, indicating that these injuries are often initially unrecognized and diagnosed only later.

This study is notable for being the first to investigate a pediatric sample with OCL treated through AMIC biological reconstruction using arthroscopy. Additionally, it is the first to correlate clinical data with foot biomechanics.

Although literature data for the pediatric population are limited, specific treatment factors have been considered (Hurley et al., 2022) , such as the state of skeletal maturity, which can predict the potential for spontaneous healing and guide the surgeon in determining whether a safe osteotomy is possible if surgical repair is undertaken. (Letts et al., 2003; Perumal et al., 2007)

Another important factor, supported by the ISAKOS 2022 expert group, is the alignment of the hindfoot, which plays a key role in symptomatic ankle cartilage lesions. It should be taken into account for both surgical and conservative treatment decisions. Previous studies have acknowledged the significance of hindfoot alignment in relation to ankle cartilage lesions. (Higuera, J. M.D.; Laguna, R. M.D.; Peral, M. M.D.; Aranda, E. M.D.; Soleto, 1998; Karrholm J, Hansson LI, 1984; Letts et al., 2003; Perumal et al., 2007; Su et al., 2012)

Regarding biomechanical alignment, the study results show a correlation between a pronated biomechanical alignment (FPI) and lower AOFAS scores. A correlation between FPI and FFI also indicates that lower FFI scores were found in patients with physiological/slightly pronated feet. (table 7-8)

However, Pinski 2016 (Pinski JM, Boakye LA, Murawski CD, Hannon CP, Ross KA, 2016) has emphasized that the quality of supporting studies is still low and lacks sufficient evidence. The 2022 Cartilage Consensus suggests that conservative treatment is preferable for pediatric OCLs for the first 6 months, except in cases of displaced fragments, considering the potential for biological healing in this population. Karrholm J (Karrholm J, Hansson LI, 1984) has demonstrated that this potential for healing increases in pediatric OLTs with open physes. Other authors like Bruns, Letts, and Perumal suggest that conservative treatment in the pediatric population can extend up to 12 months, even in symptomatic cases. (Bruns J, Rosenbach B., 1992)

Lam and Perumal (Lam & Siow, 2012; Perumal et al., 2007) highlight satisfactory results of conservative treatment, while numerous authors underline that in case of unstable lesions or failure of conservative treatment, surgical treatment should be undertaken. According to Van Dijk 2014 (Reilingh et al., 2014) 92% of the population underwent post-conservative surgery, probably due to the influx of patients from different structures working with different conservative protocols. All the studies do not show a rehabilitation protocol of the conservative treatment that takes into consideration the orthotic treatment of the biomechanical alignment of the foot, and this could be a limit to the result of the conservative treatment in some cases. Our sample is also in line with literature data, as it shows that conservative treatment was varied, unresponsive and perhaps sometimes even incomplete.

The current literature suggests satisfactory outcomes with conservative treatment, but many authors highlight that surgical treatment should be considered for unstable lesions or if conservative treatment fails. The study's results align with the literature as they show that conservative treatment varied and was sometimes ineffective or incomplete.

The protocol followed by the study's participants is in line with the current literature, wherein failed conservative treatment often leads to surgical intervention due to misdiagnosis or lack of responsiveness. Literature consensus supports the use of internal fixation techniques (with/without bone grafting) as the primary choice for pediatric patients with fragments >15mm (Reilingh et al., 2014). Retrograde drilling or debridement (with/without bone marrow stimulation) is also recommended for treating pediatric OLTs, with advice to avoid osteotomies until physes are closed. In fact, Van Dijk himself in 2014, before performing an osteotomy, recommended subjecting the patient to a CT with ankle in plantarflexion to determine whether a medial malleolar osteotomy was also necessary for fixation and, if necessary, postponing the operation until at skeletal maturity.

However, according to Körner 2021 (Körner et al., 2021), the reintervention rate after surgical treatment with retrograde drilling or BMS in pediatric patients is high (approximately 25.9%), leading the authors to recommend retrograde drilling only in conditions of overlaying intact cartilage.

The first study that utilized bone marrow-derived cells through concentrated marrow aspirate in a pediatric population was conducted by Pagliazzi et al. in 2018 (Pagliazzi et al., 2018). They applied this technique to pediatric patients, taking advantage of their skeletal immaturity and high potential for healing.

In 2021, Körner et al. (Körner et al., 2021) performed an intervention using the MACI technique for stage 4 ICRS lesions with cartilage damage >1cm^2 and/or depth ≥5mm in a population of 12 adolescents with 13 ankles affected by OLT.

Currently, the statements from the Cartilage Consensus hold a level V evidence, indicating limited data. However, these statements currently remain the best practices for pediatric OLT cases.

Some authors, like Pagliazzi et al. in 2018 (Pagliazzi et al., 2018), suggest that patients might return to sports activity after surgical intervention, but at lower levels compared to before. This is in line with your study's findings, where prior to the issue, 6 out of 9 patients were engaged in sports with significant functional involvement. After the intervention, only 5 out of 9 continued with sports, often with a different activity and at a reduced intensity.

6 CONCLUSION

Osteochondral lesions of the ankle represent a niche within foot and ankle pathology, especially in the pediatric context. Their clinical history and delayed diagnosis place healthcare professionals in a position of increased demand for knowledge.

The study has shown that pediatric osteochondral lesions often occur in feet that are morphologically physiological or predominantly pronated. However, the sample size is limited to establish a strong correlation. It can certainly be asserted from the patients' clinical history that traumatic causes, especially sprain-related traumas, often underlie these lesions, although there are also cases of non-traumatic origins. Pain is the guiding element for clinicians in their clinical reasoning, and in the future, it would be desirable to establish a universally applicable conservative treatment protocol as the initial therapeutic step in the pediatric setting. Similarly, a post-surgical rehabilitative protocol would also be beneficial. In the adult population undergoing similar procedures, we often find ourselves addressing foot biomechanics to manage recurring OLT symptoms; however, as of now, this has not been the case in the pediatric sample.

The field of pediatric foot and ankle care still lacks in many aspects. It is often approached with the same evaluations as those for adults, just on a smaller scale. However, it's evident that this isn't an accurate perspective, and my internships and second year of Master's studies have continually reinforced this realization. Scientific studies in the pediatric foot and ankle domain must become more numerous and of higher quality in order to safeguard the health of our young patients and enhance clinical practice through validated guidelines specific to pediatric podiatry.

6.1 LIMITATIONS OF THE STUDY

The outcome assessment and foot health evaluation forms used for the patients are indeed evaluation forms, except for FPI-6, that have not been validated for the pediatric population. It is certainly important to conduct investigations into the foot health of the pediatric population using dedicated and appropriate assessment forms. For example, transitioning from the Visual Analog Scale (VAS) to the Wrong Face Scale for pain assessment could be considered.

The study showcases a notably small sample size, which is understandable given the specialized nature of this niche pathology and the need to involve specialized foot centers. Additionally, the absence of a pre-operative biomechanical evaluation is a limitation worth noting.

Addressing these limitations and further refining the evaluation tools for pediatric foot health and surgical outcomes could significantly enhance the understanding and management of osteochondral lesions in this specific population.

6.2 FUTURE RECOMMENDATIONS: THE INTERDISCIPLINARY REHABILITATIVE TREATMENT

It is important that in the presence of pain in a pediatric patient at the ankle level, the possibility of an osteochondral lesion (OLT), whether traumatic or not, should be considered. It is crucial to establish uniform guidelines for conservative treatment, even in a pediatric setting, taking into account the key role that a podiatrist could play. Certainly, the role of examining the biomechanical or pathomechanical aspects of these feet during walking or sports activities is significant. We know from the literature that, for example, shifts of 1mm in the talus can increase the load percentage on the cartilage surface, subjecting it to stress. Educating the patient about the proper use of their feet, any orthotics, and/or footwear is the responsibility of the podiatrist. In the presence of an OLT, the patient needs to walk with closed, laced, and well-supportive shoes that secure the heel, not only outside the home but also indoors. The patient should also consistently use any prescribed orthotics, avoid walking on inclined surfaces (e.g., beach shore, mountain slopes, uneven terrains), as these terrains increase stress on the subtalar joint. All of this is aimed at controlling joint stability as much as possible.

Furthermore, collaborative rehabilitative treatment with a physiotherapist involves pain control, addressing swelling, restoring range of motion, muscle strength, motor coordination, and joint economy. Range of motion recovery begins with passive mobilization, followed by controlled active mobilization, aquatic rehabilitation to better control load progression, early gait pattern re-education, maintaining an "athletic condition," and the controlled introduction of sport-specific movements. Patient education about joint economy requires awareness of pathogenetic mechanisms, avoidance of self-protective behaviors, learning proper techniques, targeted exercises, and the correct use of appropriate orthotics and footwear. Therefore, the role of rehabilitative healthcare professionals could involve supporting the orthopedic surgeon in the management of pediatric patients with OLT.

To enhance the quality of foot health in patients, it is advisable to consider incorporating biomechanical assessment into the surgical approach for this pathology.

7 BIBLIOGRAPHY

Alexander AH, Lichtman DM. (1980). Surgical treatment of transchondral talar-dome fractures (osteochondritis dissecans). Long-term follow-up. *J Bone Joint Surg Am.J Bone Joint Surg Am.*, *62*(4), 646–652.

Anastasio, A. T., Bagheri, K., Peairs, E. M., Grant, C., & Adams, S. B. (2023). *Juvenile Osteochondral Lesions of the Talus : Current Concepts Review and an Update on the Literature*.

Anderson IF, crichton KJ, Grattan- Smith T, Cooper RA, Brazier D. (1989). Osteochondral fractures of the dome of the talus. *J Bone Joint Surg Am.*, *71*(8), 1143–1152.

Athanasiou KA, Niederauer GG, S. R. J. (1995). Biomechanical topography of human ankle cartilage. *Ann Biomed Eng*, *23*(5), 697–704.

Aurich, M., Poole, A. R., Reiner, A., Mollenhauer, C., Margulis, A., Kuettner, K. E., & Cole, A. A. (2002). Matrix homeostasis in aging normal human ankle cartilage. *Arthritis and Rheumatism*, *46*(11), 2903–2910. https://doi.org/10.1002/art.10611

Barnett C, N. J. (1952). The axis of rotation at the ankle joint in man, its influence upon the form of the talus and mobility of the fibula. *Journal of Anatomy*, *86*, 1–9.

Battaglia, M., Rimondi, E., Monti, C., Guaraldi, F., Sant'Andrea, A., Buda, R., Cavallo, M., Giannini, S., & Vannini, F. (2011). Validity of T2 mapping in characterization of the regeneration tissue by bone marrow derived cell transplantation in osteochondral lesions of the ankle. *European Journal of Radiology*, *80*(2), 132–139. https://doi.org/10.1016/j.ejrad.2010.08.008

Bauer RS, Ochsner PE. (1987). Nosology of osteochondrosis dissecans of the trochlea of the talus. *Z Orthop Ihre Grenzgeb*, *125*(2), 194–200.

Behrens, P., Bitter, T., Kurz, B., & Russlies, M. (2006). Matrix-associated autologous chondrocyte transplantation/implantation (MACT/MACI)-5-year follow-up. *Knee*, *13*(3), 194–202. https://doi.org/10.1016/j.knee.2006.02.012

Benazzo, F., Cadossi, M., Cavani, F., Fini, M., Giavaresi, G., Setti, S., Cadossi, R., & Giardino, R. (2008). Cartilage repair with osteochondral autografts in sheep: Effect of biophysical stimulation with pulsed electromagnetic fields. *Journal of Orthopaedic Research*, *26*(5), 631–642. https://doi.org/10.1002/jor.20530

Benthien, J. P., & Behrens, P. (2010). Autologous matrix-induced chondrogenesis (AMIC): Combining microfracturing and a collagen I/III matrix for articular cartilage resurfacing. *Cartilage*, *1*(1), 65–68. https://doi.org/10.1177/1947603509360044

Berndt, A. L., & Harty, M. (1959). Transchondral Fractures (Osteochondritis Dissecans) of the Talus. *The Journal of Bone and Joint Surgery-American Volume*, *41*(A), 988–1020. https://doi.org/10.2106/00004623-200406000-00031

Boss AP, H. B. (2002). Anatomical study of the medial ankle ligament complex. *Foot & Ankle International*, *23*(6), 547–553.

Bruns J, Rosenbach B. (1992). Osteochondrosis dissecans of the talus. Comparison of results of surgical treatment in adolescents and adults. *Arch Orthop Trauma Surg*, *112*(1), 23–27.

Cain, J. D., & Dalmau-Pastor, M. (2021). Anatomy of the Deltoid-Spring Ligament Complex. *Foot and Ankle Clinics*, *26*(2), 237–247. https://doi.org/10.1016/j.fcl.2021.03.001

Camarero-Espinosa S, Rothen-Rutishauser B, Foster EJ, W. C. (2016). Articular cartilage: from formation to tissue engineering. *BIOMATERIAL SCIENCE*, *4*(5), 734–767.

Canale ST, B. R. (1980). Osteochondral lesions of the talus. *J Bone Joint Surg Am.*, *62*(1), 97–102.

Carballo CB, Nakagawa Y, Sekiya I, R. S. (2017). Basic Science of Articular Cartilage. *Clinics in Sports Med*, *36*(3), 413–425.

Carlson, M. J., Antkowiak, T. T., Larsen, N. J., Applegate, G. R., & Ferkel, R. D. (2020). Arthroscopic Treatment of Osteochondral Lesions of the Talus in a Pediatric Population: A Minimum 2-Year Follow-up. *American Journal of Sports Medicine*, *48*(8), 1989–1998. https://doi.org/10.1177/0363546520924800

Chen Z, Yan F, L. Y. (2016). The function of mechanical loading on chondrogenesis. *Front Biosci (Landmark Ed)*, *21*(6), 1222–1232.

Cheng MS, Ferkel RD, Applegate GR. (1995). Osteochondral lesions of the talus: a radiologic and surgical comparison. *In: Annual Meeting of the American Academy of Orthopedic Surgeons, New Orleans*.

Chi Zhang, You-Zhi Cai, X.-J. L. (2016). One-Step Cartilage Repair Technique as a Next Generation of Cell Therapy for Cartilage Defects: Biological Characteristics, Preclinical Application, Surgical Techniques, and Clinical Developments. *Arthroscopy*, *32*(7), 1444–1450.

Chubinskaya AS, Huch K, Mikecz K, Cs-Szabo G, Hasty KA, Kuettner KE, C. A. (1996). Chondrocyte matrix metalloproteinase-8: up-regulation of neutrophil collagenase by interleukin-1 beta in human cartilage from knee and ankle joints. *Lab Invest.*, *74*(1), 232–240.

CLOSE, J. R. (1956). Some applications of the functional anatomy of the ankle joint. *The Journal of Bone and Joint Surgery. American Volume*, *38 A*(4), 761–781. https://doi.org/10.2106/00004623-195638040-00005

Close JR, I. V. (1952). *The action of the ankle joint prosthetic devices research project Institute of Engineering Research,*.

Cole, A. A., & Kuettner, K. E. (2002). Molecular basis for differences between human joints. *Cellular and Molecular Life Sciences*, *59*(1), 19–26. https://doi.org/10.1007/s00018-002-8401-2

Cole, A. A., Margulis, A., & Kuettner, K. E. (2003). Distinguishing ankle and knee articular cartilage. *Foot and Ankle Clinics*, *8*(2), 305–316. https://doi.org/10.1016/S1083-7515(03)00012-3

Conti, S. F., & Taranow, W. S. (1996). Transtalar retrograde drilling of medial osteochondral lesions of the talar dome. *Operative Techniques in Orthopaedics*, *6*(4), 226–230. https://doi.org/10.1016/S1048-6666(96)80008-5

Curl WW, Krome J, Gordon ES, Rushing J, Smith BP, P. G. (1997). Cartilage injuries: a review of 31,516 knee arthroscopies. *Arthroscopy - Journal of Arthroscopic and Related Surgery*, *13*(4), 456–460.

Dahmen, J., Bayer, S., Toale, J., Mulvin, C., Hurley, E. T., Batista, J., Berlet, G. C., DiGiovanni, C. W., Ferkel, R. D., Hua, Y., Kearns, S., Lee, J. W., Pearce, C. J., Pereira, H., Prado, M. P., Raikin, S. M., Schon, L. C., Stone, J. W., Sullivan, M., … Murawski, C. D. (2022). Osteochondral Lesions of the Tibial Plafond and Ankle Instability With Ankle Cartilage Lesions: Proceedings of the International Consensus Meeting on Cartilage Repair of the Ankle. *Foot and Ankle International*, *43*(3), 448–452. https://doi.org/10.1177/10711007211049169

De Mattei, M., Pellati, A., Pasello, M., Ongaro, A., Setti, S., Massari, L., Gemmati, D., & Caruso, A. (2004). Effects of physical stimulation with electromagnetic field and insulin growth factor-I treatment on proteoglycan synthesis of bovine articular cartilage. *Osteoarthritis and Cartilage*, *12*(10), 793–800. https://doi.org/10.1016/j.joca.2004.06.012

De Palma L, Santucci A, Falcioni D, M. M. (2014). Anatomia e biomeccanica dell'articolazione tibiotarsica. In *Monografia Le grandi deformità* (Timeo, pp. 71–79).

de Vries, J. S., Kingma, I., Blankevoort, L., & van Dijk, C. N. (2010). Difference in balance measures between patients with chronic ankle instability and patients after an acute ankle inversion trauma. *Knee Surgery, Sports Traumatology, Arthroscopy*, *18*(5), 601–606. https://doi.org/10.1007/s00167-010-1097-1

Decker RS. (2017). Articular cartilage and joint development from embryogenesis to adulthood. *Semin Cell Dev Biol*, *62*, 50–56.

D'Hooghe, P., Murawski, C. D., Boakye, L. A. T., Osei-Hwedieh, D. O., Drakos, M. C., Hertel, J., Lee, K. B., Popchak, A., Wiewiorski, M., van Dijk, C. N., Ackermann, J., Adams, S. B., Andrews, C. L., Angthong, C., Batista, J. P., Baur, O. L., Bayer, S., Becher, C., Berlet, G. C., … Zhang, Z. (2018). Rehabilitation and Return to Sports: Proceedings of the International Consensus Meeting on Cartilage Repair of the Ankle. *Foot and*

Ankle International, *39*(1_suppl), 61S-67S. https://doi.org/10.1177/1071100718781862

Dipaola JD, Nelson DW, Colville MR. (1991). Characterizing osteochondral lesions by magnetic resonance imaging. *Arthroscopy*, *7*(1), 101–104.

Dürr, H. R., Martin, H., Pellengahr, C., Schlemmer, M., Maier, M., & Jansson, V. (2004). The cause of subchondral bone cysts in osteoarthrosis: A finite element analysis. *Acta Orthopaedica Scandinavica*, *75*(5), 554–558. https://doi.org/10.1080/00016470410001411

Engebretsen, L., Steffen, K., Alsousou, J., Anitua, E., Bachl, N., Devilee, R., Everts, P., Hamilton, B., Huard, J., Jenoure, P., Kelberine, F., Kon, E., Maffulli, N., Matheson, G., Mei-Dan, O., Menetrey, J., Philippon, M., Randelli, P., Schamasch, P., … Verrall, G. (2010). IOC consensus paper on the use of platelet-rich plasma in sports medicine. *British Journal of Sports Medicine*, *44*(15), 1072–1081. https://doi.org/10.1136/bjsm.2010.079822

Evans, A. M. (2020). Pain:consult with the five "Is." In *Disorders of the foot and ankle* (elsevier, pp. 332–333).

Flick AB, Gould N. (1985). Osteochondritis dissecans of the talus (transchondral fractures of the talus): review of the literature and new surgical approach for medial dome lesions. *Foot Ankle.*, *5*(4), 165–185.

Giannini, S., Buda, R., Faldini, C., Vannini, F., Bevoni, R., Grandi, G., Grigolo, B., & Berti, L. (2005). *COPYRIGHT © 2005 BY THE JOURNAL OF BONE AND JOINT SURGERY, INCORPORATED Surgical Treatment of Osteochondral Lesions of the Talus in Young Active Patients*. 28–41.

Giannini, S., Buda, R., Grigolo, B., & Vannini, F. (2001). Autologous chondrocyte transplantation in osteochondral lesions of the ankle joint. *Foot and Ankle International*, *22*(6), 513–517. https://doi.org/10.1177/107110070102200612

Gijon-Nogueron, G., Marchena-Rodriguez, A., Montes-Alguacil, J., & Evans, A. M. (2020). Evaluation of the paediatric foot using footprints and foot posture index: A cross-sectional study. *Journal of Paediatrics and Child Health*, *56*(2), 201–206. https://doi.org/10.1111/jpc.14558

Gijon-Nogueron, G., Martinez-Nova, A., Alfageme-Garcia, P., Montes-Alguacil, J., & Evans, A. M. (2019). International normative data for paediatric foot posture assessment: A cross-sectional investigation. *BMJ Open*, *9*(4), 1–8. https://doi.org/10.1136/bmjopen-2018-023341

Golano P, Farineas O, S. I. (2004). The anatomy of the navicular and periarticular structures. *Foot and Ankle ClinicsFoot and Ankle Clinics*, *9*(1), 1–23.

Golano P, Vega J, de Leeuw PA, Malagelada F, Manzanares MC, Götzens V, van Dijk CN. (2010). Anatomy of the ankle ligaments: a pictorial essay. *Knee Surgery, Sports Traumatology, Arthroscopy*, *18*(5), 557–569.

Grambart, S. T., Passet, A., & Holte, N. (2023). Osteochondral Lesions of the Talus: The Questions We Would Like Answered. *Clinics in Podiatric Medicine and Surgery*, *40*(3), 425–437. https://doi.org/10.1016/j.cpm.2023.02.004

Grath GB. (1960). Widening of the ankle mortise. A clinical and experimental study. *Acta Chir Scand Suppl*, *263*, 1–88.

Griffith JF, Lau DT, Yeung DK, W. MW. (2012). High-resolution MR imaging of talar osteochondral lesions with new classification. *Skeletal Radiol.*, *41*(4), 387–399.

Haynes JA, Gosselin M, Cusworth B, McCormick J, Johnson J, K. S. (2017). The arterial anatomy of the deltoid ligament: a cadaveric study. *Foot & Ankle International*, *38*(7), 785–790.

Hendren, L., & Beeson, P. (2009). A review of the differences between normal and osteoarthritis articular cartilage in human knee and ankle joints. *Foot*, *19*(3), 171–176. https://doi.org/10.1016/j.foot.2009.03.003

Heyse, T. J., Schüttler, K. F., Schweitzer, A., Timmesfeld, N., Efe, T., Paletta, J. R., Fuchs-Winkelmann, S., & Fernandez, F. F. (2015). Juvenile osteochondritis dissecans of the talus: predictors of conservative treatment failure. *Archives of Orthopaedic and Trauma Surgery*, *135*(10), 1337–1341. https://doi.org/10.1007/s00402-015-2260-4

Higuera, J. M.D.; Laguna, R. M.D.; Peral, M. M.D.; Aranda, E. M.D.; Soleto, J. M. D. (1998). Osteochondritis Dissecans of the Talus During Childhood and Adolescence. *J Pediatric Orthop*, *18*(3), 328–332.

Hintermann B. (2005). *Total Ankle Arthroplasty* (Springer W).

Hochschild J. (2003). *Apparato locomotore –anatomia e funzioni* (Edi.Ermes).

Hollis JM, Blaiser RD, F. C. (1995). Simulated lateral ankle ligamentous injury. Change in ankle stability. *Am J Sports Med*, *23*(6), 6672–6677.

Huch, K., Kuettner, K. E., & Dieppe, P. (1997). Osteoarthritis in ankle and knee joints. *Seminars in Arthritis and Rheumatism*, *26*(4), 667–674. https://doi.org/10.1016/S0049-0172(97)80002-9

Hunziker, E. B. (2002). Articular cartilage repair: Basic science and clinical progress. A review of the current status and prospects. *Osteoarthritis and Cartilage*, *10*(6), 432–463. https://doi.org/10.1053/joca.2002.0801

Hurley, D. J., Davey, M. S., Hurley, E. T., Murawski, C. D., Calder, J. D. F., D'Hooghe, P., van Bergen, C. J. A., Walls, R. J., Ali, Z., Altink, J. N., Batista, J., Bayer, S., Berlet, G. C., Buda, R., Dahmen, J., DiGiovanni, C. W., Ferkel, R. D., Gianakos, A. L., Giza, E., … Kennedy, J. G. (2022). Paediatric ankle cartilage lesions: Proceedings of the International Consensus Meeting on Cartilage Repair of the Ankle. *Journal of ISAKOS*, *7*(5), 90–94. https://doi.org/10.1016/j.jisako.2022.04.001

Inman VT. (1976). *The joints of the ankle* (Baltimore:).

Johnson EE, M. K. (1983). Contribution of the anterior talofibular ligament to ankle laxiq. *Journal of Bone and Joint Surgery - American Volume*, *65*(a), 81.

Juras, V., Zbýň, Š., Mlynarik, V., Szomolanyi, P., Hager, B., Baer, P., Frollo, I., & Trattnig, S. (2016). The compositional difference between ankle and knee cartilage demonstrated by T2 mapping at 7 Tesla MR. *European Journal of Radiology*, *85*(4), 771–777. https://doi.org/10.1016/j.ejrad.2016.01.021

Kappis M. (1922). Weitese Beitrage zur Traumatisch-mechanischen-Entstehung der "Spontanen" Knospelablosungen. *Dtsch Z Chir*, *17*, 13–29.

Karrholm J, Hansson LI, S. G. (1984). Changes in tibiofibular relationships due to growth disturbances after ankle fractures in children. *J Bone Joint Surg Am.*, *66*(1198–210).

Keenan, A. M., Redmond, A. C., Horton, M., Conaghan, P. G., & Tennant, A. (2007). The Foot Posture Index: Rasch Analysis of a Novel, Foot-Specific Outcome Measure. *Archives of Physical Medicine and Rehabilitation*, *88*(1), 88–93. https://doi.org/10.1016/j.apmr.2006.10.005

Kelikian AS. (2011). *Sarrafian's anatomy of the foot and ankle* (3^ed. LWW, Ed.).

Kempson GE. (1991). Age-related changes in the tensile properties of human articular cartilage: a comparative study between the femoral head of the hip joint and the talus of the ankle joint. *Biochim Biophys Acta*, *1075*(3), 223–230.

Kessler, J. I., Weiss, J. M., Nikizad, H., Gyurdzhyan, S., Jacobs, J. C., Bebchuk, J. D., & Shea, K. G. (2014). Osteochondritis dissecans of the ankle in children and adolescents: Demographics and epidemiology. *American Journal of Sports Medicine*, *42*(9), 2165–2171. https://doi.org/10.1177/0363546514538406

Kitaoka HB, Alexander IJ, Adelaar RS, Nunley JA ,Myerson MS, Sanders M. (1994). Clinical rating systems for the ankle-hindfoot, midfoot, hallux, and lesser toes. *Foot & Ankle International*, *15*(7), 349–353.

Kitaoka HB, Alexander IJ, Adelaar RS, Nunley JA, Myerson MS, Sanders M, Lutter LD. (1997). Clinical rating systems for the ankle-hindfoot, midfoot, hallux, and lesser toes. *Foot & Ankle International*, *18*(3), 187–188.

Kon E, Viglione V, V. F. (2022). Lesioni osteocondrali dell'articolazione tibiotarsica. In *Ortopedia e traumatologia* (Piccin, pp. 457–460).

Konig F. (1887). Ueber freie korper in den gelenken. *Dtsch Z Chir*, *27*, 90–109.

Körner, D., Gonser, C. E., Döbele, S., Konrads, C., Springer, F., & Keller, G. (2021). Matrix-associated autologous chondrocyte implantation with autologous bone grafting of osteochondral lesions of the talus in adolescents: patient-reported outcomes with a median follow-up of 6 years. *Journal of Orthopaedic Surgery and Research*, *16*(1), 1–10. https://doi.org/10.1186/s13018-021-02384-8

Kouvalchouk JF, Schneider-Maunoury G, Rodineau J, Paszkowski A, W.-A. L. (1990). Osteochondral lesions of the dome of the talus with partial necrosis. Surgical treatment by curettage and filling. *Rev Chir Orthop Reparatrice Appar Mot .*, *76*(7), 480–489.

Kraeutler, M. J., Chahla, J., Dean, C. S., Mitchell, J. J., Santini-Araujo, M. G., Pinney, S. J., & Pascual-Garrido, C. (2017). Current Concepts Review Update: Osteochondral Lesions of the Talus. *Foot and Ankle International*, *38*(3), 331–342. https://doi.org/10.1177/1071100716677746

Kuettner, K. E., & Cole, A. A. (2005). Cartilage degeneration in different human joints. *Osteoarthritis and Cartilage*, *13*(2), 93–103. https://doi.org/10.1016/j.joca.2004.11.006

Lam, K. Y., & Siow, H. M. (2012). Conservative treatment for juvenile osteochondritis dissecans of the talus. *Journal of Orthopaedic Surgery (Hong Kong)*, *20*(2), 176–180. https://doi.org/10.1177/230949901202000208

Leardini A, O'Connor JJ, Catani F, G. S. (1999). A geometric model of the human ankle joint. *J Biomech.*, *32*(6), 585–591.

Leardini A, O'Connor JJ, G. S. (2014). Biomechanics of the natural, arthritic, and replaced human ankle joint. *Journal of Foot and Ankle Research*.

Lee, K. B., Bai, L. Bin, Park, J. G., & Yoon, T. R. (2008). A comparison of arthroscopic and MRI findings in staging of osteochondral lesions of the talus. *Knee Surgery, Sports Traumatology, Arthroscopy*, *16*(11), 1047–1051. https://doi.org/10.1007/s00167-008-0607-x

Lee, Y. H. D., Suzer, F., & Thermann, H. (2014). Autologous Matrix-Induced Chondrogenesis in the Knee: A Review. *Cartilage*, *5*(3), 145–153. https://doi.org/10.1177/1947603514529445

Leigheb M, Janicka P, Andorno S, Marcuzzi A, Magnani C, G. F. (2016). Italian translation, cultural adaptation and validation of the "American Orthopaedic Foot and Ankle Society's (AOFAS) ankle-hindfoot scale". *Acta Biomed.*, *87*(1), 38–45.

Letts, M., Davidson, D., & Ahmer, A. (2003). Osteochondritis dissecans of the talus in children. *Journal of Pediatric Orthopaedics*, *23*(5), 617–625. https://doi.org/10.1097/01241398-200309000-00008

Loomer R, Fisher C, Lloyd-Smith R, Sisler J, Cooney T. (993). Osteochondral lesions of the talus. *Am J Sports Med1*, *21*(1), 13–69.

Loreti, S., Berardi, A., & Galeoto, G. (2023). Translation, Cross-Cultural Adaptation, and Validation of the Foot Posture Index (FPI-6)—Italian Version. *Healthcare (Switzerland)*, *11*(9), 1–11. https://doi.org/10.3390/healthcare11091325

M Brittberg 1, A Lindahl, A Nilsson, C Ohlsson, O Isaksson, L. P. (1994). Treatment of deep cartilage defects in the knee with autologous chondrocyte transplantation. In *N Engl J Med* (Vol. 331, Issue 14, pp. 889–895).

Mach, D. B., Rogers, S. D., Sabino, M. C., Luger, N. M., Schwei, M. J., Pomonis, J. D., Keyser, C. P., Clohisy, D. R., Adams, D. J., O'leary, P., & Mantyh, P. W. (2002). Origins of skeletal pain: Sensory and sympathetic innervation of the mouse femur. *Neuroscience*, *113*(1), 155–166. https://doi.org/10.1016/S0306-4522(02)00165-3

Madry, H., van Dijk, C. N., & Mueller-Gerbl, M. (2010). The basic science of the subchondral bone. *Knee Surgery, Sports Traumatology, Arthroscopy*, *18*(4), 419–433. https://doi.org/10.1007/s00167-010-1054-z

Mei-Dan, O., Carmont, M. R., Laver, L., Mann, G., Maffulli, N., & Nyska, M. (2012). Platelet-rich plasma or hyaluronate in the management of osteochondral lesions of the talus. *American Journal of Sports Medicine*, *40*(3), 534–541. https://doi.org/10.1177/0363546511431238

Millington SA, Li B, Tang J, Trattnig S, Crandall JR, Hurwitz SR, A. S. (2007). Quantitative and topographical evaluation of ankle articular cartilage using high resolution mri. *J OrthopRes*, *25*(2), 143–151.

Mintz DN, Tashjian GS, Connell DA, Deland JT, O'Malley M, Potter HG. (2003). Osteochondral lesions of the talus: a new magnetic resonance grading system with arthroscopic correlation. *Arthroscopy*, *19*(4), 353–359.

Morrison, S. C., & Ferrari, J. (2009). Inter-rater reliability of the Foot Posture Index (FPI-6) in the assessment of the paediatric foot. *Journal of Foot and Ankle Research*, *2*(1), 1–5. https://doi.org/10.1186/1757-1146-2-26

Murawski, C. D., Jamal, M. S., Hurley, E. T., Buda, R., Hunt, K., McCollum, G., Paul, J., Vannini, F., Walther, M., Yasui, Y., Ali, Z., Altink, J. N., Batista, J., Bayer, S., Berlet, G. C., Calder, J. D. F., Dahmen, J., Davey, M. S., D'Hooghe, P., … Hogan, M. C. V. (2022). Terminology for osteochondral lesions of the ankle: proceedings of the International Consensus Meeting on Cartilage Repair of the Ankle. *Journal of ISAKOS*, *7*(2), 62–66. https://doi.org/10.1016/j.jisako.2021.12.001

Natali S, Ruffilli A, Pintus EE, Luciani D., Cortese E., Buda R. (2017). La tibio-tarsica. In *Monografia La mini-invasività a 360°* (Ed. Timeo, pp. 7–32).

Niladri Kumar Mahato, S. N. M. (2012). Articular and angular dimensions of the talus: inter-relationship and biomechanical significance. *Foot (Edinb).*, *22*(2), 85–89.

Oji DE, McCall DA, Schon LC, F. R. (2014). Diagnosis of osteochondral defects by arthroscopy. In *Talar Osteochondrla defects* (Springer, pp. 43--50).

O'Neill, P. J., Van Aman, S. E., & Guyton, G. P. (2010). Is MRI adequate to detect lesions in patients with ankle instability? *Clinical Orthopaedics and Related Research*, *468*(4), 1115–1119. https://doi.org/10.1007/s11999-009-1131-0

Pagliazzi, G., Baldassarri, M., Perazzo, L., Vannini, F., Castagnini, F., & Buda, R. (2018). Tissue Bioengineering in the Treatment of Osteochondritis Dissecans of the Talus in Children with Open Physis: Preliminary Results. *Journal of Pediatric Orthopaedics*, *38*(7), 375–381. https://doi.org/10.1097/BPO.0000000000000827

Patel, M., Francavilla, M. L., Lawrence, J. T. R., Barrera, C. A., Nguyen, M. K., Longoria, C., & Nguyen, J. C. (2020). Osteochondral lesion of the talus in children: Are there MRI findings of instability? *Skeletal Radiology*, *49*(8), 1305–1311. https://doi.org/10.1007/s00256-020-03436-6

Peretti GM, Lombardo MDM, B. L. (2022). Cartilagine. In *Ortopedia e traumatologia* (Piccin, pp. 8–9).

Perry J, B. J. (2010). *Gait Analysis* (2^ed, Slac).

Perumal, V., Wall, E., & Babekir, N. (2007). Juvenile osteochondritis dissecans of the talus. *Journal of Pediatric Orthopaedics*, *27*(7), 821–825. https://doi.org/10.1097/BPO.0b013e3181558961

Pinski JM, Boakye LA, Murawski CD, Hannon CP, Ross KA, K. J. (2016). Low Level of Evidence and Methodologic Quality of Clinical Outcome Studies on Cartilage Repair of the Ankle. *Arthroscopy*, *32*(1), 214–222.

Pritsch M, Horoshovski H, Farine I. (1986). Arthroscopic treatment of osteochondral lesions of the talus. *J Bone Joint Surg Am.*, *68*(6), 862–865.

Raikin, S. M., Elias, I., Zoga, A. C., Morrison, W. B., Besser, M. P., & Schweitzer, M. E. (2007). Osteochondral lesions of the talus: Localization and morphologic data from 424 patients using a novel anatomical grid scheme. *Foot and Ankle International*, *28*(2), 154–161. https://doi.org/10.3113/FAI.2007.0154

Redmond, A. C., Crane, Y. Z., & Menz, H. B. (2008). Normative values for the Foot Posture Index. *Journal of Foot and Ankle Research*, *1*(1), 1–9. https://doi.org/10.1186/1757-1146-1-6

Redmond, A. C., Crosbie, J., & Ouvrier, R. A. (2006). Development and validation of a novel rating system for scoring standing foot posture: The Foot Posture Index. *Clinical Biomechanics*, *21*(1), 89–98. https://doi.org/10.1016/j.clinbiomech.2005.08.002

Reilingh, M. L., Kerkhoffs, G. M. M. J., Telkamp, C. J. A., Struijs, P. A. A., & van Dijk, C. N. (2014). Treatment of osteochondral defects of the talus in children. *Knee Surgery, Sports Traumatology, Arthroscopy : Official Journal of the ESSKA*, *22*(9), 2243–2249. https://doi.org/10.1007/s00167-013-2685-7

RODEN S, TILLEGARD P, UNANDERSCHARIN L. (1953). Osteochondritis dissecans and similar lesions of the talus: report of fifty-five cases with special reference to etiology and treatment. *ACTA ORTHOP SCAND.*, *23*(1), 51–66.

Rolauffs B, Williams JM, Grodzinsky AJ, Kuettner KE, C. A. (2008). Distinct horizontal patterns in the spatial organization of superficial zone chondrocytes of human joints. *J Struct Biol.*, *162*(2), 335–344.

Root M, Orien WP, W. J. (2001). *La funzionalità del piede normale e patologico* (Piccin).

Roughley, P. J., & Mort, J. S. (2014). The role of aggrecan in normal and osteoarthritic cartilage. *Journal of Experimental Orthopaedics*, *1*(1), 1–11. https://doi.org/10.1186/s40634-014-0008-7

Schachter AK, Chen AL, Reddy PD, Tejwani NC. (2005). Osteochondral lesions of the talus. *J Am Acad Orthop Surg.*, *13*(3), 152–158. https://doi.org/10.1016/S1083-7515(03)00007-X

Scharfbillig R, Evans AM, Copper AW,Williams M, Scutter S,Iasiello H,Redmond A. (2004). Criterion validation of four criteria of the foot posture index. *J Am Podiatr Med Assoc*, *94*(1), 31–38.

Schneider, W., & Jurenitsch, S. (1997). Normative data for the American Orthopedic Foot and Ankle Society ankle-hindfoot, midfoot, hallux and lesser toes clinical rating system. *Foot & Ankle International*, *18*(3), 187–188.

Siegler S, Block J, S. C. (1988). The mechanical characteristics of the collateral ligaments of the human ankle joint. *Foot Ankle.*, *8*(5), 234–242.

Silfverskiöld N. (1924). Reduction of the uncrossed two joint muscle of the leg too one joint muscle in spastic conditions. *Acta Chir.Scan.*

Skraba JS, G. A. (1984). The role of the interosseous membrane on tibiofibular weightbearing. *Foot Ankle.*, *4*(6), 301–304.

Slattery, C., & Kweon, C. Y. (2018). Classifications in Brief: Outerbridge Classification of Chondral Lesions. *Clinical Orthopaedics and Related Research*, *476*(10), 2101–2104. https://doi.org/10.1007/s11999.0000000000000255

Stone, J. W. (1996). Osteochondral lesions of the talar dome. *J Am Acad Orthop Surg.*, *4*(2), 63–73.

Su, N. P., Schmal, H., & Niemeyer, P. (2012). Surgical treatment of osteochondritis dissecans of the talus : a systematic review. *Arch Orthop Trauma Surg*, *132*(9), 1241–1250. https://doi.org/10.1007/s00402-012-1544-1

Sullivan, M., Fraser, E. J., Linklater, J., Harris, C., & Morgan, K. (2017). Arthroscopic Surgical Technique for an Acute Talar Dome Osteochondral Lesion in a Professional Rugby League Player. *Foot and Ankle Specialist*, *10*(3), 263–269. https://doi.org/10.1177/1938640016669797

Taranow, W S, G A Bisignani, J D Towers, S. F. C. (1999). Retrograde drilling of osteochondral lesions of the medial talar dome,. *Foot Ankle Int*, *20*(8), 474–480.

Treppo, S., Koepp, H., Quan, E. C., Cole, A. A., Kuettner, K. E., & Grodzinsky, A. J. (2000). Comparison of biomechanical and biochemical properties of cartilage from human knee and ankle pairs. *Journal of Orthopaedic Research*, *18*(5), 739–748. https://doi.org/10.1002/jor.1100180510

Vadell AM, P. M. (2012). Calcaneonavicular ligament: anatomy, diagnosis, and treatment. *Foot and Ankle Clinics*, *17*(3), 437–448.

Valderrabano, V., Barg, A., Alattar, A., & Wiewiorski, M. (2014). Osteochondral Lesions of the Ankle Joint in Professional Soccer Players: Treatment With Autologous Matrix-induced Chondrogenesis. *Foot and Ankle Specialist*, *7*(6), 522–528. https://doi.org/10.1177/1938640014539811

Valderrabano V, Hintermann B, Nigg BM, Stefanyshyn D, S. P. (2003). Kinematic changes after fusion and total replacement of the ankle: part 2: Movement transfer. *Foot & Ankle International*, *24*(12), 888–896.

Valmassy RL. (1996). *Clinical bionechanics of the lower extremities* (Mosby).

van Bergen, C. J. A., Baur, O. L., Murawski, C. D., Spennacchio, P., Carreira, D. S., Kearns, S. R., Mitchell, A. W., Pereira, H., Pearce, C. J., Calder, J. D. F., Ackermann, J., Adams, S. B., Andrews, C. L., Angthong, C., Batista, J. P., Bayer, S., Becher, C., Berlet, G. C., Boakye, L. A. T., … Zhang, Z. (2018). Diagnosis: History, Physical Examination, Imaging, and Arthroscopy: Proceedings of the International Consensus Meeting on Cartilage

Repair of the Ankle. *Foot and Ankle International*, *39*(1_suppl), 3S-8S. https://doi.org/10.1177/1071100718779393

Van den Bekerom MP, Mutsaerts EL, V. D. C. (2009). Evaluation of the integrity of the deltoid ligament in supination external rotation ankle fractures: a systematic review of the literature. *Arch Orthop Trauma Surg.*, *129*, 227–235.

van Dijk, C. N., Reilingh, M. L., Zengerink, M., & van Bergen, C. J. A. (2010). Osteochondral defects in the ankle: Why painful? *Knee Surgery, Sports Traumatology, Arthroscopy*, *18*(5), 570–580. https://doi.org/10.1007/s00167-010-1064-x

Vega, J., Malagelada, F., Manzanares Céspedes, M. C., & Dalmau-Pastor, M. (2020). The lateral fibulotalocalcaneal ligament complex: an ankle stabilizing isometric structure. *Knee Surgery, Sports Traumatology, Arthroscopy*, *28*(1), 8–17. https://doi.org/10.1007/s00167-018-5188-8

Vellet AD, Marks PH, Fowler PJ, Munro TG. (1991). Occult posttraumatic osteochondral lesions of the knee: prevalence, classification, and short-term sequelae evaluated with MR imaging. *Radiology*, *178*(1), 271–276.

Venditto, T., Tognolo, L., Rizzo, R. S., Iannuccelli, C., Di Sante, L., Trevisan, M., Maggiolini, F. R., Santilli, V., & Ioppolo, F. (2015). 17-Italian Foot Function Index with numerical rating scale: Development, reliability, and validity of a modified version of the original Foot Function Index. *Foot*, *25*(1), 12–18. https://doi.org/10.1016/j.foot.2014.09.004

Verhagen, R. A. W., Struijs, P. A. A., Bossuyt, P. M. M., & Van Dijk, C. N. (2003). Systematic review of treatment strategies for osteochondral defects of the talar dome. *Foot and Ankle Clinics*, *8*(2), 233–242. https://doi.org/10.1016/S1083-7515(02)00064-5

Vukicević S, Stern-Padovan R, Vukicević D, K. P. (1980). Holographic investigations of the human tibiofibular interosseous membrane. *Clin Orthop Relat Res.*, *Sep*(151), 210–214.

Vuurberg G, van D. C. (2016). Osteochondral defect of the ankle. In *Arthroscopy* (Springer-, pp. 985–996).

Weber MA, A., Wünnemannm F, & Jungmann PM, Kuni B, Rehnitz C. (2017). Modern Cartilage Imaging of the Ankle Moderne Knorpelbildgebung des Sprunggelenks. *Fortschr Röntgenstr*, *189*, 945–956. https://doi.org/10.1055/s-0043-110861

Wodicka, R., Ferkel, E., & Ferkel, R. (2016). Osteochondral Lesions of the Ankle. *Foot and Ankle International*, *37*(9), 1023–1034. https://doi.org/10.1177/1071100716654691

Woods K, Harris I. (1995). Osteochondritis dissecans of the talus in identical twins. *J Bone Joint Surg Br.*, *77*(2), 331.

Yammine K. (2017). The Morphology and Prevalence of the Deltoid Complex Ligament of the Ankle. *Foot and Ankle Specialist*, *10*(1), 55–62.

Zwiers, R., Weel, H., Mallee, W. H., Kerkhoffs, G. M. M. J., & van Dijk, C. N. (2018). Large variation in use of patient-reported outcome measures: A survey of 188 foot and ankle surgeons. *Foot and Ankle Surgery*, *24*(3), 246–251. https://doi.org/10.1016/j.fas.2017.02.013

Anexo I – Carta de pedido de autorização do orientador

MARIA PALMUCCI

Aluna do Mestrado em Podiatria infanti!

Estimada Ora. Laura Pérez Palma,

Agtualmente estoy realizando el trabajo de fin dè master correspondiente al Master Oficial de Podologia Infanti! de la Universidad de CESPU, en Portugal.

El motivo de la presente, es la solicitud de tutorizaciòn por su parte del trabajo que estoy realizando y que trata sobre la relaciòn entre la especializaciòn deportiva precoz y la postura del pie en el futbol.

Atentamente,

Barcellona, 20/05/2022

MARIA PALMUCCI

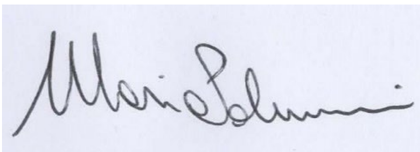

Maria Palmucci
24.11.2023
11:59:35
GMT+01:00

Anexo II – Carta de pedido de autorização da aluna

MARIA PALMUCCI

Aluna do Mestrado em Podiatria infanti!

Estimada Ora. Umberto Alfieri Montrasio

Agtualmente estoy realizando el trabajo de fin dè master correspondiente al Master Oficial de Podologia Infanti! de la Universidad de CESPU, en Portugal.

El motivo de la presente, es la solicitud de tutorizaciòn por su parte del trabajo que estoy realizando y que trata sobre la relaciòn entre la especializaciòn deportiva precoz y la postura del pie en el futbol.

Atentamente,

Barcellona, 08/03/2022

MARIA PALMUCCI

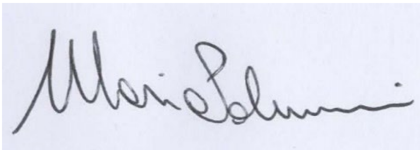

Maria Palmucci
24.11.2023
11:59:35
GMT+01:00

Anexo III – Apresentação do estudo

Declaração do orientador

Para os devidos efeitos, eu Laura Pérez Palma, declaro que aceito ser orientador do relatório final de estágio profissionalizante da estudante_MARIA PALMUCCI__ do 2° ano do curso de Mestrado em Podiatria Infantil da Escola Superior se Saúde do Vale do Ave – Instituto Politécnico de Saúde do Norte, com o tema "BIOMECHANICAL FOOT ASSESSMENT IN PEDIATRIC PATIENTS POST INTERVENTION WITH AMIC TECHNIQUE FOR OSTEOCONDRAL LESION _".

26/05/2022

O (a) orientador(a)

LAURA PÉREZ PALMA - DNI 38105016L

Firmado digitalmente por LAURA PÉREZ PALMA - DNI 38105016L
Fecha: 2022.07.22 16:17:34 +02'00'

Anexo IV – Apresentação do estudo

CESPU
INSTITUTO POLITÉCNICO
DE SAÚDE DO NORTE
ESCOLA SUPERIOR DE SAÚDE
DO VALE DO AVE

I

À Comissão Coordenadora do Curso de Mestrado em Podiatria Infantil da Escola Superior de Saúde do Vale do Ave

Eu, _MARIA PALMUCCI_(nome do estudante), venho por este meio apresentar a proposta do tema para o relatório de estágio a apresentar no âmbito da unidade curricular de estágio Profissionalizante do 2º ano do curso de Mestrado em Podiatria Infantil.

Proponho-me a desenvolver o tema " BIOMECHANICAL FOOT ASSESSMENT IN PEDIATRIC PATIENTS POST INTERVENTION WITH AMIC TECHNIQUE FOR OSTEOCONDRAL LESION." sob orientação do (a) (nome do orientador).
Junto anexo a declaração de aceitação do orientador.

Data: 01/06/2022

Com os melhores cumprimentos,

O (a) estudante

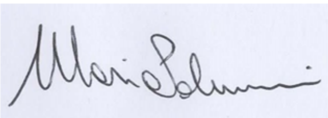

Maria Palmucci
24.11.2023 11:59:35
GMT+01:00

Anexo V – Declaração de consentimento informado

Gentile Signore/a,

desideriamo informarLa che la Dott.ssa Palmucci Maria (di seguito "la Professionista") considera di fondamentale importanza la privacy dei propri pazienti, dei loro familiari e/o di eventuali figure di sostegno e garantisce che il trattamento dei dati personali effettuati con qualsiasi mezzo di elaborazione sia informatico che cartaceo, si svolga nel rispetto dei diritti dell'interessato, con particolare riferimento alla riservatezza, alla tutela dell'identità e della dignità personale e al diritto alla protezione dei dati personali.

La presente informativa, rilasciata ai sensi dell'art.13 del Regolamento UE n. 2016/679 (di seguito "GDPR") e della normativa nazionale, compresi i singoli provvedimenti dell'Autorità di controllo (Garante per la protezione dei dati personali), ove applicabile, è articolata in paragrafi ognuno dei quali tratta in maniera approfondita uno specifico aspetto.

a) Titolare delTrattamento e Responsabili del Trattamento

Il titolare del trattamento dei Vs. dati è la Dott.ssa Palmucci Maria, sede legale via U. Foscolo 20, Giussano (MB).

I soggetti responsabili del trattamento dei dati personali sono stati opportunamente nominati dalla professionista e l'elenco, contenuto all'interno del "Registro dei Trattamenti", è disponibile a richiesta presso lo studio della Professionista.

b) Finalità e modalità deltrattamento

La Professionista potrà trovarsi a trattare i Suoi dati personali, anche sensibili (disciplinati dall'art.9 del GDPR), utilizzando sia strumenti informatici sia cartacei per una o più delle finalità di seguito illustrate:

1. <u>Finalità connesse e strumentali all'erogazione delle prestazioni podologiche</u>

   Rientrano in questa categoria tutte le attività di erogazione delle prestazioni di valutazione e cura, le prestazioni di assistenza e fornitura di dispositivi medici su misura (plantari, siliconi, tutori, etc…), nonché le attività di calendarizzazione degli appuntamenti e delle visite effettuate presso le strutture nelle quali opera.
   Per tutte le finalità sopra riportate il conferimento dei Suoi dati personali, ancorché libero è necessario per il raggiungimento degli obbiettivi correlati con le attività erogate dalla Professionista.
   L'art. 6 par. 1 del GDPR, prevede la prestazione del Suo consenso che potrà esprimere utilizzando l'apposito form in calce a questa informativa.

2. <u>Finalità connesse all'espletamento di obblighi normativi e contrattuali</u>

Rientrano in questa categoria tutte le attività per ottemperare ad obblighi di legge/regolamento imposti dalla normativa nazionale o comunitaria (ad esempio in materia di igiene e sanità, relazione ad adempimenti fiscali, verifiche di carattere amministrativo, ispezione degli organi vigilanza sanitaria, investigazioni di polizia giudiziaria, ecc.) nonché tutti gli adempimenti di natura amministrativa e contabile collegati al pagamento delle prestazioni sanitarie erogate e/o alla gestione degli obblighi contrattuali con compagnie assicuratrici di terzi.
Per tutte le finalità sopra riportate il conferimento dei Suoi dati personali, ancorché libero, è necessario per il raggiungimento degli obbiettivi correlati con le attività erogate dalla Professionista.
L'art. 6 par. 1 del GDPR, prevede la prestazione del suo consenso che potrà esprimere utilizzando l'apposito form in calce a questa informativa.

c) Ambito di circolazione dei dati personali

Per il perseguimento delle finalità di cui al precedente punto a) la Professionista, a seconda dei casi, si può trovare nella necessità di comunicare i Suoi dati personali e sensibili (disciplinati dall'art. 9 del GDPR) ad alcuni tra i seguenti soggetti:

1. Suoi familiari e/o a persone di sostegno cui dare le informazioni relative alla sua condizione di salute o ad aspetti correlati alle prestazioni sanitarie erogate
2. Medici specialistici

Per le suddette operazioni di comunicazione Le viene richiesto di esprimere, utilizzando l'apposito form, il suo consenso. Inoltre, i suoi dati potranno essere comunicati a:

3. Servizio Sanitario Regionale e/o Nazionale per le pratiche di rimborso delle prestazioni podologiche erogate o ad altri organismi sanitari di controllo e vigilanza (ASP) per le attività di verifica sull'erogazione delle prestazioni sanitarie
4. Enti previdenziali ed assistenziali e/o compagnie assicurative che, nella loro qualità di autonomi titolari del trattamento offrono servizi di assistenza sanitaria integrativa nei suoi confronti
5. Forze di polizia, autorità giudiziaria ed altri organismi o soggetti pubblici per scopi di difesa o sicurezza dello Stato ovvero per prevenzione, accertamento o repressione di reati nei limiti di cui all'art. 6 par. 1 del GDPR.

In queste ipotesi non è necessario acquisire il suo consenso stante il carattere obbligatorio delle comunicazioni che avvengono in forza di leggi o di obblighi contrattuali.

d) Trasferimento di dati all'estero

La professionista non effettua alcun trasferimento di dati all'estero. La professionista si riserva di informare tempestivamente i propri pazienti nel caso in cui si rendesse necessario effettuare il trasferimento di dati verso Paesi non appartenenti alla comunità europea esclusivamente per finalità correlate all'erogazione di prestazioni sanitarie.

e) Conservazione dei dati personali

Fatti salvi gli obblighi di legge che impongono alla Professionista la conservazione ed il mantenimento dei dati personali raccolti durante tutto il processo di cura e di prevenzione, i Suoi dati saranno conservati coerentemente per un periodo di tempo non superiore a quello necessario agli scopi per i quali essi sono raccolti e successivamente trattati. I dati personali funzionali all'assolvimento di obblighi di legge saranno conservati anche successivamente al termine del processo di cura e prevenzione, in ottemperanza a detti obblighi, nel rispetto delle tempistiche di conservazione previste dalle norme di volta in volta applicabili. Per un maggiore dettaglio è disponibile presso la sede della professionista il "Registro dei Trattamenti".

f) Diritti di accesso ai Dati ed altri diritti

In relazione al trattamento dei Suoi dati personali, Lei ha il diritto in qualunque momento di ottenere la conferma dell'esistenza o meno dei medesimi dati e di conoscerne il contenuto e l'origine, verificarne l'esattezza o chiederne l'integrazione o l'aggiornamento, oppure la rettificazione; Ella, inoltre, ha il diritto di chiedere la cancellazione dei dati trattati in violazione di legge o in caso di revoca del consenso [articolo 17, comma 1, lett. a), b), c), e) ed f) GDPR] e la limitazione del trattamento in caso di contestazione, nonché di opporsi al loro trattamento, per motivi legittimi oppure, in ogni caso e discrezionalmente, per tutte quelle finalità basate sul consenso. Lei ha inoltre il diritto di ottenere il rilascio dei dati personali oggetto di trattamento in un formato compatibile con le applicazioni informatiche standard, per permetterne il trasferimento su altre piattaforme di Sua scelta, anche tramite trasmissione diretta, ove questa stessa sia tecnicamente fattibile [c.d. diritto alla portabilità dei dati].

Tali diritti potranno essere esercitati rivolgendosi:

- via e-mail, all'indirizzo: maria.palmucci@gmail.com
- via posta, all'indirizzo: Dott.ssa Maria Palmucci: in via U. Foscolo,20, Giussano (MB)

Nel caso di mancato o parziale riscontro alle predette richieste, avrà diritto di proporre reclamo o ricorso al Garante per la protezione dei datipersonali.

Consenso al trattamento dei dati personali

ai sensi dell'Art. 13 del Regolamento UE n. 2016/679

Il/La sottoscritto/a____

Nato/a a________________________________ il_____________________________

Codice fiscale____

Residente a ____CAP_________________

In via/piazza ______________________________________n.___________________

Telefono ____

e-mail____

Preso atto dell'Informativa Privacy fornita, dichiaro di prestare il consenso al trattamento dei miei dati personali e sensibili da parte della Dott.ssa Palmucci Maria per le Finalità di cui al **punto b) nn. 1 e 2**, consapevole del fatto che il conferimento dei dati risulta indispensabile ai fini del perseguimento delle finalità di cura della salute.

☐ Acconsento ☐ Nonacconsento

Con riguardo al **punto c) nn. 1 e 2** dell'informativa:

☐ Acconsento ☐ Nonacconsento

alla comunicazione dei dati personali e sensibili ai seguenti soggetti sotto indicati:

NOME: _______________ COGNOME___________________________

☐ tutore ☐ amministratore di sostegno ☐ parente

di____

NOME: _______________ COGNOME___________________________

☐ tutore ☐ amministratore di sostegno ☐ parente

di____

consapevole del fatto che tali comunicazioni risultano funzionali ai fini del perseguimento delle finalità di cura della salute.

Data ______________________ Firmadelpaziente ___________________________

Anexo VI – Foot Function Index

Italian Version

quanto è severo il dolore al piede?		
es. nell'ultima settimana quanto dolore ha avuto?	0=nessun dolore	10=il peggior dolore immaginabile
1. al momento della max intensità		
2. all'inizio della mattina?		
3. quando stava in piedi?		
4. quando camminava?		
5. alla fine della giornata?		
quanto difficoltà ha avuto?		
es. quando cammina in casa	0=nessuna difficoltà	10= difficoltà tale da dover chiedere aiuto
6. quando camminava in casa		
7. quando camminava all’aperto		
8. quando camminava per 500mt		
9. quando saliva le scale		
10. quando scendeva le scale		
11. quando stava in piedi		
12. quando si rialzava da una sedia		
13. quando superava un ostacolo di 20cm		
14. quando correva o camminava velocemente		
per quanto tempo lei ha		
es. limitato le sue attività	0=mai	10=sempre
15. usato un ausilio (bastone, stampelle, deambulatore,...) in casa		
16. usato un ausilio all'aperto		
17.limitato le sue attività		
punt tot= __________/170*100=_____%		

English version

How severe is the pain in the foot?		
E.g. in the last week how much pain have you had?	0=no pain	10=the worst pain imaginable
1. at the time of maximum intensity		
2. Early in the morning?		
3. When was he standing?		
4. When did he walk?		
5. At the end of the day?		
How much difficulty did you have?		
e.g. when walking around the house	0=no difficulty	10= difficulty such that you have to ask for help
6. when he walked in the house		
7. when walking outdoors		
8. when he walked 500mt		
9. when he climbed the stairs		
10. when he went down the stairs		
11. when he was standing		
12. when he got up from a chair		
13. when overcoming a 20cm obstacle		
14. when he ran or walked fast		
How long have you		
es. limited its activities	0=never	10=All the time
15. used an aid (stick, crutches, walker,...) in the house		
16. used an outdoor aid		
17.limited its activities		
score tot= __________/170*100=_____%		

Anexo VII – Foot Posture Index

Italian version

palpazione della testa dell'astragalo	lat no med	lat e legg med	simmetrica	med e legg lat	med no lat	TOT
	-2	-1	0	1	2	
dx						
sx						
curvatura sopra e sotto malleolare	dritta/convessa	Curva sotto al malleolo concava ma più piatta/più bassa della curva sopramalleolare	uguali	Curva sotto al malleolo più concava della curva sopramalleolare	molto concava	
	-2	-1	0	1	2	
dx						
sx						
posizione calcagno sul piano frontale	inv<-5	-5°<inv<0	verticale	0°<inv<5°	>5°	
	-2	-1	0	1	2	
dx						
sx						
sporgenza nella regione dell'art. talo-navicolare	molto concava	concava	nessuna sporgenza	sporgente	molto sporgente	
	-2	-1	0	1	2	
dx						
sx						
altezza e congruenza dell'arco longitudinale mediale	alto ce acuto, angolato vs estremità posteriore dell'arco mediale	arco moderatamente alto e leggermente acuto posteriormente	altezza arco normale e congruenza della curva	arco abbassato appiattito nella porzione centrale	arco molto basso con sporgenza acuta nella porzione centrale - arco totalmente a contatto con il terreno	
	-2	-1	0	1	2	
dx						
sx						
abduzione7adduzione dell'avampiede rispetto al retropiede	nessuna delle dita visibile lateralmente, dita mediali chiaramente visibili	dita mediali maggiormente visibili di quelle laterali	dita mediali e laterali visibili in egual misura	dita laterali + visibili di quelle mediali	nessuna delle dita visibile medialmente, dita laterali chiaramente visibili	
	-2	-1	0	1	2	
dx						
sx						

English Version

FPI					
Talar head palpation	talar head palpable on lateral side/but not on medial side	talar head palpable on lateral side/slightly palpable on medial side	talar head equally palpable on lateral and medial side	talar head palpable on medial side/slightly palpable on lateral side	talar head palpable on medial side/but not on lateral side
	-2	-1	0	1	2
right		-1			
left		-1			
Curves above and below lateral malleoli	curve below the malleolus either straight or convex	curve below the malleolus concave, but flatter/more shallow than curve above the malleolus	both infra and supra malleolar curves roughly equal	curve below the malleolus more concave, than curve above the malleolus	curve below malleolus markedly more concave, but than curve above the malleolus
	-2	-1	0	1	2
right	-2				
left		-1			
calcaneal inversion/eversion o	more than an estiamted 5°inverted (varus)	between vertical and an estimated 5° inverted (varus)	vertical	between vertical an estimated 5° evrted (valgus)	more than an estimated 5° everted (valgus)
	-2	-1		1	2
right		-1			
left		-1			
Bulge in the region of talo-navicular jont	markedly concave	slightly, but definitely concave	area of TNJ flat	bulging slightly	bulging markedly
	-2	-1	0	1	2
right	-2				2
left		-1			2
medial arch height	arch high and acutely angled towards the posterior end of the medial arch	arch moderately high and slightly acute posteriorly	arch height normal and concentrically curved	arch lowered with some flattening in the central portion	arch very low with severe flattening in the central position - arch making ground contact
	-2	-1	0	1	2
right		-1			
left		-1			
abduction/adduction of the forefoot on rearfoot (too-many-toes)	no lateral toes visible. Medial toes clearly visible	medial toes clearly more visible than lateral	medial and lateral toes equally visible	lateral toes clearly more visible than medial	no medial toes visible. Lateral toes clearly visible
	-2	-1	0	1	2
right	-2				
left	-2				

Anexo VIII – AOFAS

Italian version of the “AOFAS Ankle-Hindfoot evaluation scale”		
Categoria		punti
Dolore (40 punti)	nessuno	40
	lieve, sporadico	30
	moderato, quotidiano	20
	severo, quasi semrpe presente	0
Funzione (50 punti)		
Limitazioni nelle attività necessità di ausili	nessuna limitazione, nessun ausilio	10
	Nessuna limitazione nelle attività quotidiane, limitazioni nelle attività ricreative, nessun ausilio	7
	Attività quotiiane e ricreative limitate, bastone	4
	Seria limitazione nelle attività quotidiane e ricreative, deambulatore, stampelle, sedia a rotelle, tutore ortopedico	0
Massima distanza che riesce a percorrere, in centinaia di metri	>6	5
	4-6	4
	1-3	2
	<1	0
Superfici percorribili	Nessuna difficoltà su qualsiasi superficie	5
	Qualche difficoltà su terreno irregolare, scale, pendenze, gradini	3
	Seria difficoltà su terreno irregolare, scale, pendenze, gradini	0
Anormalità nell’andatura	Nessuna, lieve	8
	Evidente	4
	Marcata	0
Movimento sagittale	Normale/leggera restrizione(≥30°)	8
	Restrizione moderata(15°-29°)	4
	Restrizione marcata(≤15°)	0
Movimento del retropiede	Normale/leggera restrizione(75%-100% del normale)	6
(inversione + eversione)	Restrizione moderata(25%-74% del normale)	3
	Restrizione marcata(<25% del normale)	0
Stabilità della caviglia e retropiede	Stabile	8
(anteroposteriore, varo, valgo)	decisamente instabile	0
Allineamento (10 punti)	Buono, piede plantigrado, caviglia e retropiede ben allineato	10
	Discreto, piede plantigrado, si osserva qualche segno di mal allineamento della caviglia e retropd, nessun sintomo	5
	Scarso, piede non plantigrado, grave mal allineamento, presenza di sintomi	0

English version of the “AOFAS Ankle-Hindfoot evaluation scale”

Category		points
Pain (40 points)	None	40
	Mild, occasional	30
	Moderate, daily	20
	Severe, almost always present	0
Function (50 points)		
Activity limitations, support requirement	No limitations, no support	10
	Njo limitation of daily activities, limitation of recreational activities, no support	7
	Limited daily and recreational activities, cane	4
	Sever limitationm of daily and recreational activities, walker, crutches, wheelchair, brace	0
Maximum walking distance, blocks	>6	5
	4-6	4
	1-3	2
	<1	0
Walking surfaces	No difficulty on any surface	5
	Some difficulty on uneven terrain, stairs, inclines, ladders	3
	Serious difficulty on uneven terrain, stairs, inclines, ladders	0
Gait abnormality	None, slight	8
	Obvious	4
	Marked	0
Sagittal Motion (flexion plus extension)	Normal/mild restriction(≥30°)	8
	Moderate restriction(15°-29°)	4
	Severe restriction(≤15°)	0
Hindfoot motion	Normal/mild restriction (75%-100% normal)	6
(inversion + eversion)	Moderate restriction (25%-74% normal)	3
	Severe restriction (<25% normal)	0
Ankle and hindfoot stability	Stable	8
(anteroposterior, varus, valgus)	Definitely unstable	0
Alignment (10 points)	Good, plantigrade foot, ankle and hindfoot well aligned	10
	Fair, plantigrade foot, some degree of ankle-hindfoot malalignment observed, no symptoms	5
	Poor, non-plantigrade foot, severe malalignment, symptoms	0

Anexo IX – Datos for SPSS

pz	iniziali	DATA INTERVENTO	FOLLOW-UP	distanza da intervento in mesi	sport	sport
1	PV	20/12/2021	22/10/2022	8	NO	no
2	SM	19/02/2021	01/11/2022	21	calcio3-4v/sett	si
3	TM	24/07/2015	01/10/2022	86	palestra	si
4	DGA	10/07/2020	01/10/2022	27	no	no
5	GL	08/06/2018	01/10/2022	52	PALESTRA-PESI	si
6	GG	27/11/2020	24/09/2022	22	NO	no
7	PS	16/12/2013	22/10/2022	104	NO	no
8	RA	07/04/2017	23/10/2022	66	PALESTRA+CORSA	si
9	ZN	13/12/2017	22/10/2022	56	MMA	si

pz	zona lesione	zona astragalica	lato lesione	fpi dx	fpi sx	FFI %	AOFAS RETROPD
1	mediale	post	d	2	3	15	100
2	laterale	centrale	s	5	8	18	85
3	mediale	post	d	8	8	20	84
4	tibiale		s	2	1	14	100
5	mediale	post	s	5	6	15	93
6	mediale	post	d	2	1	15	88
7	mediale	post-centr	s	0	0	14	100
8	mediale	post	d	2	0	14	100
9	mediale	post	d	2	1	18	90

pz	JACK	HINTERMANN	RCSP	NAVICULAR DROP	AV	rp	tbt	M1	LASSITà
1	pos	neg	2	1	4°sup				
2	neg	neg	4	1,4	8°varo	6°varo			
3	neg	pos	6	1,7	7varo	3varo	planatrflessa 4°		
4	pos	neg	2	0,9	0	2°varo		dorsifle sr	
5	neg	neg	4	1,3	4°valgo flex	6°varo		plant fl	
6	pos	neg	2	-0,6				dorsifle fl	

7	neg	neg	4	0,9				dorsifle sr	
8	neg	neg	0	1,2	4°valgo flex	6°varo			
9	pos	neg	2	0,9		4°varo		Dors	x

pz	dinamica	Età INT in mesi	sesso	eziologia
1	pronazione durante 2^rocker + evidente, rispetto statica	174	f	t
2	evidente pos squat test a sx, andatura molleggiante, stacco precoce del tallone	200	m	t
3		159	f	t
4		191	f	i
5		163	f	t
6	hav sx	178	f	i
7		169	f	t
8		204	f	t
9	polpaccio <0,5cm	200	m	t

Anexo X – Internship evaluation form Podologia UB con Fundacion de Osteopatia Barcellona

História Núm.:	**Fecha 1ª visita:**
Enviado por:	

Datos del niño/niña
Nombre:
Apellidos:
Fecha de nacimiento:

Datos del padre/madre/tutor		
Nombre:		
Apellidos:		
Fecha de nacimiento:		
Dirección:	C.P.:	Provincia:
NIF/Pasaporte:		
Telf. De contacto:		
Dirección de correo:		
Otros datos de interés:		

C/ Consolat de mar, 45 2º planta. 08003 Barcelona. fob@osteopatiabarcelona.com

Servei d'Osteopatia Solidària

FUNDACIÓ d'Osteopatia de Barcelona

HISTORIA CLÍNICA

MOTIVO DE CONSULTA

EMBARAZO

- Edad madre :
- Salud / estado emocional:
- Trastornos endocrinos / peso :
- Posición / encaje del bebé :
- Embarazos anteriores :

PARTO

- Semana embarazo :
- Espontáneo / Inducido
- Evolución:
  - Dilatación
  - Expulsivo :
- Instrumentalización/Maniobras
  - Kristeller
  - Ventosa
  - Forceps/palas
- Anestesia / Medicalización
- Episiotomía

C/ Consolat de mar, 45 2º planta. 08003 Barcelona. fob@osteopatiabarcelona.com

RECIÉN NACIDO

- Apgar
- Llanto
- Reanimación / aspiración
- Incubadora
- Contacto materno
- Color
- Forma del cráneo
- Pecho /lactancia
- Comportamiento

PRIMER AÑO

- Crecimiento: talla y peso
- Alimentación
- Sueño
- Desarrollo psicomotor
- Comportamiento (llanto, irritabilidad, sonrisa)
- Estado de salud / enfermedades

Servei d'Osteopatia Solidària

FUNDACIÓ d'Osteopatia de Barcelona

ANAMNESIS Y MOTIVO DE LA VISITA: Altura:_______ Peso:_____ Talla:_____

INSPECCIÓN:

EXPLORACIÓN CAMILLA:

	IZQ	DCHO
Tipo de pie		
DF TPA rodilla en extensión (15º)		
DF TPA rodilla en flexión (15º)		
Linias frontereras rotas		
Relación AP/RP		
Metatarso aducto		
Movilidad 1Radio		
DF o PF 1cmtt		
1AMTF (70-90º)		
Movilidad 5Radio		
DF o PF 5cmtt		
Función TP		
Función TA		
Función PLL y PLC		
Función t Aquiles		

EXPLORACIÓN BIPEDESTACIÓN:

	IZQ	DCHO
Test Adams		
Bending test		
Basculaciones (DIBUJO)		
Plomada		
Block test		
AV/RV pélvica		
Torsión pélvica		
Genu varo/valgo		
Genu recurvatum/flexum		
DIM		
Ròtulas conv/divergentes		
Tibia vara		

C/ Consolat de mar, 45 2º planta. 08003 Barcelona. fob@osteopatiabarcelona.com

*marca con flechas basculaciones y/o dibuja desviaciones de raquis

	IZQ	DCHO
Helbing talar PRCA		
Helbing talar PNCA		
SHRT		
DHRT		
TMP (máx pronación)		
TRS (resisténcia a la supinación)		
Huella plantar		
FPI		

Palpación astrágalo	Curvas maleolares	Posición calcáneo	Prominencia talonavicular	ALI	Abd/add antepié

Muy supinado	Supinado	Normal	Pronado	Muy pronado
-5 a -12	-1 a -4	0 a +5	+6 a +9	+10 a +12

DINÁMICA:

		IZQ	DCHO
Ángulo de progresión (0-15º)			
Marcha de puntillas			
Fase de apoyo de talón	DF TPA (10-15º)		
	Posición ASA		
Fase de apoyo de mediopié	DF TPA (10º)		
Fase de despegue	DF hallux (65º)		
Otros			

CALZADO: DESGASTE:

Tipo: ______________________

C/ Consolat de mar, 45 2º planta. 08003 Barcelona. fob@osteopatiabarcelona.com

Servei d'Osteopatia Solidària

FUNDACIÓ d'Osteopatia de Barcelona

EXPLORACIÓN

IMPRESIÓN DIAGNÓSTICA

OBJETIVOS A CORTO Y A LARGO PLAZO

TRATAMIENTO

Nombre del terapeuta:

C/ Consolat de mar, 45 2º planta. 08003 Barcelona. fob@osteopatiabarcelona.com